Geologic Report for the
NAVARIN BASIN
Planning Area

Bering Sea, Alaska

Geologic Report for the Navarin Basin
Planning Area, Bering Sea, Alaska

by

Ronald F. Turner
Gary C. Martin
Tabe O. Flett
David A. Steffy

edited by

Ronald F. Turner

1985

United States Department of the Interior
Minerals Management Service
Alaska OCS Region

English-Metric Conversion

(The following table gives the factors used to convert English units to metric units.)

multiply English units	by	to obtain metric units
feet	0.3048	meters
miles (statute)	1.6093	kilometers
acres	0.4047	hectares
barrels (U.S. petroleum)	158.9828	liters
	0.1589	cubic meters
inches	2.5400	centimeters
pounds per gallon	0.1198	grams per cubic centimeter
knots	1.8520	kilometers per hour
miles per hour	1.6093	kilometers per hour
square miles	2.5899	square kilometers

To convert from Fahrenheit (°F) to Celsius (°C), subtract 32 then divide by 1.8.

Abbreviations and Acronyms

AAPG	American Association of Petroleum Geologists
aff.	affinis (to have affinities with)
APD	Application for Permit to Drill
ARCO	Atlantic Richfield Company
BHT	Bottom Hole Temperature
b.p.	before present
BSR	Bottom-Simulating Reflector
C	carbon
°C	degrees Celsius
CDP	common depth point
cf.	confer (to be compared with)
Co.	Company
commun.	communication
COST	Continental Offshore Stratigraphic Test
D	darcy, darcies
D	downthrown
DST	Drill Stem Test
e, E	early, Early
E	east

EA	Environmental Assessment
ed.	editor(s), edited by
°F	degrees Fahrenheit
fig.	figure
ft.	feet
g	gram
GSA	Geological Society of America
H	high
H.R.	high resolution
HRT	High Resolution Thermometer
Inc.	Incorporated
K-Ar	potassium-argon
l, L	late, Late
lat	latitude
long	longitude
LSS	Long-Spaced Sonic
m, M	middle, Middle
m	milli
	meter
	million
μ	micro
MMS	Minerals Management Service
m.y.	million years
N	north
NMFS	National Marine Fisheries Service
No.	number
OCS	Outer Continental Shelf
opal-CT	opal cristobalite-tridymite
p.	page(s)
PPG	pounds per gallon
R_o	random vitrinite reflectance
RFT	Repeat Formation Tester
S	south
s	second
SP	Spontaneous Potential
sp.	species (singular)
spp.	species (plural)
SSD	subsea depth
St.	Saint
TAI	thermal alteration index
TD	total depth
TOC	total organic carbon
TTI	time-temperature index
U	upthrown
US	United States
USGS	United States Geological Survey
USSR	Union of Soviet Socialist Republics
var.	varietas (variety)

Abbreviations and Acronyms--Continued

---

vol.	volume
W	west
WG	Western Geophysical Company
yr(s)	year(s)

Contents

Figures

Figures--Continued

Figures--Continued

Plates

Tables

Introduction

This report is a summary of the regional geology, petroleum potential, and environmental characteristics of the continental shelf portion of the Navarin Basin Planning Area. The parts of the planning area encompassing continental slope and rise bathymetries were not assessed because of the paucity of seismic data. The report is based, in great part, on detailed analyses of data obtained from the ARCO Navarin Basin COST No. 1 Well, the first deep stratigraphic test in the area. This well received exhaustive treatment in OCS Report MMS 84-0031, Geological and Operational Summary, Navarin Basin COST No. 1 Well, Bering Sea, Alaska (Turner and others, 1984). Although significant portions of that report are reproduced here, an equal amount of new and reinterpreted data is included. In particular, the common-depth-point (CDP) seismic reflection data base has been greatly expanded and improved by the inclusion of key Western Geophysical lines. Permission to use these lines, with some restrictions, was granted by Western Geophysical Company. A number of U.S. Geological Survey (USGS) studies were also used.

The Navarin Basin Planning Area (figs. 1 and 2) is bounded on the north and south by the 63° and 58° latitude lines, respectively. The southern boundary extends from 174° longitude on the east to 180° longitude on the west. The northwest boundary follows the disputed international boundary between the United States and the Soviet Union (US-USSR Convention of 1867). This line also approximates the boundary between the Navarin Basin and the Anadyr and Khatyrka Basins (fig. 3).

Risked mean leaseable economically recoverable hydrocarbon resources in the Navarin Basin as of July 1984 are estimated to be 890 million barrels oil equivalent (U.S. Department of the Interior, 1985). The economic and logistical factors associated with the production of any hydrocarbons discovered are not within the scope of this report.

Analyses of COST well data and seismic mapping indicate that the volume and distribution of source rock, reservoir rock, seals, and trapping configurations are sufficient to ensure further
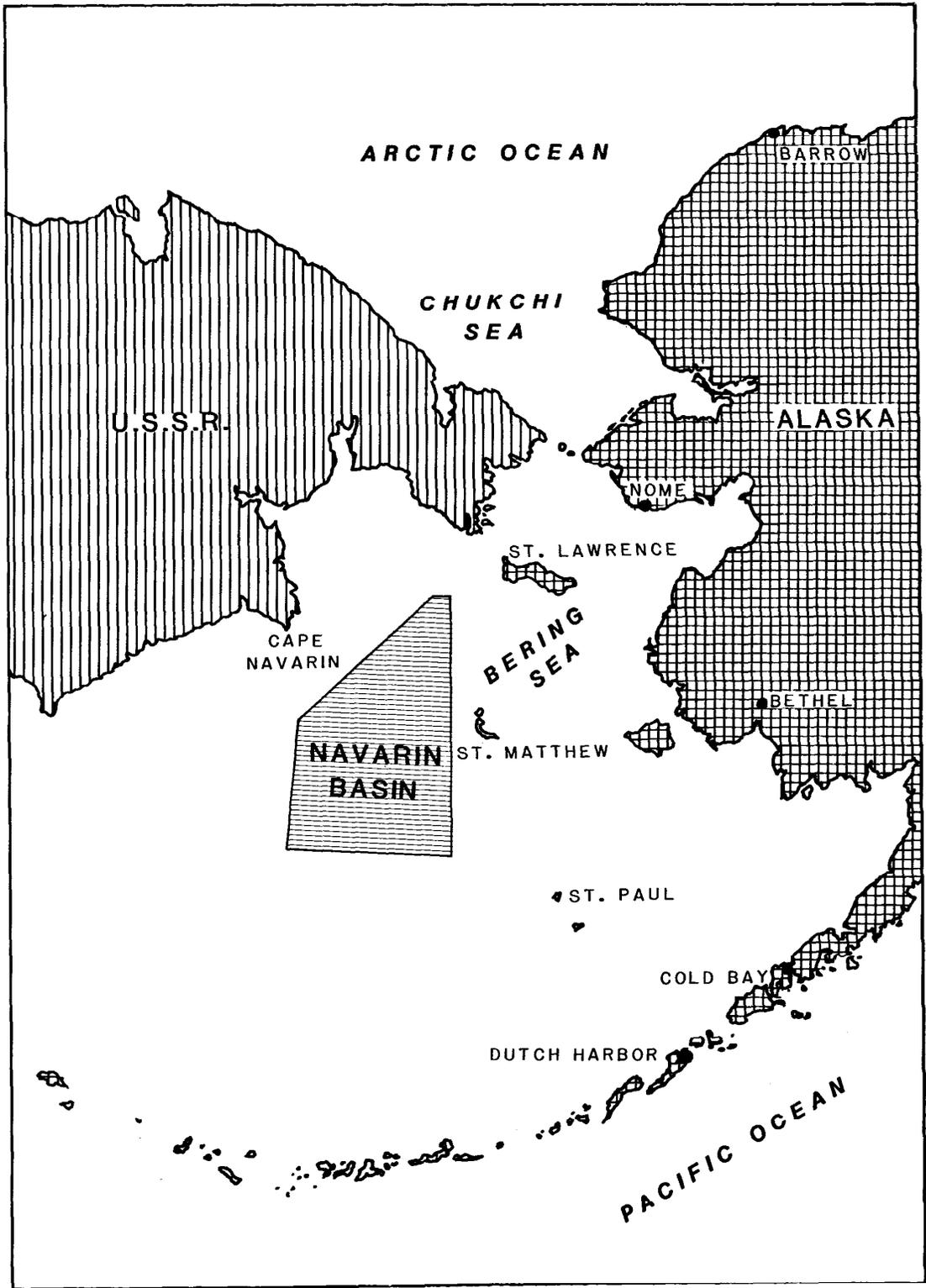
FIGURE 1. Location of Navarin Basin Planning Area.

NAVARIN BASIN

LEASE SALE 83
APRIL 1984

▥ BLOCKS RECEIVING
  BIDS IN SALE 83

■ BIDS REJECTED

⊗ COST NO. 1 WELL

▬ SALE AREA
  BOUNDARY

US-USSR CONVENTION OF 1867

USSR
US

63°

NP 1-4

NP 1-5

NP 1-6

NP 1-7

NP 1-8

NO 1-1

NO 1-2

0   50
         ⌐ MILES
SCALE 1:2,407,680

NO 1-3

NO 1-4   58°

180°   177°   174°
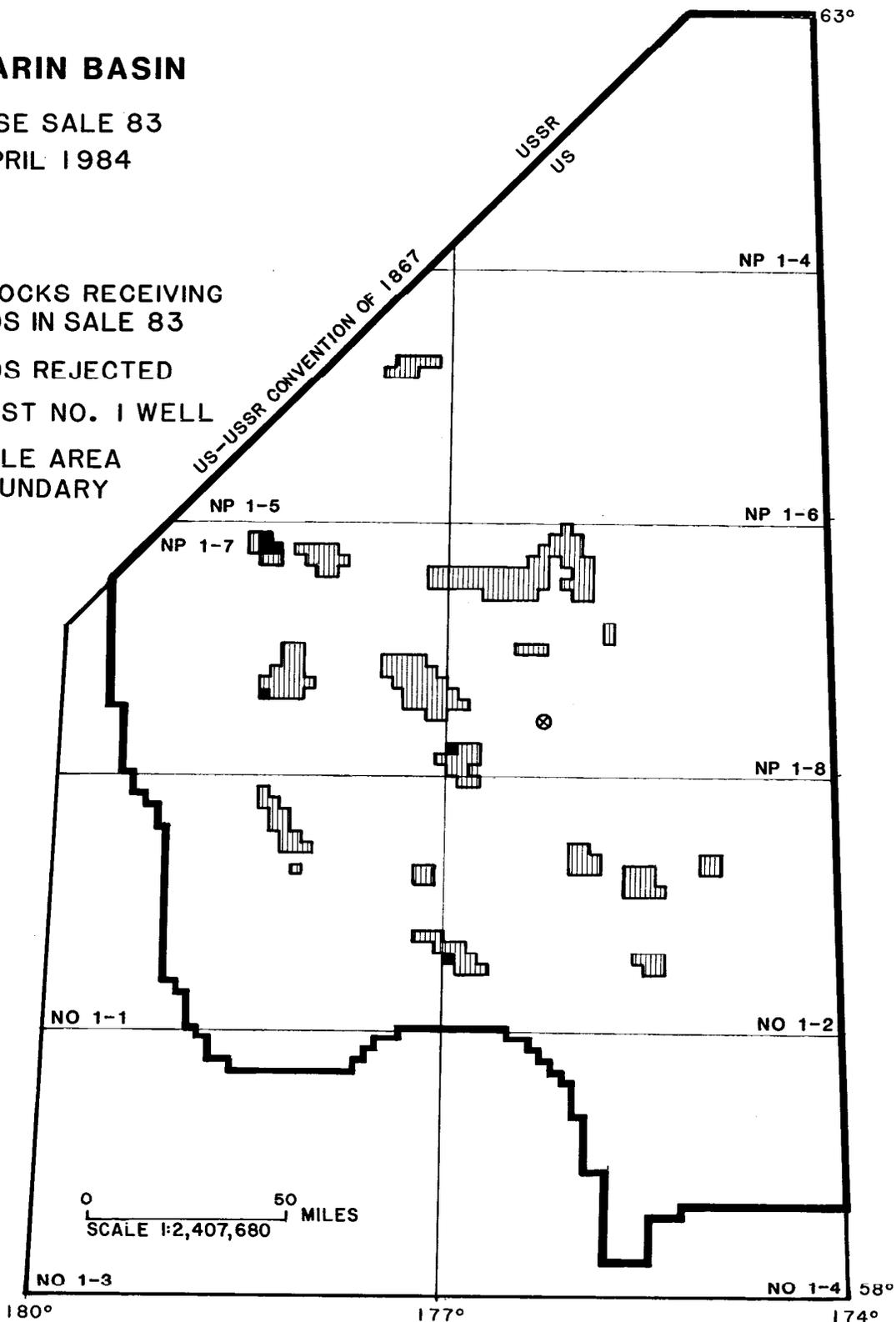
FIGURE 2. Lease Sale 83 bid history map.

exploration efforts in the basin. Maturity, migration, and timing do not appear to pose serious problems at this time.

The first Navarin Basin lease offering, Sale 83, was held by the Minerals Management Service (MMS) in April 1984 (fig. 2). A total of 5,036 lease blocks covering about 28 million acres were offered. Despite the remoteness of the area, 186 blocks covering about 1 million acres received $1.148 billion in total bids. High bids totaled over $631 million. The highest bid was over $39 million for a block on a large structure in the central part of the basin (approximately 25 miles northwest of the COST well). The first exploratory drilling is expected to take place in 1985.

I. Regional Geology

Geologic Framework

The Navarin Basin is one of five large Tertiary basins on the Bering Sea shelf (fig. 3). The basin covers an area approximately the size of the State of Maine (32,000 square miles), as delineated by the 7,000-foot structure contour on acoustic basement. The basin is bounded by the continental shelf break to the southwest, the Okhotsk-Chukotsk volcanic belt to the east and southeast, and the Anadyr Ridge, a basement high, to the northwest.

Marlow and others (1976) first recognized the basin as a site of significant Tertiary sedimentation. Subsequent seismic mapping has shown that the Navarin Basin consists of three en echelon subbasins filled with up to 36,000 feet of layered Tertiary sedimentary rocks; we have informally named these three subbasins the Navarinsky, Pervenets, and Pinnacle Island subbasins (fig. 16).

Fisher and others (1979) grouped areas with similar pre-Tertiary geology into regional lithostratigraphic provinces. The Navarin Basin lies within their forearc basin province. The Okhotsk-Chukotsk volcanic belt and a miogeoclinal belt represent the remaining pre-Tertiary provinces to the north.

FOREARC BASIN PROVINCE

Paleozoic and Mesozoic rocks composed of deep-water melange and olistostromes, mafic volcanics, and nonmarine and marine sediments may extend beneath the Tertiary forearc basins. The northern portion of the Koryak Range of eastern Siberia contains complexly juxtaposed slabs of olistostrome and melange sequences and ultramafic masses. These possibly allochthonous blocks are unconformably overlain by Paleozoic sedimentary rocks and Mesozoic volcanics or terrigenous deposits. Devonian through Permian limestones are also present (Meyerhoff, 1980; Marlow and others, Tectonic Evolution, 1983). The Anadyr Ridge is probably an offshore extension of the Koryak Range and defines the northern boundary of the Navarin Basin.

The Navarin Basin COST No. 1 well encountered Late Cretaceous nonmarine clastics and coals and marine clastics and tuff that may

EXPLANATION FOR FIGURE 3.

era	period	symbol	sedimentary	igneous
Cenozoic	Quaternary	Q		
Cenozoic	Tertiary	T		Tv
Mesozoic	Cretaceous	K	KPz	Kv
Mesozoic	Jurassic	J	KPz	KJ
Mesozoic	Triassic	Ŧ		
Paleozoic	Permian	P		
Paleozoic	Pennsylvanian	ℙ	POs	
Paleozoic	Mississippian	M	POs	
Paleozoic	Devonian	D	POs	
Paleozoic	Silurian	S		
Paleozoic	Ordovician	O		
Paleozoic	Cambrian	Є	OpЄ	
	Precambrian	pЄ	OpЄ	

Tv: undifferentiated volcanic rocks.

Kv: undifferentiated volcanic rocks.

KJ: lava, tuff, agglomerate, argillite, shale, greywacke, quartzite, and conglomerate. Slightly metamorphosed in places.

KPz: south of 64° N latitude sandstone, siltstone, limestone, chert, and volcaniclastic rocks of Permian through Late Cretaceous age. Locally includes melange and olistostrome sequences. North of 64° N latitude are sandstone, siltstone, argillite, conglomerate, coal, spilite, and basalt.

POs: sedimentary rocks of Permian and Mississippian age. Includes some Ordovician, Silurian, and Mississippian limestone.

OpЄ: phyllite, sandstone, siltstone, limestone, chert, and quartzite.

pЄ: undifferentiated metasedimentary and metamorphic rocks.

FIGURE 3. General geologic map of eastern Siberia, Bering Sea, and western Alaska. Major Tertiary basins and pre-Tertiary geologic provinces of Fisher and others (1979) are indicated. Adapted from Link and others (1960), Beikman (1980), and Marlow and others (Tectonic Evolution, 1983).

be correlative with USGS dredge samples of basement exposures along
the Navarin continental shelf and slope. The dredge samples include
Late Cretaceous sandy siltstone and sandstone, Late and Middle Jurassic
volcanic sandstone (table 1), and Late Jurassic shallow-water
arkosic sandstone (Marlow and others, 1979). Dredge samples from
the Pribilof Canyon included Late Cretaceous mudstones and
siltstones (McLean, 1979c), and the St. George COST No. 2 well
encountered Late Jurassic through Early Cretaceous nonmarine
clastics and coal (Turner and others, 1984). Late Jurassic to
Early Cretaceous siltstones and sandstones of the Naknek Formation
on the western end of the Alaska Peninsula may correlate with the
Late Jurassic sandstone and siltstone dredged from the Pribilof
Canyon (Vallier and others, 1980). The recovery of Late to Middle
Jurassic rock in dredge samples from the Zemchug Canyon and Navarin
continental slope suggests that the Naknek Formation (or a
chronostratigraphic equivalent) extends into the Navarin shelf
(Marlow and others, 1979; Turner and others, Navarin COST No. 1,
1984). This supports the contention of Marlow and others (1979;
Tectonic Evolution, 1983) that the basement rock in the Navarin
shelf is an extension of the Alaskan Mesozoic terrane and suggests
that the outer Beringian shelf is a single, continuous terrane.

OKHOTSK-CHUKOTSK VOLCANIC BELT

The Okhotsk-Chukotsk volcanic belt (fig. 3) is a continuous,
narrow zone of mostly upper Mesozoic volcaniclastic and associated
plutonic rocks. It lies to the west and north of the Koryak-Anadyr
fold belt, parallel to the Siberian coast. From the Siberian coast
the volcanic belt trends southeast and extends from the southern
Chukotsk Peninsula of eastern Siberia to the Yukon-Koyukuk province
of western Alaska (Belyi, 1973; Fisher and others, 1979). In the
Bering Sea, the volcanic belt encompasses western St. Lawrence
Island, St. Matthew Island, the Pribilof Islands, and Nunivak Island.
In western Alaska, the volcanic belt is correlative with a broad
zone of Cretaceous and early Tertiary volcanic and sedimentary
rocks that make up the Yukon-Koyukuk province and extend into the
Brooks Range (Patton, 1973; Fisher and others, 1979). Marlow and
others (1976) speculated that this belt is a magmatic arc associated
with the Late Cretaceous to early Tertiary oblique subduction of
the Kula plate at the Beringian margin.

MIOGEOCLINAL BELT

The miogeoclinal belt of Fisher and others (1979) is composed
of Precambrian, Paleozoic, and early Mesozoic sedimentary rocks.
This belt lies north of the Okhotsk-Chukotsk volcanic belt and
extends from the northern Chukotsk Peninsula and Wrangel Island
to the Seward Peninsula and into the Brooks Range (fig. 3). The
Siberian rocks are mostly Paleozoic and early Mesozoic carbonates

and nonvolcanics. The Brooks Range consists of Paleozoic carbonates and early Mesozoic sedimentary rocks. In the Bering Sea, the miogeoclinal belt is present in the central and eastern parts of St. Lawrence Island and on the Seward Peninsula (Patton and Dutro, 1969). A comprehensive description of the miogeoclinal geology of this area is given by Dutro (1981).

Introduction to Offshore Stratigraphy

The Navarin Basin is a true frontier area both in the sense that there has been virtually no exploration there, and in the fact that it is located in an exceptionally remote area characterized by a rigorous, subarctic marine environment. The nearest applicable geological exposures are outcrops in eastern Siberia. The nearest subsurface analog, if it truly is such, is the relatively poorly known Anadyr Basin, also in Siberia. Because of these factors, the offshore stratigraphy section of this report is based almost entirely on detailed analyses and interpretations of data from the ARCO Navarin Basin COST No. 1 Well. These data were then integrated with the seismic stratigraphy seen at the well site and extrapolated into the basin by means of correlation with regional seismic profiles. In essence, an area the size of the State of Maine is being evaluated using a stratigraphic column derived from a single well. This is the only reasonable approach, given the paucity of data.

The offshore stratigraphy is treated in three rather exhaustive chapters: Biostratigraphy, Lithostratigraphy, and Seismic Stratigraphy. The nature of the data dictates that each chapter approach an elucidation of the subsurface stratigraphy from a different perspective, each utilizing different "tools" with different powers of resolution. When possible, the stratigraphy is discussed in terms of geologic time, but defined lithologic zones, seismic sequences, and seismic reflectors are also commonly used. Plate 1 and figure 7 illustrate the various stratigraphic units and their relationships.

Most depths referred to in the Biostratigraphy and Lithostratigraphy chapters were measured from the COST well kelly bushing, which was 85 feet above sea level. Most depths in the Seismic Stratigraphy chapter were measured from sea level. Discrepancies between depths given for seismic horizons and depths for nearly equivalent lithologic and time-stratigraphic boundaries not attributable to datum differences (kelly bushing or sea level) are probably a result of differences in the vertical resolution of seismic, well log, and paleontologic techniques.

Biostratigraphy

The chronostratigraphic basis for correlations in the Navarin
Basin is the biostratigraphic, paleontologic, and paleoecologic
analysis of the sedimentary section penetrated by the Navarin Basin
COST No. 1 well (Turner and others, 1984). Age and environmental
determinations in the well were based on detailed analyses of
microfossil assemblages containing Foraminifera, ostracodes,
silicoflagellates and ebridians, diatoms, calcareous nannoplankton,
Radiolaria, and marine and terrestrial palynomorphs (dinoflagellates,
pollen, and spores). MMS personnel processed and examined rotary
drill bit samples (taken at 30-foot intervals) from the first
sample at 1,536 feet to the total depth of 16,400 feet. Data from
conventional and sidewall cores were also examined and used. In
addition, slides, processed samples, and reports prepared for the
participants by micropaleontological consultants (BioStratigraphics,
1983; ERT biostrat, 1983) were examined, interpreted, and integrated
into this report. Differences between consultant reports, principally
the location of biostratigraphic tops, appear to be due, in varying
measure, to philosophical differences concerning the taxonomy and
biostratigraphic significance of certain microfossils, to variations
in initial sample content, and to variations in microfossil content
caused by different sample preparation techniques.

The MMS biostratigraphic interpretation incorporated analyses
of megafossils recovered from conventional cores (Marks, 1983; E.
G. Kauffman, written commun., 1983), ostracode studies (Elizabeth
Brouwers, written commun., 1984), and identifications of the rare
planktonic Foraminifera in the well (Gerta Keller, written commun.,
1984). Foraminiferal identification and the synthesis of other
data were done by the author. Siliceous microfossil analysis was
done by Donald L. Olson, of the MMS Alaska OCS Region.

Strata are discussed in the order in which they were penetrated.
The integrated biostratigraphic units delineated were derived from
various micropaleontological subdisciplines that do not agree in
every biostratigraphic particular. Figure 4 summarizes the MMS
biostratigraphic and paleobathymetric interpretation. Figure 5 is
a comparison of the MMS interpretation with those of the two

ERA	PERIOD	EPOCH	AGE
		no data	
		PLIOCENE	late
	Neogene		early
		MIOCENE	late
CENOZOIC			middle to early?
	Paleogene	OLIGOCENE	late
			early
		EOCENE	late to middle?
MESOZOIC	Cretaceous	LATE CRETACEOUS	Maastrichtian
			?Campanian or older

Depth (feet below kelly bushing)

	NON-MARINE	INNER NERITIC (0-60 ft)	MIDDLE NERITIC (60-300 ft)	OUTER NERITIC (300-600 ft)	UPPER BATHYAL (600-1500 ft)	MIDDLE BATHYAL (1500-3000 ft)

1,000
1,536
2,000
3,000
4,000
5,000
6,000
7,000
8,000
9,000
10,000
11,000
12,000
13,000
14,000
15,000
16,000
16,400
TD

FIGURE 4.

Biostratigraphy and paleobathymetry of the Navarin Basin COST No. 1 well.
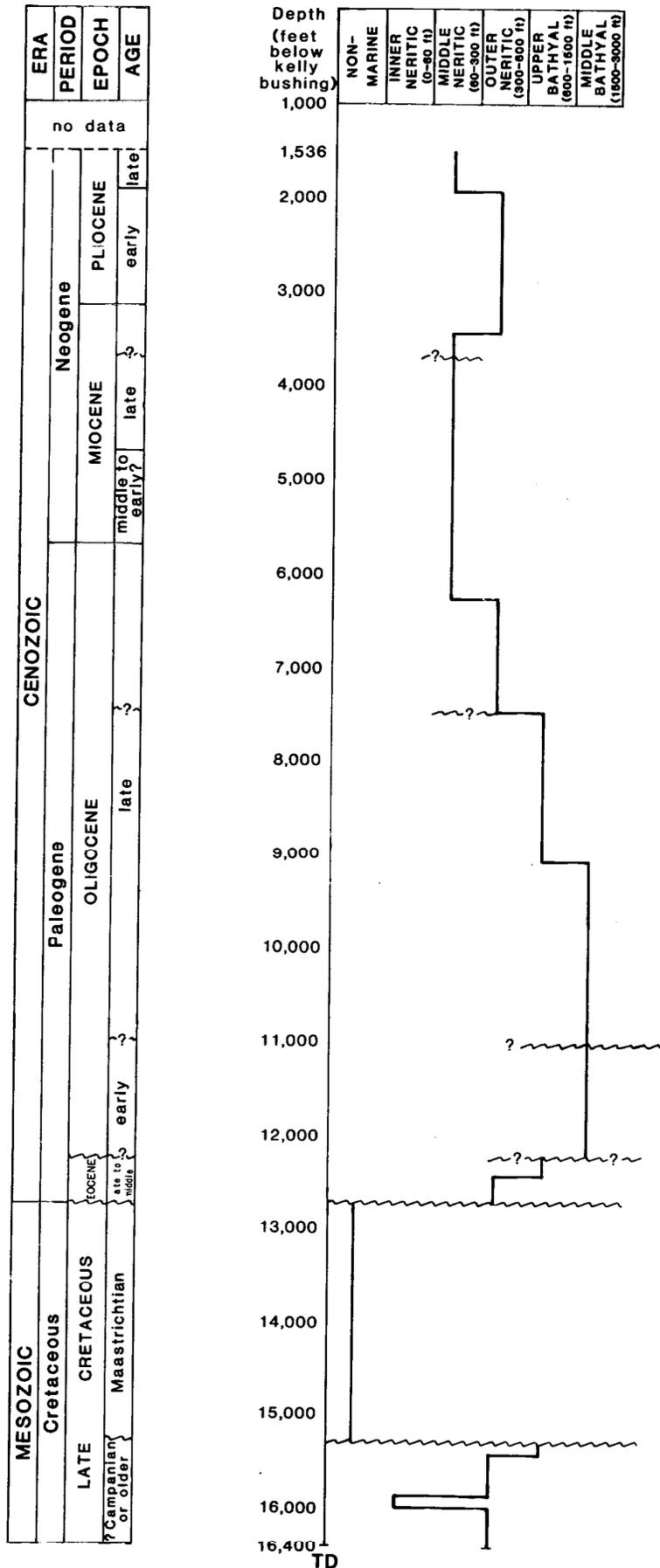
FIGURE 4. Biostratigraphy and paleobathymetry of the Navarin Basin COST No. 1 well.

14

consultants. It is unlikely that any of these three zonations represents the final word on the Navarin Basin biostratigraphy. Sample depths may disagree slightly with measured depths. Fossil occurrences are listed as highest and lowest rather than the potentially confusing first and last. Data obtained from conventional cores are given somewhat more weight than those from cuttings. Sidewall core data were not as reliable as usual because there was some trouble with uphole contamination from circulating drilling mud. The various lithologic zones and seismic sequences referred to in the text are discussed at length in the applicable sections of this report and at some length in the Navarin Basin COST well report (Turner and others, 1984). Regional correlation is discussed at the conclusion of this section.

Paleoenvironmental determinations are based on both microfossil and macrofossil suites. Paleoclimatological interpretations are based on spore and pollen assemblages and, to a lesser extent, on diatoms, silicoflagellates, Foraminifera, ostracodes, and molluscs. Fluvial, lacustrine, and paludal environments are classified as continental or nonmarine. Transitional environments include marshes, brackish estuaries, and hypersaline and hyposaline lagoons. For sediments deposited in marine environments, the paleoenvironment is expressed in terms of bathymetry (fig. 4) and is divided into inner neritic (0 to 60 feet), middle neritic (60 to 300 feet), outer neritic (300 to 600 feet), upper bathyal (600 to 1,500 feet), and middle bathyal (1,500 to 3,000 feet). Paleobathymetric determinations are primarily based on foraminiferal criteria, but dinoflagellates and other marine organisms such as bryozoans, molluscs, brachiopods, echinoids, ophiuroids, and cirripeds were taken into account. Lithological and sedimentological criteria were also used.

PLIOCENE

The Pliocene section of the well (1,536 to 3,180 feet) was subdivided into early and late ages primarily on the basis of diatom and silicoflagellate distributions. Although the siliceous microfloras were both abundant and diverse, the zonal subdivisions are somewhat tenuous. Even after factors such as reworking and up- and downhole contamination are taken into account, siliceous microfossil assemblages from the well are still characterized by unusual stratigraphic ranges and associations. Zonal equivalences were difficult to establish because "flagship taxa" were frequently either absent or out of place. That different taxonomic and zonal systems were used by the three siliceous microfossil investigators only compounded the problem. A provisional zonation was erected nevertheless.

The late Pliocene (1,536 to 1,920 feet) contains the middle and lower part of the Denticulopsis seminae var. fossilis Zone

2,000

3,000

4,000

5,000

6,000

7,000

8,000

9,000

10,000

11,000

12,000

13,000

14,000

15,000

16,000

16,400 T.D.

ERT biostrat (1983)

Pliocene

late Miocene

middle Miocene

late Oligocene

early Eocene

Late Cretaceous, Maastrichtian (12,854-12,875')

Late Cretaceous, ? Maastrichtian (13,143-16,400')

—1,536'
—3,420'
—6,300'
=?———?———?= 10,984'
10,993'
12,077'
12,171'
12,743'
12,854'
—16,400'

BioStratigraphics (1983)

late Pliocene

early Pliocene

late Miocene

prob mid to late Miocene
probable middle Miocene

possible early to middle Miocene. Oligocene?

Oligocene or Eocene to Oligocene

late Eocene to Oligocene

Late Cretaceous, Campanian to Maastrichtian

—1,536'
—1,920'
—3,180'
—4,260'
—4,440'
—4,710'
—5,790'
—12,750'
12,854'
—16,400'

MMS (this paper)

late Pliocene

early Pliocene

late Miocene
?—(NH6?)————

late Miocene

middle and early Miocene

late Oligocene

—?(TO2.2?) — — —

late Oligocene

—?(TO2.1?)——

early Oligocene, P21 Zone, Subzone a

? ——— ?—
late to late middle Eocene

Late Cretaceous, Maastrichtian

Late Cretaceous, probable Campanian(or Older?)

—1,536'
1,920'
—3,180'
—3,716'
—4,710'
—5,704'
—7,500'
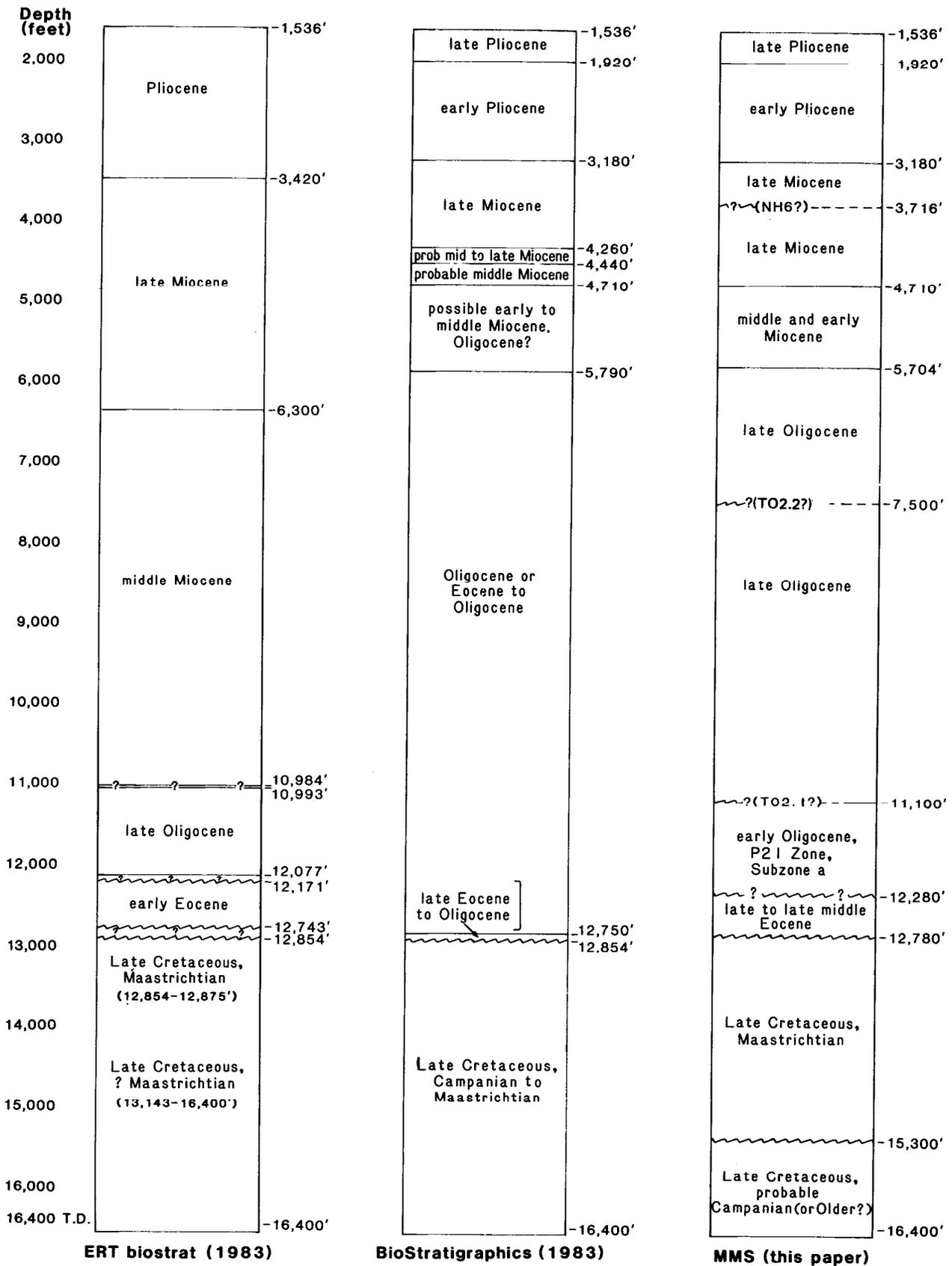—11,100'
—12,280'
—12,780'
—15,300'
—16,400'

FIGURE 5. Comparison of biostratigraphic summaries of ERT biostrat, BioStratigraphics, and Minerals Management Service. Depths are measured from the kelly bushing.

and the entire Denticulopsis seminae var. fossilis - Denticulopsis kamtschatica Zone. The former zone (1,536 to 1,710 feet) is characterized by the highest occurrences of Stephanopyxis horridus, Thalassiosira zabelinae, Coscinodiscus pustulatus, Rhizosolenia curvirostrus inermis, and Ammodochium rectangulare; the latter zone (1,710 to 1,920 feet) is somewhat more problematical, and is defined here by the highest occurrence of Thalassiosira antiqua and the lowest occurrence of Denticulopsis seminae var. fossilis.

The late Pliocene siliceous microflora contains at least 70 species, many of which have long or uncertain stratigraphic ranges. Genera present include Actinocyclus, Ammodochium, Arachnoidiscus, Aulacodiscus, Bacteriosira, Biddulphia, Coscinodiscus, Chaetoceros, Cladogramma, Cosmiodiscus, Delphineis, Denticulopsis, Distephanus, Ebriopsis, Grammatophora, Goniothecium, Hyalodiscus, Melosira, Navicula, Nitzschia, Porosira, Pseudopodosira, Pseudopyxilla, Rhaponeis, Rhizosolenia, Stephanopyxis, Thalassionema, Thalassiosira, Thalassiothrix, and Xanthiopyxis.

The early Pliocene (1,920 to 3,180 feet) is subdivided into Subzones b and c of the Denticulopsis kamtschatica Zone. Subzone c (1,920 to 2,550 feet) is defined by the highest stratigraphic occurrence of Thalassiosira nativa and the presence of common Denticulopsis kamtschatica and Ebriopsis antiqua. The top of Subzone b (2,550 to 3,180 feet) is defined by the highest occurrences of Cosmiodiscus insignis and Coscinodiscus temperei; the base is defined by the lowest occurrence of Thalassiosira oestrupii and the top of the subjacent zone.

The generic composition of the diverse early Pliocene microflora is similar to that of the overlying late Pliocene. Additional genera include Actinoptychus, Cocconeis, Cymatosira, Dictyocha, Diploneis, Endictya, Mesocena, Rhabdonema, Rouxia, and Stephanogonia.

The moderately diverse, though quite sparse, ostracode assemblage present from 1,536 to 3,180 feet indicates a Pliocene age for the interval (Elizabeth Brouwers, written commun., 1984). The late Pliocene (1,536 to 1,920 feet) contains specimens of Normanicythere leioderma, Eucytheridea bradyi, Acanthocythereis dunelmensis, ?Rabilimis sp. B, "Rabilimis" sp. A, and Robertsonites tuberculata. The early Pliocene ostracode fauna is similar, but also contains a single specimen of Australimoosella sp. at 2,070 feet. Several of these taxa were previously recorded in the Pliocene section of the Norton Sound COST No. 1 and No. 2 wells (Turner and others, 1983).

The Pliocene foraminiferal faunas are typical of high-latitude cold-water shelf environments. There are no truly age-diagnostic species in the assemblage. The late Pliocene fauna is characterized by Elphidium clavatum, Elphidium bartletti, Protoelphidium orbiculare, Elphidiella sibirica, Elphidiella cf. E. gorbunovi, Buccella frigida, Buccella tenerrima, Dentalina baggi, Dentalina soluta,

Pullenia sp., Poropullenia cf. P. bulloides, Cassidulina californica, Cassidulina laticamerata, Cassidulina teretis, Cassidulina norcrossi, Nonionella miocenica, Glandulina sp., Polymorphina sp., Quinqueloculina akneriana, and Epistominella cf. E. bradyi. Molluscan shell shards, barnacle plates, fish teeth and bones, echinoid and ophiuroid plates, and bryozoan fragments are common.

The early Pliocene foraminiferal fauna is essentially the same as that of the late Pliocene, with the addition of Trifarina angulosa, Marginulina cf. M. adunca, Melonis cf. M. barleeanum, Melonis cf. M. pompilioides, and Uvigerina juncea. Thin-shelled terebratulid brachiopods and rare vinculariiform bryozoan zoaria are also present.

The palynological assemblages present from 1,536 to 3,180 feet indicate a Pliocene age for the interval. The pollen and spore assemblage is characterized by Alnipollenites spp., Tsugaepollenites spp., Ulmipollenites sp., Caryapollenites sp., Pterocaryapollenites sp., Piceapollenites spp., Betulaepollenites spp., Liquidambarpollenites sp., Juglanspollenites sp., Malvaceae, Ericaceae, Onagraceae, Compositae, Quercus sp., Pinus spp., Pediastrum sp. (fresh-water algae), Jusseia sp., Diervilla echinata, Chenopodium leptophyllum, Deltoidospora spp., Lycopodiumsporites sp., Sphagnumsporites sp., Laevigatosporites spp., Stereisporites spp., Epilobium latifolium, and Cyathidites minor.

The dinoflagellate assemblage contains Tectatodinium pellitum, Spiniferites spp., Cymatiosphaera sp., Operculodinium sp., Kallosphaeridium sp., Lejeunia spp., Lejeunia fallax, Nematosphaeropsis labyrinthea, and Impagidinium pacificum. Reworked Cretaceous dinocysts are also present.

Judy Lentin, of ERT biostrat, recognized two palynological zones in the Pliocene section: the spore-pollen Laevigatosporites Zone of Geoffrey Norris (in preparation) and the dinoflagellate Impagidinium pacificum Zone of Bujak (1984). The former was developed by using well data from the Beaufort-Mackenzie Basin; the latter, from core hole data from Leg 19 of the Deep Sea Drilling Project in the Bering Sea.

Environment

The Pliocene section reflects shelf deposition in relatively cold water. The late Pliocene environment ranged from cold temperate to subfrigid. The early Pliocene was predominantly cold temperate. Water depths in the late Pliocene were middle neritic. The early Pliocene section was deposited in outer neritic depths.

MIOCENE

The interval from 3,180 to 5,704 feet is Miocene in age. This section is subdivided into several biostratigraphic zones, for the

most part on the basis of diatom and palynomorph distributions. In addition to the biostratigraphic problems discussed in the Pliocene section, the zonation of the Miocene is further complicated by barren intervals. Seismic horizon A is unconformable on the flanks of the basin; at the well site this reflector corresponds to the top of lithologic zone A-2 and to the top of a paleontologically barren interval beginning at 3,716 feet. Seismic horizon A may correspond in part to the NH6 hiatus of Barron and Keller (1982). There are significant differences of opinion between the various consultants and between the various subdisciplines concerning the position of the Miocene-Oligocene boundary.

The interval from 3,180 to 4,710 feet is late Miocene in age and is subdivided into the Denticulopsis kamtschatica Zone, Subzone a (3,180 to 3,670 feet), and the Denticulopsis hustedtii Zone (3,670 to 4,710 feet). The top of the Denticulopsis kamtschatica Zone, Subzone a, is defined by the highest occurrences of Goniothecium tenue and Rouxia californica; the base is defined by the top of the subjacent zone. There are approximately 170 siliceous microfossil species in this interval. Additional genera not present in the overlying Pliocene section include Asteromphalus, Dicladia, Dictyocha, Hemiaulus, Isthmia, Lithodesmium, Muelleriella, Rocella, Synedra, and Tetracyclus.

The top of the Denticulopsis hustedtii Zone is here defined by the highest occurrence of Thalassionema hirosakiensis and the lowest occurrence of Denticulopsis kamtschatica. The base of the zone is placed at 4,710 feet on the basis of the lowest occurrences of Coscinodiscus aff. C. endoi and Denticulopsis aff. D. hustedtii. The siliceous microflora in this interval is relatively diverse and abundant but very poorly preserved. The zone of mineralogical phase change from opal-A to opal-CT appears to begin at approximately 3,565 feet; the change from opal-CT to quartz appears to begin below 4,440 feet. These changes were qualitatively observable optically, although exhaustive X-ray diffraction analysis (AGAT, 1983; James Hein, oral commun., 1984; Maurice Lynch, written commun., 1984) failed to disclose unequivocal evidence for the presence or location of these diagenetic boundaries. Definitive peaks are not generally discernible on X-ray diffractograms when opaline silica is present in amounts of 5 percent or less. However, some sidewall and conventional cores below 3,600 feet contained sediments composed of more than 50 percent diatoms. This is discussed at some length in Turner and others (Navarin COST No. 1, 1984, p. 129-38).

The interval from 4,710 to 5,704 feet probably represents the middle and early Miocene. Most of the microfossils are too poorly preserved to be useful for detailed zonal biostratigraphy. The middle to early Miocene age determination is supported by the presence of Stictodiscus aff. S. kittonianus. Dean Milow, of BioStratigraphics, noted that in this interval, populations of Stephanopyxis turris sensu stricto are equal to or more abundant than those of Stephanopyxis

turris var. intermedia. He suggests that this relationship is typical of Neogene populations, whereas populations dominated by Stephanopyxis turris var. intermedia are restricted to the Paleogene.

The ostracode fauna is sparse and poorly preserved. Many of the species also occur in the Pliocene section. New taxa indicative of a Miocene age include "Costa" sp., "Leguminocythereis" sp., and Elofsonella aff. E. concinna.

Palynological evidence also supports a Miocene age for the interval from 3,180 to 5,704 feet, although in the Miocene section the palynological consultants begin to differ significantly both in taxonomy and in the placement of stratigraphic tops. This interpretive divergence continued until Late Cretaceous strata were encountered and described. Species of Tsugaepollenites occur as high as 3,090 feet (early Pliocene) but become progressively more abundant downhole. The highest occurrence of Tsugaepollenites alexandriana (3,420 feet) marks the top of the unpublished Miocene Tsugaepollenites Zone of Geoffrey Norris (in preparation). In the Navarin Basin COST No. 1 well, this pollen zone appears to more or less coincide with the unpublished dinoflagellate Spiniferites ovatus Zone of Bujak (1984). Dinoflagellates became more abundant and stratigraphically useful below 3,800 feet. Taxa present include Spiniferites ovatus, Spiniferites spp., Cannosphaeropsis spp., Hystrichosphaeropsis sp. A (Williams, 1975), Tuberculodinium vancampoae, Tuberculodinium rossignoliae, Cordosphaeridium gracilis, Pentadinium laticinctum, Achomosphaera alcicornu, Paralecaniella indentata, Operculodinium centrocarpum, Nematosphaeropsis balcombiana, Oligosphaeridium sp., Lejeunia fallax, and Lejeunia globosa.

Calcareous nannoplankton were of limited value in the well. A single specimen of Cyclicargolithus floridanus was recovered from cuttings composited over the interval 5,520 to 5,610 feet. It indicated an age range of middle Eocene to early middle Miocene. The upper part of the range is consistent with the evidence from other fossil groups.

The foraminiferal faunas support a Miocene age for the interval 3,180 to 5,704 feet. Foraminifera are rare above 3,400 feet. The most significant foraminiferal markers are the highest occurrences of Porosorotalia clarki at 3,450 feet and Ammonia japonica varianta (= Rotalia beccarii) at 5,280 feet. Other distinctive faunal elements are Elphidiella oregonensis, Elphidiella problematica, Elphidiella aff. E. discoidalis, Elphidiella cf. E. okhotica, Elphidiella cf. E. hannai, Cribroelphidium cf. C. crassum, Elphidium clavatum, Elphidium bartletti, Haplophragmoides trullissata, Haplophragmoides deformes, Uvigerina juncea, Uvigerina cf. U. hootsi, Bolivina advena, Sigmomorphina sp., Cassidulina californica, Cassidulina laticamerata, Cassidulina norcrossi, and Sphaeroidina bulloides variabilis.

The fauna is similar to that described from the Norton Sound COST No. 1 and No. 2 wells, but may represent a somewhat deeper water depositional environment. The Navarin Basin Miocene foraminiferal fauna does not appear to have as close affinities with the Sakhalin Island and Kamchatka Peninsula assemblages as do those from the Norton Basin wells. Conflict between the published and unpublished biostratigraphic ranges of high-latitude Foraminifera is a problem that is compounded by the large amount of taxonomic synonymy in the American, Russian, and Japanese northern Pacific literature. These complications add immeasurably to the difficulty of biostratigraphic correlation in this area.

Molluscan fossils recovered from core 4 (5,572 to 5,580 feet) indicate a Miocene age. Bivalve taxa identified were _Macoma?_, _Tellina?_, and a cardiid.

Environment

The upper part of the Miocene section was deposited in outer neritic depths; below 3,450 feet the paleoenvironment was middle neritic. The climate was probably temperate to cold temperate.

OLIGOCENE

Oligocene strata (5,704 to 12,280 feet) represent the thickest sedimentary section in the Navarin well. The top of the Oligocene is placed at the highest occurrence of diatom populations composed entirely of poorly preserved _Stephanopyxis turris_ var. _intermedia_. Although this evidence alone does not warrant a firm age assignment, taken in conjunction with the palynological assemblage at 5,790 feet, it is quite defensible. The base of the Oligocene (12,280 feet) is placed at a lithologic boundary (zone F) that marks an apparently unconformable contact with Eocene strata.

The section is paleontologically subdivided into late Oligocene (5,704 to 11,100 feet) and early Oligocene (11,100 to 12,280 feet). The boundary between lithologic zones D-2 and E (10,800 feet; pl. 1 and fig. 7), as well as the unconformity on the basin flanks that correlates with the reflector at 11,100 feet (figs. 4, 7, and 8), may both be related to a mid-Oligocene drop in sea level caused by a global cooling event 28 to 32 million years ago (Keigwin and Keller, 1984). This event is characterized by cooler oceanic water and is thought to be associated with an accumulation of continental ice in the Antarctic (Matthews and Poore, 1980; Kerr, 1984). The early Oligocene paleontologic top (11,100 feet) is correlative with the top of seismic sequence IV (seismic horizon C), which onlaps and truncates older strata and basement highs. Seismic sequence IV grades into apparent proximal turbidites on the southwestern flanks of the Pinnacle Island subbasin. Lithologic zone E is within the lower part of the _Globorotalia opima_ Zone

(P21 Zone, Subzone a) of Bolli (1957) and Blow (1969), as defined
by Keller (1983). The early Oligocene age assignment is based
primarily on planktonic foraminiferal data.

The abundant and diverse late Oligocene dinoflagellate assemblage
is characterized by Paleocystodinium benjaminii, Paralecaniella
indentata, Diphyes spp., Lejeunia fallax, Lejeunia hyalina,
Lingulodinium pugiatum, Evittosphaerula paratabulata, Operculodinium
centrocarpum, Hystrichokolpoma rigaudiae, Apteodinium australiense,
Achomosphaera spp., Nematosphaeropsis balcombiana, Rottnestia
borussica, Tuberculodinium vancampoae, Tuberculodinium rossignoliae,
Membranilarnecia ursula, Polysphaeridium pastielsii, Areoligera
senonensis, Spiniferites spp., Distatodinium craterum,
Phthaneroperidinium amoenum, and Cordosphaeridium multispinosum.

There are ecotypic variants of species of Paleocystodinium
that resemble Paleocystodinium benjaminii. If the specimens
present in samples from the Navarin well represent such forms, the
degree of certainty about the precise location of the Oligocene-
Miocene boundary is lessened considerably.

The range of Tuberculodinium vancampoae in Alaska has also
been questioned. One school of thought considers it to be a
Miocene marker; another considers it to be more typical of the
Oligocene. Williams and Bujak (1977) show it ranging from the
"middle" Oligocene to the Pleistocene on the Labrador shelf of
eastern Canada. Harland (1978) shows it ranging from the early
Miocene into the Holocene on the northwestern European shelf.
Wall and Dale (1971) have placed Holocene cysts assignable to
Tuberculodinium vancampoae in the modern genus Pyrophacus, and
Lentin and Williams (1977) list Tuberculodinium vancampoae as a
Pleistocene species. In the St. George Basin COST No. 1 and No. 2
wells, Tuberculodinium vancampoae was present in strata dated as
Oligocene on the basis of calcareous nannoplankton. In the Norton
Sound COST No. 1 and No. 2 wells, this species was a common element
of the Miocene marine microflora. Recent discussions with
approximately 20 palynostratigraphers from all parts of the globe
suggest that although this taxon may actually range back into the
late Eocene, it is generally abundant only in the Miocene.

The spore and pollen assemblage is similar to the overlying
Miocene Tsugaepollenites assemblage.

Foraminifera are relatively abundant, diverse, and well preserved
in the Oligocene section. With the exception of the definitive
early Oligocene planktonic assemblage, however, most of the species
present are not strictly age diagnostic. Although benthic Foraminifera
were important for paleoenvironmental determinations, there are some
ambiguities involving the paleobathymetric significance of Ammonia
and Cyclammina. The late Oligocene section (5,704 to 11,100 feet)
contains both neritic and bathyal assemblages. Ammonia japonica

(= Rotalia beccarii and several ecotypic varieties), generally considered a shallow-water species, is present in both environments. This suggests either a wider bathymetric range than commonly assumed or a depositional environment characterized by downslope mixing. The latter case is the most likely, although the relatively consistent presence of the species in deeper water deposits in other Bering Sea wells suggests that it may not have always been restricted to inner neritic and transitional environments. Ammonia japonica and Ammonia japonica varianta were both recorded from near the top of the section considered to be Oligocene in both Norton Sound COST wells; they were also present in the Oligocene of both St. George Basin COST wells (Turner and others, 1984). In the St. George Basin COST No. 1 well, the section was unequivocally dated as Oligocene on the basis of calcareous nannoplankton. In the Navarin Basin well, the highest occurrence of Ammonia japonica varianta is early Miocene. In most of the Bering Sea wells it has usually been encountered somewhat below the highest occurrence of Porosorotalia clarki.

Although Cyclammina is a dominantly bathyal genus in modern and ancient seas, Robinson (1970) showed that in the Gulf of Mexico it commonly ranged up into shelf depths as recently as late Miocene. In the Norton Sound COST No. 2 well, Cyclammina cf. C. pacifica was present in shelf sediments. The highest occurrence of the genus in the Navarin Basin COST No. 1 well (5,400 feet, middle and early Miocene) was in sediments deposited in less than bathyal depths.

Other foraminiferal species present in the late Oligocene include Elphidiella oregonensis, Elphidiella cf. E. katangliensis, Elphidiella spp., Elphidium spp., Ammonia spp., Porosorotalia clarki, Porosorotalia cf. P. tumiensis, Psammosphaera carnata, Cassidulina cf. C. laevigata, Haplophragmoides trullisata, Haplophragmoides transluscens, Cyclammina cf. C. cancellata, Cyclammina japonica, Cyclammina spp., Budashevaella spp., Melonis pompilioides, Melonis cf. M. barleeanum, Gyroidina orbicularis planata, Gyroidina soldanii, Anomalina glabrata, Cassidulinoides bradyi, Sphaeroidina bulloides variabilis, Bathysiphon spp., Martinottiella pallida, Silicosigmoilina sp., Pullenia sp., Pseudoglandulina inflata, Eponides spp., and Sigmomorphina schencki. The presence of Globigerina cf. G. ciperoensis at 8,100 feet suggests that at least the lower part of this section is within the P22 planktonic zone.

The early Oligocene section (11,100 to 12,280 feet) contains, in addition to most of the above species, Fissurina sp., Pyrgo sp., Gyroidina sp., Oridorsalis sp., and Cornuspira cf. C. byramensis. The most distinctive faunal elements are age-diagnostic planktonic species such as Globigerina linaperta, Globigerina angiporides, Globigerina cf. G. officinalis, Globigerina cf. G. senilis, Globigerina praebulloides, and Catapsydrax pera that are

present from 11,110 to 11,850 feet. This interval is early Oligocene (P21 Zone, Subzone a) in age (Gerta Keller, written commun., 1984). A reworked specimen of the middle Eocene species Globorotalia bullbrooki was also present at 11,120 feet.

Ostracodes are rare but interesting in the late Oligocene section. With the exception of "Hemicythere" sp., the few specimens recovered above 9,090 feet are similar to those in the overlying Miocene. Below 9,090 feet, several additional genera with Paleogene affinities are present, including Krithe sp., ?Pectocythere sp., "Leguminocythereis" sp., "Robertsonites" sp., and Wichmanella sp. Of these, the latter genus is of particular interest. Wichmanella has heretofore been found in the Cretaceous of eastern South America and the Neogene of Japan. It probably migrated via straits bisecting the isthmus of Panama into the Pacific, then north and west, appearing first in the Alaskan Paleogene, then in the Japanese Neogene (Elizabeth Brouwers, written commun., 1984).

The early Oligocene ostracode fauna includes Wichmanella sp., Xestoleberis sp., Krithe sp., Eucytherura sp., ?Buntonia sp., ?Spinileberis sp., and "Patagonacythere" sp.

Calcareous nannoplankton are rare and nondiagnostic in the Oligocene section. A single specimen of the very long ranging species Braarudosphaera bigelowi was recovered from samples composited over the interval 6,240 to 6,330 feet.

Isolated molluscan specimens were recovered from cores 9, 10, and 11 in the late Oligocene section. The best age determination was "post-Eocene." Taxa present include the bivalves Macoma? sp. and Lucinoma acutilineata, and an unidentified gastropod. Rare molluscan and arthropod fossils were recovered from core 13 in the early Oligocene section. Possible solenid and tellinid bivalves, Ostrea? sp., the gastropod "Buccinum?" sp., and a crab claw were identified between 11,707 and 11,711 feet. On the basis of this macrofossil data, Marks (1983) considered the depositional environment to have been outer neritic to bathyal in a temperate or warm sea with rather low bottom temperatures. This interpretation fits that derived from microfossils.

Environment

The upper part of the Oligocene section (5,704 to 6,300 feet) was deposited in a middle neritic environment, possibly shallower. There is some calcareous nannoplankton evidence that suggests reduced salinity or a freshwater influence in this interval. From 6,300 to 7,500 feet the depositional environment was probably outer neritic. The base of seismic sequence II (seismic horizon B, at approximately 7,400 feet) marks a regressive event that may represent the third-order sea level drop TO2.2 of Vail and others (1977). The basal part of seismic sequence II represents the

first marine transgression to extend substantially beyond the
structurally defined margins of the basin. The interval from
7,500 to 9,100 feet was deposited in upper bathyal depths. The
interval from 9,100 to 12,280 feet was probably deposited, for the
most part, in middle bathyal depths. Paleontological evidence for
the mid-Oligocene sea level drop (TO2.1 of Vail and others, 1977)
is subtle. There is a rather sharp reduction in faunal diversity
between 11,100 and 11,300 feet that coincides with the top of the
interval containing early Oligocene planktonic Foraminifera. This
diversity decrease may mark the eustatic event more precisely than
either the lithologic boundary between zones D-2 and E or the top
of seismic sequence IV (seismic horizon C). Given the different
parameters being defined and differences in resolution, all of
these "boundaries" may reflect the same suite of related events.

The overall Oligocene paleoclimate was probably temperate to
warm temperate.

EOCENE

A 500-foot-thick Eocene section is present from 12,280 to
12,780 feet. The upper contact appears to be unconformable on the
basis of a combination of well log, lithological, and geochemical
criteria, but there is no geophysical evidence for an unconformity.
The lower unconformable contact is defined by strong seismic
evidence as well as the above criteria. Lithologic zone F appears
to represent the entire Eocene section present in the well. There
is no compelling geochemical evidence for large amounts of missing
section at either unconformity. There is some disagreement between
foraminiferal and palynological ages. The Foraminifera present
tend to suggest a late Eocene age; the dinoflagellates indicate a
slightly earlier age. If the foraminiferal age is correct, the
Eocene-Oligocene unconformity could be either minor or nonexistent.
The paleobathymetry tends to suggest continuous deposition across
the epoch boundary. The interval is assigned a late to late middle
Eocene age.

The marine palynomorph assemblage is characterized by
Areosphaeridium diktyoplokus, Apectodinium homomorphum,
Operculodinium centrocarpum, Micrhystridium sp., Paralecaniella
indentata, Lejeunia hyalina, and Impletosphaeridium insolitum.
The overlapping ranges of Areosphaeridium diktyoplokus and
Apectodinium homomorphum (as shown by Williams and Bujak, 1977)
support a late middle Eocene age.

The foraminiferal fauna is similar to that seen in the
overlying Oligocene. The fauna includes Globobulimina ilpinica,
Bulimina cf. B. lirata, Bulimina cf. B. pupoides, Pullenia eocenica,
Sigmomorphina undulata, Eponides spp., Cibicides sp., Nuttallites
sp., Gyroidina sp., Melonis pompilioides, Bathysiphon spp.,

<u>Rhabdammina</u> sp., <u>Martinottiella palida</u>, <u>Ammobaculites</u> sp.,
<u>Trochammina</u> sp., <u>Haplophragmoides</u> spp., <u>Cyclammina</u> spp., <u>Elphidiella</u>
cf. <u>E</u>. <u>californica</u>, <u>Porosorotalia tumiensis</u>, <u>Ammonia japonica</u>,
<u>Pyrgo</u> sp., and <u>Globocassidulina globosa</u>.

No molluscs, ostracodes, siliceous microfossils, or calcareous
nannoplankton were identified in the Eocene section.

Environment

The depositional environment was upper bathyal from 12,280
to 12,450 feet and outer neritic from 12,450 to 12,780 feet. The
paleoclimate was probably temperate or warmer.

CRETACEOUS

The interval from 12,780 to 16,400 feet is Late Cretaceous in
age on the basis of both marine and nonmarine fossils. The rocks
beneath the angular unconformity (seismic horizon D) that defines
the top of the section are nonmarine from 12,780 to 15,300 feet
(combined lithologic zone G/H) and marine from 15,300 to 16,400
feet (lithologic zone I). The contact between the marine and
nonmarine sections appears to be unconformable on the basis of
paleontological, lithological, and well log criteria. Diabase
sills radiometrically dated (K-Ar) as early Miocene by Teledyne
Isotopes (1983) are intercalated with the coal and siltstone beds
of the nonmarine section.

The nonmarine section (12,780 to 15,300 feet) is Maastrichtian
in age on the basis of the pollen <u>Aquilapollenites</u> <u>parallelus</u> and
<u>Manicorpus</u> cf. <u>M</u>. <u>trapeziforme</u>.

The marine section (15,300 to 16,400 feet) is probably
Maastrichtian or Campanian (or older) in age. Foraminifera present
include <u>Praebulimina kickapooensis</u>, <u>Praebulimina venusae</u>, <u>Praebulimina</u>
<u>carseyae</u>, <u>Gavelinella whitei</u>, <u>Gyroidinoides nitidus</u>, <u>Gyroidinoides</u>
<u>goudkoffi</u>, <u>Haplophragmoides excavatus</u>, <u>Haplophragmoides incognatus</u>,
<u>Nodosaria</u> sp., <u>Dentalina</u> spp., <u>Pullenia cretacea</u>, <u>Saccammina</u> sp.,
<u>Silicosigmoilina californica</u>, <u>Saracenaria</u> cf. <u>S</u>. <u>triangularis</u>,
and <u>Osangularia cordieriana</u>. The foraminiferal fauna is similar
to the ?Campanian to Maastrichtian assemblage identified from the
Lower Cook Inlet COST No. 1 well (Wills and others, 1978).

A single specimen of the calcareous nannoplankton <u>Zygodiscus</u>
cf. <u>Z</u>. <u>acanthus</u> is present in samples composited over the interval
from 15,300 to 15,390 feet. This species indicates a Late Cretaceous
(Maastrichtian or Campanian) age.

Rare, poorly preserved pseudoaulophacid Radiolaria were recovered
from core 19 (15,500 feet). These specimens suggest a Cretaceous age.

Rare Inoceramus prisms, both in situ and reworked, were present throughout the Cretaceous section. In addition, a single valve from an inoceramid bivalve was recovered from core 20 (16,316 feet). The specimen was identified by E. G. Kauffman (written commun., 1983) as a species of Platyceramus, a genus that ranges from the Coniacian to the Campanian. The specimen compared most closely with Coniacian to Santonian species. It is possible that the strata at the bottom of the well could be that old. Palynomorphs from the marine section below the unconformity at 15,300 feet have been thermally degraded and yield no definitive age older than ?Campanian to Maastrichtian. There are nearby dredge sample data that indicate the presence of older Cretaceous rocks in the immediate area. Paleomagnetic data, however, tend to support an age of no older than Campanian at total depth.

Environment

The nonmarine section (12,780 to 15,300 feet) probably represents a fluvial-paludal floodplain system. The marine section (15,300 to 16,400 feet) was deposited in inner neritic to upper bathyal depths. Both faunal and geochemical evidence (kerogen profile) suggests several transgressive-regressive cycles in the Late Cretaceous marine section. The paleoenvironment of the interval from 15,300 to 15,400 feet was upper bathyal. From 15,400 to 15,840 feet the environment was dominantly outer neritic, perhaps occasionally shallower, with a considerable amount of terrigenous organic input. From 15,840 to 15,960 feet the environment was probably inner neritic. From 15,960 to 16,400 feet the paleobathymetry was probably outer neritic.

The Late Cretaceous paleoclimate was probably warm temperate, possibly subtropical.

CORRELATION

The Navarin Basin COST No. 1 well can be correlated with the other Bering Sea deep stratigraphic test wells in a very general way. The Neogene section, in particular, is similar to that seen in the two Norton Sound and two St. George Basin COST wells. In all of these, the Neogene biostratigraphy was based on zones primarily defined by siliceous microfossils. Foraminifera were of more use for paleoenvironmental determinations, although there were some age-diagnostic species present in the early Miocene sections. Ostracodes proved to be surprisingly useful for both paleoecology and biostratigraphy. Neogene palynological zonations are still in the developmental stage in the Bering Sea area, and calcareous nannoplankton have proven to be of very limited utility in this section. Nevertheless, the Neogene sections of these five deep stratigraphic test wells can be correlated with some degree of confidence.

Paleogene correlations are far more difficult to establish. In particular, there is disagreement among industry, academic, and government biostratigraphers as to the nature and extent of Oligocene strata in the Bering Sea area. Much of the confusion stems from correlation with Russian onshore sections on the Kamchatka Peninsula and Sakhalin Island that were initially described as Miocene but are now considered to be, in part, Oligocene (Gladenkov, 1980). The ages of Paleogene foraminiferal and palynological assemblages are often the subject of dispute. Siliceous microfossils are difficult to work with in the older sections because they have generally been diagenetically replaced by pyrite. Calcareous nannoplankton and planktonic Foraminifera yield the best information, but neither group is consistently present.

The Oligocene foraminiferal assemblage of the Navarin Basin COST No. 1 well is somewhat similar to assemblages described from the Norton Sound and St. George Basin deep stratigraphic test wells, from the Kamchatka Peninsula and Sakhalin Island, and from the Poul Creek Formation (offshore) in the Gulf of Alaska. There are significant differences, however, such as the absence of the diverse shallow-water assemblages seen in the Norton Sound COST No. 1 well (which were quite similar to Sakhalin Island assemblages), and the absence of the Caucasina assemblages seen in Eocene and Oligocene strata in other Bering Sea wells and in the Eocene of the Kamchatka and Ilpinsky Peninsulas. Some of the correlation problems are facies related; others are attributable to the present imperfect knowledge of species ranges.

Palynological zonations are particularly tenuous in the late Oligocene because many key dinoflagellate species range into the early Miocene. It is also likely that the influence of facies on marine palynofloral assemblages is as significant as it is on foraminiferal assemblages. Oligocene ranges for some dinoflagellate species seen in the Navarin and Norton wells have been confirmed by calcareous nannoplankton data from the St. George Basin wells.

The Eocene section of the Navarin well may be in part correlative with the Eocene section in the St. George Basin COST No. 1 well, though there are few similarities between the faunas or floras. The possibly equivalent Eocene sections in the St. George Basin No. 2 and Norton Sound No. 1 wells were dominantly nonmarine or contained no age-diagnostic microfossils. The Eocene section in the Norton Sound No. 2 well was deposited in transitional to continental environments and yielded no marine palynomorphs.

The Navarin Basin Eocene foraminiferal fauna contains some species found in Russia (Globobulimina ilpinica, Ammonia japonica, Porosorotalia tumiensis) and others characteristic of deep-water deposits around the north Pacific rim. The presence of Globocassidulina globosa indicates a somewhat younger age for the section (late Eocene) than do dinoflagellates (late middle Eocene).

The Neogene and upper Paleogene sedimentary section in the Navarin Basin COST No. 1 well can be considered a deeper water analog of the basin fill described in the Khatyrka Basin and the southeastern part of the Anadyr Basin (McLean, 1979a; Gladenkov, 1980; Marlow and others, Tectonic Evolution, 1983). Dredge sample and seismic reflection data suggest that there is more Eocene (and probable Paleocene) section in the deeper parts of the subbasins than was encountered in the Navarin well. Dredge sample L5-78-(22-4) (table 1), for instance, contained a dinoflagellate assemblage of Paleocene (Danian) age (Jones and others, 1981; Rosemary Jacobson, written commun., 1984).

There are no correlative Late Cretaceous strata in the St. George Basin or Norton Sound COST wells. Pollen from the nonmarine Maastrichtian section of the Navarin well (12,780 to 15,300 feet) are similar to those described by Jones and others (1981) from sample L5-78-(27-1) dredged from the nearby Bering Sea continental margin, although the dredge sample was far more marine in aspect and contained a Late Cretaceous dinoflagellate assemblage. A reinvestigation of this dredge sample yielded a significant recycled assemblage of Albian to Santonian age dinoflagellates (Rosemary Jacobson, written commun., 1984). This recycled component was also present in the nonmarine Maastrichtian section of the well. There is little doubt that the rocks dredged from the continental margin represent a marine facies of the Maastrichtian strata penetrated by the well.

Dredge sample L5-78-(27-2), from the same general location as L5-78-(27-1), contained volcaniclastic sandstone and tuff. Rosemary Jacobson (written commun., 1984) identified a poorly preserved ("corroded and mineral-scarred") assemblage of marine and nonmarine palynomorphs of ?Cenomanian to Turonian age mixed with recycled Albian elements. Thin lenses of very similar tuff are present in core 20 associated with a Platyceramus shell dated as possible Campanian to Coniacian. This "correlation" is far more tenuous than that with sample L5-78-(27-1). Nevertheless, these data do lend support to the concept of a section of Late Cretaceous rocks below the unconformity at 15,300 feet that is older than Maastrichtian. The foraminiferal assemblages from 15,300 to 16,400 feet are similar to those described from the ?Campanian to Maastrichtian section of the Lower Cook Inlet COST No. 1 well (Wills and others, 1978).

The Late Cretaceous section contains faunal and floral elements found in marine and nonmarine rocks of the Impenyeyen suite of the Koryak Highlands of eastern Siberia (Dundo, 1974; Korotkevich, 1974) and in Late Cretaceous wells and outcrops from south central and western Alaska. Paleomagnetic data from conventional cores (Van Alstine, 1983) suggest that although the Cenozoic section was deposited within 5° of the present well site, the Late Cretaceous section may have been deposited as much as 50° south of the present location. The polarity data also suggest that the Late Cretaceous

section was deposited during the Maastrichtian and Campanian. The presence of recycled carboniferous spores in Mesozoic well samples can be most easily explained by transport into the basin from eroding Paleozoic rocks in eastern Siberia or Alaska (fig. 3).

Lithostratigraphy

The offshore lithostratigraphy of the Navarin Basin is based chiefly on well log and lithologic data from the Navarin Basin COST well and the integration of these data with common-depth-point (CDP) seismic reflection data. Turner and others (1984) provide the most extensive published stratigraphic summary of the No. 1 well, and much of the following discussion is based on their report.

The ARCO Navarin Basin COST No. 1 Well was drilled to a depth of 16,400 feet and penetrated approximately 12,800 feet of Neogene and Paleogene clastic sediments, and over 3,000 feet of Cretaceous clastic sediments intercalated with Miocene diabase and basalt sills. The Tertiary-Cretaceous boundary is represented by a diachronous angular unconformity that also marks acoustic basement in the Navarin Basin.

Strata in the COST well are divided into 11 informal lithostratigraphic zones based on lithologic, petrophysical, and diagenetic characteristics determined from electric logs, conventional and sidewall cores, and rotary-drill-bit cuttings (pl. 1). The lithologic zones are composed of genetically related facies, but several of the zones are further subdivided where significant lithologic or diagenetic facies differences exist within them. Lithologic zones in the following discussions are described by age and order of penetration in the COST well. Most depths referred to in this section were measured from the COST well kelly bushing, which was 85 feet above sea level.

PLIO-PLEISTOCENE

The Plio-Pleistocene section of the COST well (measured from the first sample) is over 1,640 feet thick and comprises all but the bottom 385 feet of lithologic zone A-1 (pl. 1). Sediments from this section of the well consist of poorly sorted, silty, sandy mudstone and diatomaceous ooze deposited in a mid-shelf environment. Primary sedimentary structures were destroyed by extensive bioturbation. Concentrations of granule-sized rock and shell fragments are associated with scour surfaces. Coarser grained

material may represent basal lag deposits on erosional surfaces created by storm-generated currents. The framework grains are mainly volcanic lithic fragments, angular quartz, and feldspars. Diatom and clay matrix content ranges from 50 to 80 percent. Most of the diatom fragments are broken and angular. Lithic components are dominantly basaltic and intermediate volcanic fragments, with secondary amounts of glauconite, metamorphic rock fragments, mica, chert, and clay. Accessory minerals include hornblende, epidote, apatite, and pyroxene. Diagenetic processes included compaction, weak alteration and dissolution of lithic fragments, and development of authigenic pyrite, clinoptilolite, and chlorite. Porosity and permeability have not been significantly altered by diagenesis at these shallow depths.

MIOCENE

The Miocene section of the COST well is about 2,520 feet thick and comprises the lower 385 feet of zone A-1, all of zones A-2, B, and C-1, and the upper 340 feet of zone C-2 (pl. 1). The uppermost Miocene section occurs within lithologic zone A-1, which is lithologically identical to the Plio-Pleistocene section. Zone A-2 (295 feet thick) is characterized by increased diagenesis and cementation of zone A-1 sediments. Below zone A-2, the opaline silica that originally made up the abundant diatom fraction of the sediment has been largely altered to clinoptilolite. Opal-CT (cristobalite-tridymite) was not identified by scanning electron microscopy, but was identified in trace amounts by optical and X-ray diffraction analysis. The silica phases of altered diatoms have been progressively replaced by framboidal pyrite in zone A-2. Very few diatoms composed of silica have been found below 3,900 feet.

Sediments of lithologic zone B (1,150 feet thick) consist of bioturbated, muddy, very fine and fine-grained sandstone interbedded with sandy mudstone. The depositional environment was probably middle neritic. The sand grains are poorly to well sorted and locally cemented with calcite. The only primary sedimentary structures preserved are a few wavy, discontinuous laminations. The isolated lithic granules and pebbles present were probably transported and deposited by storm activity. Whole and broken gastropod and bivalve shells are also present. The framework grains are monocrystalline and polycrystalline quartz, plagioclase and potassium feldspar, and abundant lithic clasts that include volcanic, metamorphic, and sedimentary rock fragments, hornblende, chert, mica, clay clasts, glauconite, and molluscan shell fragments. The amount of detrital matrix ranges from rare in the well-sorted sandstones to abundant in the muddy sandstones. Authigenic minerals include pyrite, siderite, smectitic clay, clinoptilolite, analcite, and calcite cement.

Lithologic zone C-1 consists of 350 feet of thin-bedded, fine- and very fine-grained muddy sandstone and siltstone interbedded with mudstone and claystone. The sandstone is poorly sorted, commonly bioturbated, and locally cemented by calcite. Lithic pebbles and broken and intact thin molluscan shells are present. The sediments in this zone were probably deposited in a middle neritic environment. Well logs indicate that most of the sandstones are less than 10 feet thick. The framework grains include chert, monocrystalline and polycrystalline quartz (22 to 30 percent), lithic fragments (32 to 44 percent), and feldspar (31 to 38 percent). Plagioclase is the predominant feldspar. Most of the lithic fragments are volcanic in origin, but some are sedimentary (probably second-cycle volcaniclastic) and metamorphic. Glauconite is common. Minor constituents include chert, hornblende, pyroxene, fossil fragments, epidote, zircon, garnet, and rare tourmaline. Diagenetic alterations include compaction, alteration of some feldspar, alteration of volcanic rock fragments, and precipitation of clinoptilolite and authigenic pyrite. The alteration of framework grains and the precipitation of authigenic zeolites have generally degraded the reservoir quality.

The Miocene part of zone C-2 is lithologically similar to the Oligocene section, which is described below.

OLIGOCENE

The Oligocene section is 6,580 feet thick in the COST well and represents a largely regressive marine sequence comprising lithologic zones D-1, D-2, E, and most of C-2. Seismic horizon B, which is at or near the boundary between lithologic zones C-2 and D-1 (pl. 1), is an unconformable surface along the shelf break. It probably reflects a sea level drop and a depositional hiatus at the COST well, and it separates the bathyal mudstones and siltstones of zones D-1 and D-2 from the shelf sandstones of zone C-2. Wave-base erosion of older Tertiary and Mesozoic strata along basin margins and local highs during this regressive event may have provided much of the clastics for the sand sequences constituting zones C-2 and C-1. Erosional truncation of subbasin highs to a common base level allowed the extension of a common marine depositional system across all three subbasins for the first time during the late Oligocene.

The marine-shelf deposits of lithologic zone C-2 represent this basin-wide depositional system. At the well, zone C-2 is 1,770 feet thick and consists of fine- to very fine-grained, relatively clean to muddy sandstone and siltstone interbedded with mudstone and claystone. The sandstones are poorly to well sorted. The sediments are locally cemented by calcite. There are some wavy interbeds and laminations of sandstone and claystone. Bioturbation has resulted in horizontal and oblique burrows. Lithic pebbles and broken and intact molluscan shells are present. Microfossil assemblages indicate middle

(possibly inner) neritic to outer neritic paleobathymetries. The framework grains are subrounded and subangular quartz, feldspar, and lithic fragments. The average abundances of framework constituents are 37 percent quartz, 22 percent feldspar (predominantly plagioclase), and 38 percent lithic fragments. The lithic fragments are about 62 percent volcanic, 20 percent metamorphic, and 18 percent sedimentary (probably volcaniclastic). Glauconite is common. Accessory minerals include micas, clay, chert, chlorite, hornblende, pyroxene, epidote, zircon, garnet, and rare tourmaline. Fossil fragments and organic matter are also present. Authigenic minerals include smectite, mixed-layer illite and smectite, calcite, siderite, pyrite, zeolites, gypsum, chlorite, quartz, and feldspar.

Zone C-2 sediments occur in coarsening- and cleaning-upward bedding sequences which probably represent individual shoaling events. These repetitively stacked bedding sequences collectively form a regressive megasequence which appears to coarsen and shoal upward. Higher in the zone, the mudstone intervals that separate discrete coarsening-upward sand sequences are thinner. Near the top of the sequence, the sandstones are amalgamated in units up to 100 feet thick. It is uncertain whether the progradational facies observed at the COST well are common elsewhere in the basin, but the consistent character of seismic sequence II (which contains lithologic zone C-2) suggests they may be extensive.

Slatt (1984) postulates that the formation of shelfal sand-ridge deposits is largely controlled by the development of topographic highs or banks, which when coupled with fluctuations in water depth, provide for the source, development, and burial of the ridges. Assuming this model is applicable in the Navarin Basin, it suggests that shelf sands observed in the COST well (which is located on a paleotopographic bench) may grade into deeper water lithofacies toward subbasin depocenters.

Lithologic zones D-1 and D-2 are 3,670 feet thick at the COST well and are characterized by sandy mudstone, fine-grained muddy sandstone, and claystone with rare lenses of siltstone and sandy carbonate. Isolated coarse-sand-to-pebble-sized volcanic rock fragments are present. Whole and broken molluscan shells and microfossils are common. The only primary sedimentary structures seen in the cores are wavy laminations. Sand- and silt-sized particles include chert, poly- and monocrystalline quartz, lithic fragments (predominantly volcanic, with secondary metamorphic), and feldspar (primarily plagioclase). Accessory minerals include micas, clay, chert, chlorite, and hornblende. Authigenic minerals include smectite, mixed-layer clays, calcite, siderite, pyrite, zeolites, gypsum, chlorite, quartz, and feldspar.

Zone D-2 differs from zone D-1 in containing more clay. In zone D-2 the smectite clays which predominated in zone D-1 have been diagenetically altered to illite, mixed-layer illite-smectite, and

chlorite. The clay diagenesis is associated with overpressuring, which occurs in and below this zone.

Microfossil assemblages indicate deposition in middle bathyal (zone D-2) and upper bathyal (zone D-1) depths. These zones reflect progressive infilling of the structural subbasins. Seismic evidence suggests that these basinal mudstones may grade into turbidites and submarine fans along basement highs.

Lithologic zone E (early Oligocene) is separated from zone D-2 by seismic horizon C, which represents an erosional event along the shelf break and a probable depositional hiatus at the COST well. Zone E consists of 1,480 feet of poorly sorted gray claystone, mudstone, and sandy mudstone with abundant detrital clay matrix. The sediments exhibit wavy lamination and have been moderately burrowed. Calcite concretions are present. The sediments in this zone are slightly finer grained than those of the two zones above. Silt-sized monocrystalline quartz, plagioclase, micas, chert, and volcanic rock fragments are all present as framework clasts. Other minerals present in small amounts are pyroxene, glauconite, hornblende, gypsum, and clays. Clays constitute about 40 to 70 percent of the rock and include chlorite, kaolinite, illite, and mixed-layer illite and smectite. Organic material and molluscan shell fragments are also present. Authigenic minerals include chert, siderite, calcite, laumontite, leonhardite, mixed-layer clay, pyrite, zeolites, quartz, potassium feldspar, and ankerite. The provenance was chiefly volcanic with a minor metamorphic input.

Zone E sediments, which contain a middle bathyal microfossil assemblage, record deposition in a deep-water structural basin. Seismic data suggest that these sediments, like those of zones D-1 and D-2, may grade laterally into coarser grained turbidite deposits along local basement highs. Sediments from zone E and the underlying zone F are believed to be the source for the shale diapirs in the Navarinsky subbasin. (Further information is given in the Seismic Stratigraphy chapter.)

EOCENE

The Eocene section (lithologic zone F) is composed of 500 feet of relatively organic-rich, dark-gray calcareous claystone and sandy mudstone. At the COST well, zone F unconformably overlies acoustic basement. There is some evidence from a combination of well log, lithological, geochemical, and paleontological criteria that the upper contact of zone F with zone E may be unconformable. However, considering the bathyal water depths extant during deposition and the lack of evidence for large amounts of missing section, it seems likely that the contact represents a depositional hiatus at most.

The microfossil assemblage in zone F indicates a relatively sudden deepening of the depositional environment from outer neritic at the base to middle bathyal at the top. This sequence records significant basin subsidence during the initial rifting that formed the Navarin Basin. The organic facies of this unit may reflect an anoxic marine depositional environment, which may indicate a restricted or silled basin (Demaison and Moore, 1980).

Zone F, like zones D-1, D-2, and E, grades laterally into what may be turbidite deposits along local basement highs. Additional evidence for this is suggested by dredge samples of brecciated mudstone and conglomerate equivalent in age to zone F (Marlow and others, Description of Samples, 1983).

MESOZOIC

The Mesozoic section in the COST well consists of 2,520 feet of Late Cretaceous (Maastrichtian) nonmarine coal-bearing sediments intruded by Miocene diabase and basalt sills (lithologic zone G/H), and 1,100 feet of Campanian or older marine shale (lithologic zone I). Eocene (zone F) sediments unconformably overlie the Mesozoic section.

Lithologic zone G/H contains siltstone, very fine grained sandstone, mudstone, claystone, diabase, basalt, and coal. Depositional environments probably included stream and distributary channels and possibly tidally influenced deltaic distributary systems. Core 16 from this zone may have been deposited in an intertidal zone. No marine microfossils were recovered, however. Sedimentary features include flaser structures and wavy and lenticular interbeds of sandstone and mudstone. Truncated ripple sets and herringbone crossbedding are present within some sandstone units. Minor soft-sediment deformation, attributable to the slumping of semiconsolidated sediments on unstable surfaces, is also present.

The framework grains in zone G/H include abundant monocrystalline and polycrystalline quartz, chert, plagioclase feldspar, volcanic and rare metamorphic rock fragments, mica, and hornblende. Many rock fragments were altered in the source area. Authigenic minerals include minor amounts of pyrite, clinoptilolite, siderite, locally abundant calcite, kaolinite, chlorite, mixed-layer illite and smectite, and traces of chert. Densely packed kaolinite and chlorite are present as alteration products of unstable grains and as pore-filling clays. The mixed-layer illite and smectite is an alteration product of labile grains as well as a regenerated detrital clay.

Lithologic zone I is composed of claystone, siltstone, mudstone, and tuff. Deposition was in a marine environment. Bioturbation traces, rare leaf fossils, Inoceramus prisms, discontinuous wavy laminations, and isolated tuff layers are present in cores 19 and 20. Core 19 (15,500 to 15,509 feet) has been tentatively interpreted

as a prodelta mud deposit. Core 20 (16,313 to 16,343 feet) was deposited in a marine shelf environment.

Rocks in zone I are composed of 70 to 80 percent clay minerals. Clays include chlorite (about 40 percent), illite and mixed-layer illite and smectite (about 50 percent), and kaolinite (about 10 percent). Nonclay components include volcanic rock fragments, quartz, plagioclase and potassium feldspar, pyrite, siderite, calcite, clinopyroxene, clinoptilolite, heulandite, hornblende, and mica. Quartz is the dominant nonclay mineral. Authigenic minerals include pyrite, calcite, and mixed-layer illite and smectite. Calcite has replaced both detrital silt grains and clay matrix. Small pyrite framboids associated with organic fragments define weak laminations. Thin, isolated layers of tuff near the bottom of this zone indicate local volcanic activity.

SUMMARY

At the COST well, Eocene rocks record a marine transgression and rapid increase in water depth during the initial stages of basin subsidence. By the early Oligocene, middle bathyal water depths had been attained. Throughout most of the Oligocene, mud and silt sedimentation infilled the three subbasins. At the well site, this is recorded by a largely shale or mudstone regressive sequence.

A sea level drop during the late Oligocene exposed local subbasin highs to wave-base erosion and reduced them to a common base level. Locally sourced shelf sands were then deposited, probably throughout much of the basin, by an area-wide shelf depositional system which persisted into the late Miocene. At the COST well, this is reflected by a predominantly sandstone sequence. The lower half of this sandstone section is a generally regressive sequence, and the upper half is a largely transgressive sequence. The regressive sequence contains the thickest and cleanest potential reservoir sands observed in the COST well.

A late Miocene angular unconformity is present in the northwest area of the basin, but at the COST well it probably represents a depositional hiatus at most. It separates the shelf sandstone sequence from the finer grained mud and silt shelf sedimentation which persisted to the Pleistocene.

The source terrane for the Navarin Basin was chiefly volcanic to volcaniclastic. A secondary, but steady, input from a metamorphic quartz-mica schist terrane persisted throughout the sedimentary history of the basin as seen in the COST well. Consequently, sandstones observed in the well, even those below the basal unconformity, are quartz-poor, mineralogically immature lithic and feldspathic varieties. The immature Tertiary sandstones are typical of the Pacific margin. Detrital mineralogy is largely controlled

by the tectonic setting displayed along converging plate boundaries. This setting is marked by volcanic arcs, by deep oceanic trenchs, and by marine shelves, slopes, and deep basins in the arc-trench gap (Dickinson, 1970). Volcanic and plutonic rocks from the arc are intermediate in composition (rich in plagioclase and mafic minerals and poor in quartz). Older sediments in this setting tend to be deformed and metamorphosed.

Thus sands from these sources tend to be rich in feldspar, mafic minerals, and metasedimentary, volcanic, and pyroclastic rock fragments (Hayes, 1984). The short distances between the locally sourced, coarser grained sediments and the deposition sites have not significantly reduced the percentage of mechanically unstable grains in the Navarin Basin. As a result, sandstones in the well are very susceptible to rapid diagenetic alteration. Sediments below the Cretaceous-Tertiary unconformity have reached an advanced stage of diagenetic and textural maturity and probably represent economic basement in the basin.

Seismic Stratigraphy

Geologic significance was assigned to individual reflections and seismic sequences seen on common-depth-point (CDP) seismic reflection survey lines that profile the Navarin Basin COST No. 1 well site. These sequences were then extrapolated into the basin to establish a regional geologic setting. Structure-contour maps of four major seismic sequence boundaries were constructed to depict the configuration of the basin, to represent the growth of the basin through time, and to locate potential hydrocarbon source beds and reservoir rocks. Dredge sample data from the nearby continental slope and lithologic, petrophysical, geochemical, and paleontological data from the COST well were integrated with the seismic data to better elucidate the geologic history of the basin. All depths discussed in this section are measured from sea level. To adjust COST well depths, subtract 85 feet for the elevation of the kelly bushing.

DATA BASE

Correlation of well information to the CDP seismic reflection survey lines was made in part by using a synthetic seismogram. The seismogram was generated from the Long-Spaced Sonic (LSS) log of the COST No. 1 well and then correlated to the 1978 Western Geophysical (WG) seismic line NB-11, which profiles the well location. Geological correlations were extrapolated from the well into the basin by tying the 1978, 1980, and 1981 WG regional CDP surveys (fig. 6) and the 1977 and 1980 USGS reconnaissance surveys of the Navarin and adjacent Anadyr Basins. The three WG seismic surveys collected over 13,000 miles of high-quality, gridded, CDP data. In compliance with the restrictions placed on the use of WG data, the MMS interpretation of two regional horizons is presented on page-size maps. This permits the depiction of a structure-contour map of horizons C and D (figs. 13 and 15), an isopach map of the section between C and D (fig. 14), a map of major geologic features of the Mesozoic basement (horizon D; fig. 16), and a map of thermal maturity for horizons C and D (figs. 23 and 24). The structure-contour maps of horizons A and B (figs. 11 and 12) are based on our interpretation of USGS data. Figures 10 and 8 are line interpretations of Petty-Ray
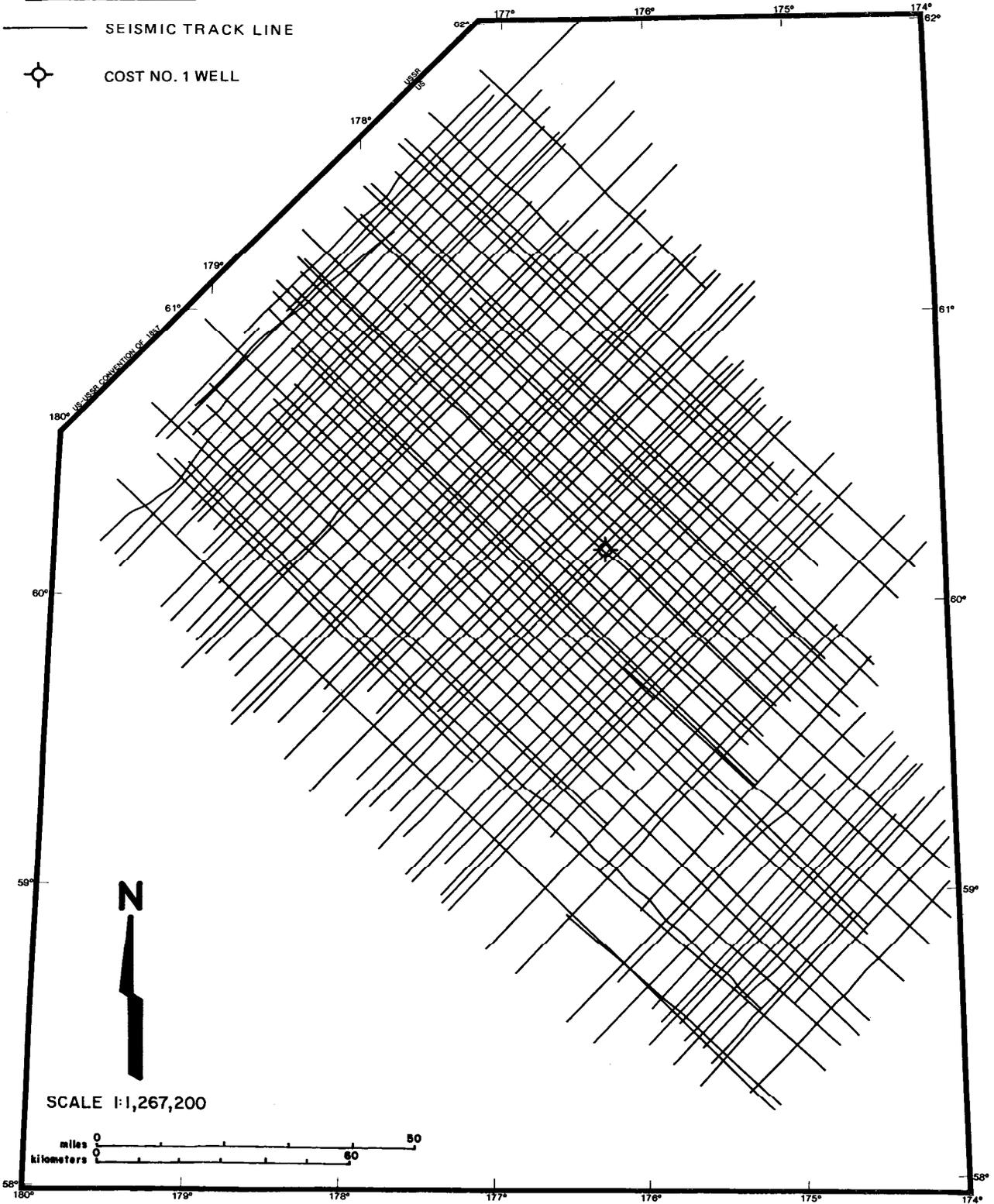
FIGURE 6. Seismic reflection data coverage by the 1978, 1980, and 1981 Western Geophysical Co. surveys.

Geophysical (Geosource, Inc.) lines PR 7411 and PR 7415; figure 9 is a seismic profile of line PR 710a. Selected dredge samples from the 1977, 1978, 1980, and 1981 USGS surveys of the continental slope were also used. Published analyses of these samples and analyses made by MMS personnel and consulting geoscientists were incorporated.

SEISMIC SEQUENCE ANALYSIS

Seismic sequence analysis of the CDP seismic reflection data reveals at least five regional depositional sequences (I through V). The upper four Tertiary sequences are composed of genetically related facies or depositional systems bounded by unconformities or by their correlative conformities (horizons A through D). Sequence V, the acoustic basement, is a structurally complex series of Mesozoic rocks. Figure 7 displays these sequences (from a CDP seismic profile of the COST well) adjacent to time-stratigraphic divisions and lithologic zones. Two local unconformities were identified within seismic sequences I and IV. Because of their restricted occurrence, the local unconformities are considered features within a regional sequence that signify a tectonostratigraphic change in the local depositional system. Because these local unconformities were not mapped or correlated to the COST well, much of their geologic significance can only be inferred.

Seismic Sequence I (Plio-Pleistocene to late Miocene)

Seismic sequence I comprises the Plio-Pleistocene section and part of the late Miocene section (fig. 7). The sequence is characterized by a zone of flat-lying, parallel, continuous reflections that are present throughout the basin (fig. 8). These reflections exhibit subtle divergences toward subbasin centers and onlap the continental sides. Sequence I is bounded by the sea bottom and horizon A (late Miocene). Horizon A occurs at 1.28 seconds (or about 3,560 feet below sea level) at the COST well site.

Horizon A is defined by a continuous, large-amplitude, positive reflection that becomes discontinuous and variable in amplitude as the reflector becomes shallower toward the basin flanks. At the well, the reflections above and below horizon A are concordant, and they remain concordant throughout much of the basin. In the northwest area of the basin (fig. 34, point B), however, horizon A becomes an angular unconformity between overlying concordant reflections and the underlying truncated reflections of seismic sequence II (fig. 9). This erosional truncation was caused in part by the intrusion of shale diapirs and the associated uplift and erosion of sequence II.

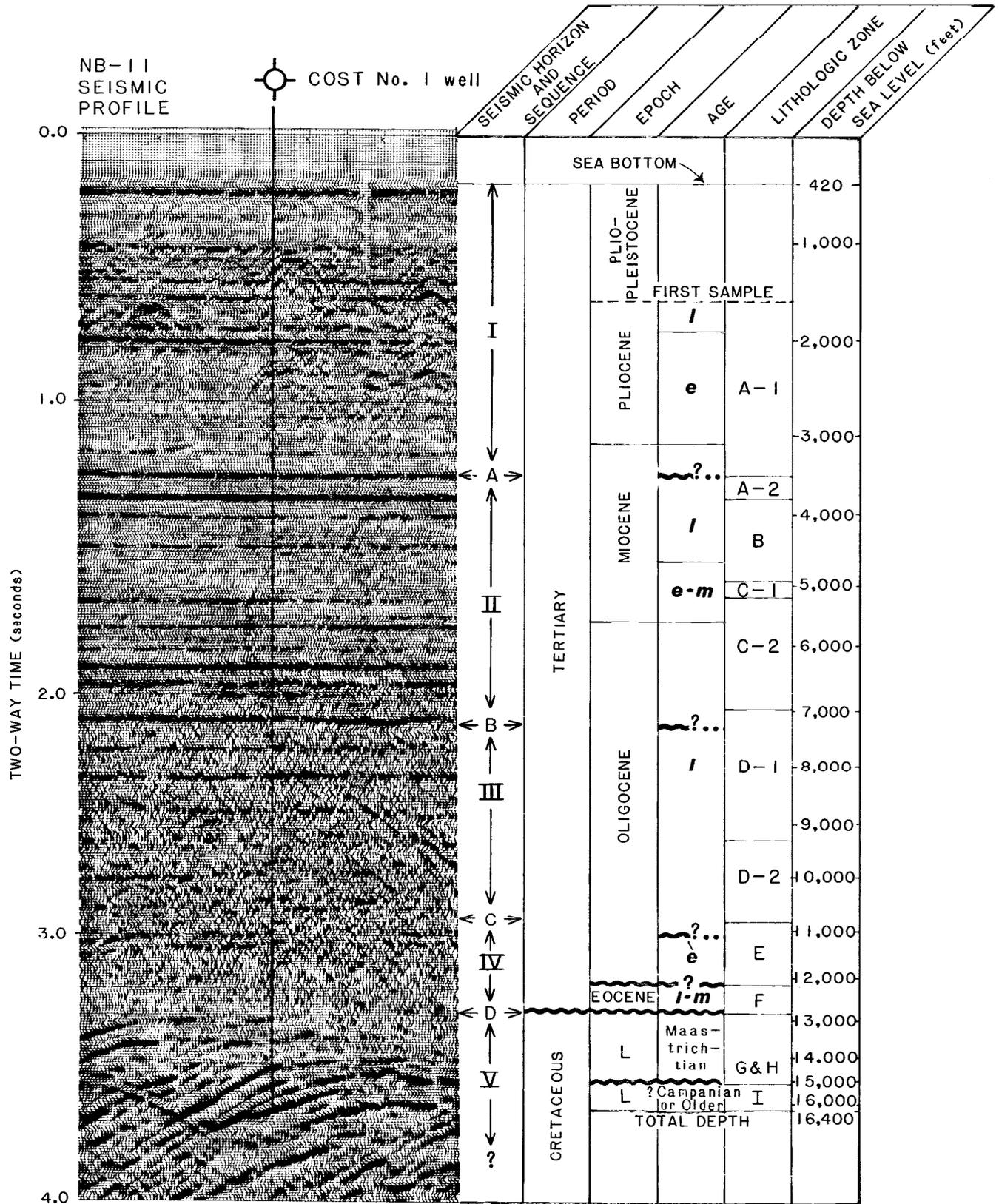**FIGURE 7.** Seismic sequences and horizons, time-stratigraphic column, lithologic column, and a Western Geophysical Co. seismic reflection profile of the Navarin Basin COST No. 1 well. (Basin flank unconformities are indicated by question marks).

Horizon A coincides with both the boundary between lithologic zones A-1 and A-2 and a possible late Miocene unconformity. At the well, horizon A probably results from constructive interference between a chronostratigraphic surface and a diagenetic boundary (the bottom-simulating reflector, or BSR). The absence of a lithologic break or any of the well log characteristics normally indicative of a disconformity suggests that, at the well, the reflection represents a depositional hiatus at most.

Diffractions are common in sequence I between 0.4 and 1.0 second (or about 950 to 2,700 feet below sea level). These diffractions are more prevalent in the two southern subbasins. Probable sources for the diffractions are segments along the continuous reflections with increased amplitude. Reflections that lie between the diffractions and above horizon A are disrupted or disappear. Thin (usually less than 10 feet), highly indurated lenses of secondary carbonate minerals in the mudstone probably caused the diffractions.

A local angular unconformity was identified at the Pervenets Ridge area of the continental shelf break (approximately 80 miles southwest of the COST No. 1 well site, fig. 34, point A). Figure 10 is a line interpretation of a CDP seismic line that profiles the Pervenets Ridge and shows that the unconformity is the base of a prograding wedge of Miocene and Pliocene sediment. The areal extent of the unconformity was not mapped nor was it tied to the well. The downlapping sigmoidal reflections may be indicative of a prograding shelf environment. These reflections are traced updip into the parallel, coherent reflections which typify sequence I. This progradation may indicate a change in the rate of sea level rise or of basin subsidence (Brown and Fisher, 1980).

At the well, seismic sequence I brackets lithologic zone A-1 and the unsampled material above 1,500 feet. Lithologic zone A-1 is composed of diatomaceous mudstone and diatomite. It is distinct from zone A-2, which has undergone diagenesis and cementation. Dredge samples from the Navarin continental slope indicate that the time-stratigraphic equivalents of lithologic zone A-1 are early to late Pliocene diatomaceous mudstone and volcanic sandstone, and late Miocene diatomaceous mudstone and diatomaceous limestone. The unsampled section above 1,500 feet contains Plio-Pleistocene and Holocene material. Dredge hauls from the lower part of the Navarin continental slope collected sandy and muddy limestone (probably concretionary), conglomeratic sandstone, and muds of Pleistocene and Holocene age. The similarities between well and dredge samples indicate relatively uniform, regional deposition.

A structure-contour map of horizon A (fig. 11) was made with available Government CDP seismic reflection data. Because of the paucity of data, only a general surface trend is depicted. The sedimentary accumulation represented by seismic sequence I appears
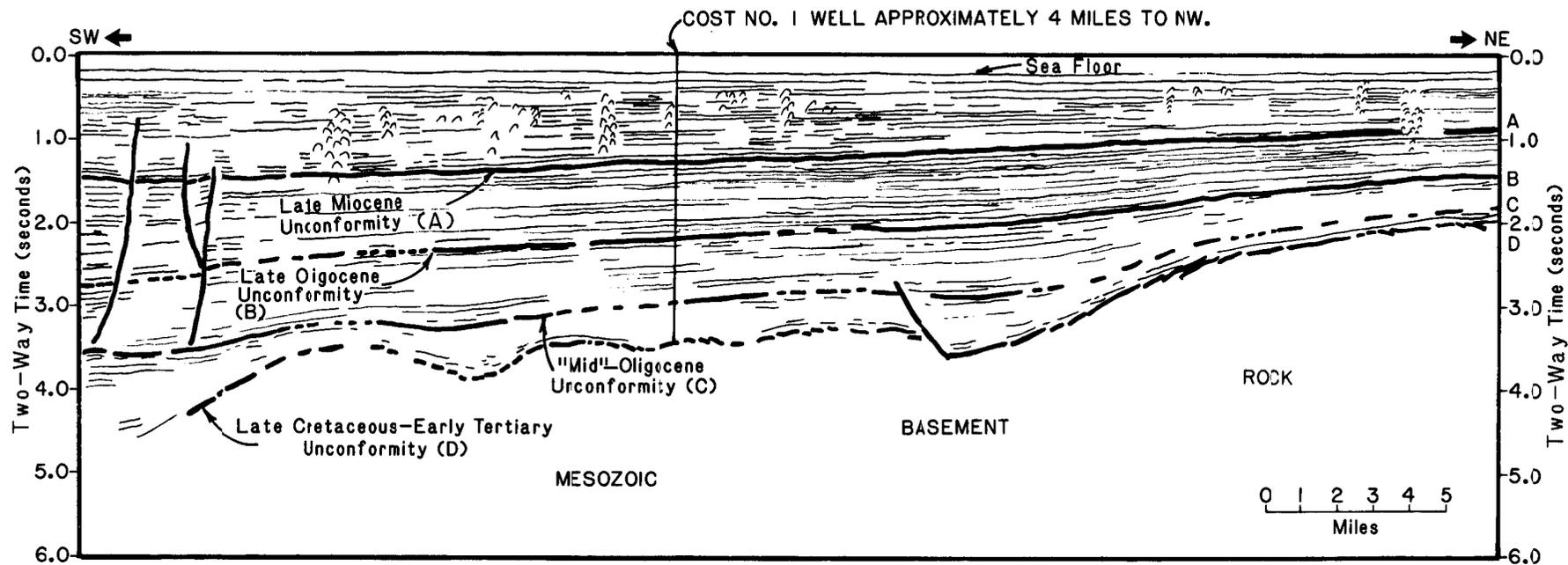
FIGURE 8. Line interpretation of Petty-Ray seismic line PR 7415. Adapted from Steffy (1984b).

FREE-AIR
GRAVITY
IN MILLIGALS
(—)

8300
8290
8280
8270
8260
8250
8240
8230
8220
8210
8200

9050
9000
8950
8900
8850
8800
8750
8700
8650
8600
8550

FILTERED
MAGNETICS
IN GAMMAS
(—)

0.0
1.0
2.0
3.0
4.0
5.0
6.0

horizon A

horizon B

SHALE
DIAPIR

TWO-WAY TIME
(seconds)

TWO-WAY TIME
(seconds)

0 1 2 3 4 5
miles

FIGURE 9.   Petty-Ray seismic line PR710a, free-air gravity profile, and filtered magnetics profile.
Adapted from Steffy (1984b).

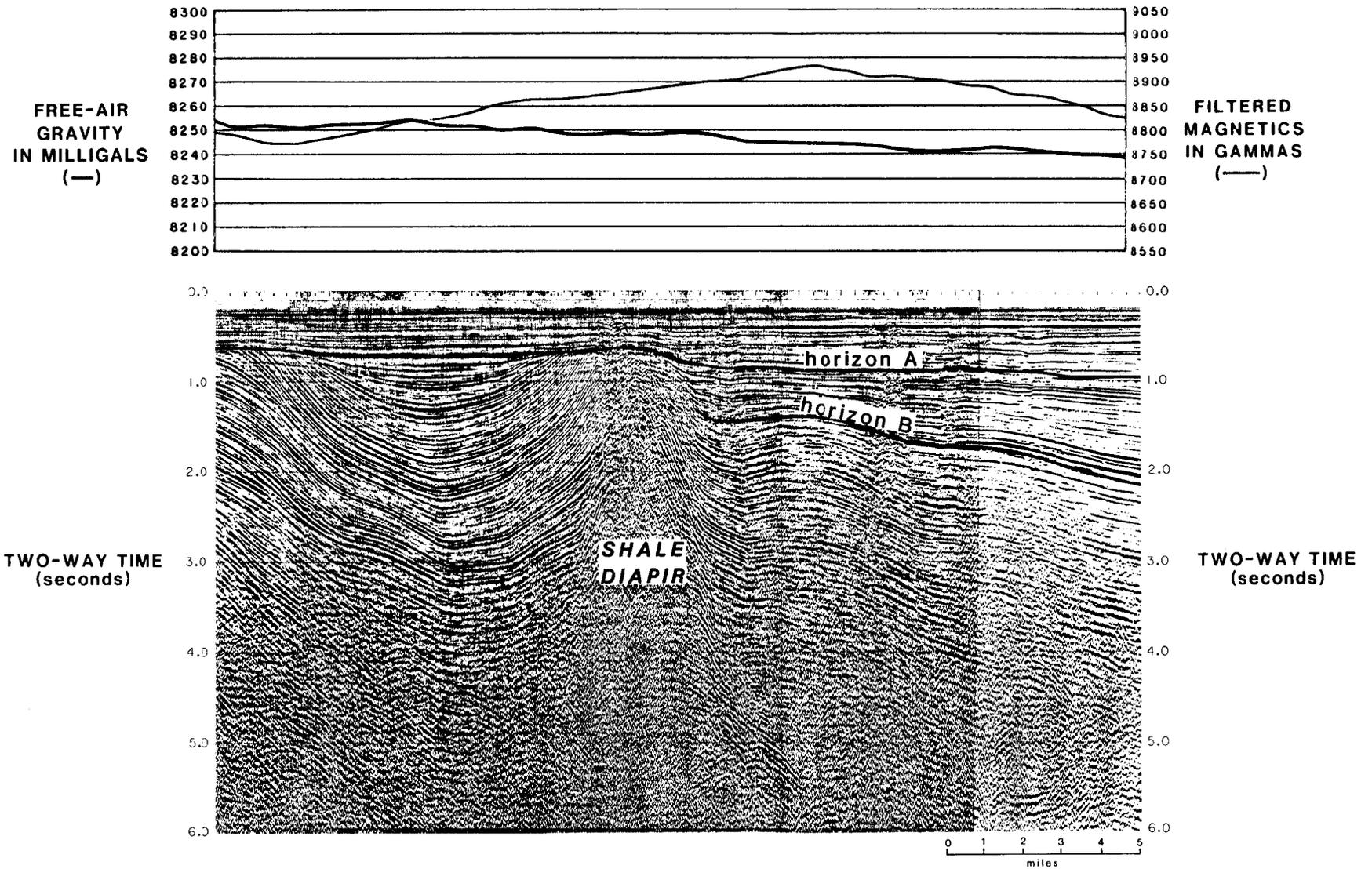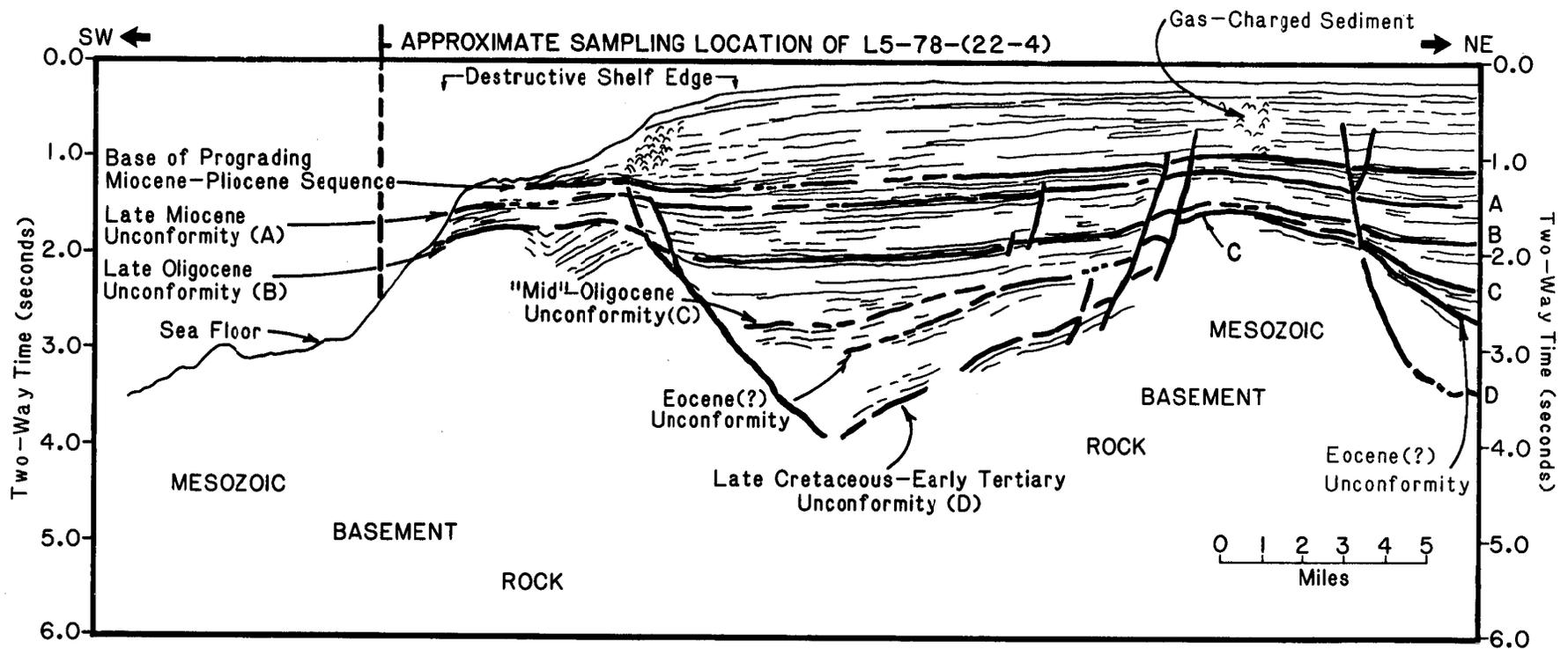**FIGURE 10.** Line interpretation of Petty-Ray seismic line PR 7411
Adapted from Steffy (1984b).

to have been uniform in that the effects of subsidence and deposition in the Navarinsky and Pervenets subbasins are not distinct. The average thickness is 3,000 feet throughout the Navarin Basin, with a maximum thickness of more than 5,000 feet in the center of the Pinnacle Island subbasin. Although Mesozoic basement highs along the continental shelf break apparently remained as positive tectonic features throughout most of Tertiary time, sequence I extends beyond the margins of these structurally controlled subbasins. This probably indicates regional subsidence in response to crustal cooling during Neogene time.

Seismic Sequence II (late Miocene to late Oligocene)

Seismic sequence II comprises part of the Miocene and part of the late Oligocene sections. The sequence is bounded by horizons A and B (fig. 7). At the well, horizon A occurs at 1.28 seconds (or about 3,560 feet below sea level), and horizon B occurs at 2.20 seconds (or about 7,400 feet below sea level).

Throughout most of the Navarin Basin, horizon B is a continuous, large-amplitude reflection that separates the concordant, parallel, continuous, large-amplitude reflections of seismic sequence II from the concordant, parallel, discontinuous, variable-amplitude reflections of seismic sequence III. Along the shelf break, horizon B represents a late Oligocene lowering of sea level (perhaps the TO2.2 eustatic event of Vail and others, 1977) that subjected older Tertiary strata and Mesozoic basement rock to wave-base erosion; in the subbasins, however, it represents a depositional hiatus at most. Horizon B separates the middle and outer neritic deposits of sequence II from the upper and middle bathyal mudstones and siltstones of sequence III.

The stratal surfaces of sequence II onlap the Mesozoic basement ridges of the Navarin Basin (fig. 10). In the northern Navarinsky subbasin these stratal surfaces were uplifted and intruded by shale diapirs (fig. 9). The uplifted strata were also truncated by the late Miocene unconformity (horizon A). Where sequence II is not affected by postdepositional tectonism, its stratal surfaces exhibit a subtle divergence toward the subbasin centers, which suggests relatively uninterrupted sedimentation and basin filling.

At the COST well, seismic sequence II contains lithologic zones A-2, B, C-1, and C-2, and the upper portion of zone D-1. Zone A-2 represents a thin transitional layer characterized by increased diagenesis and cementation of zone A-1 type sediments. Zones B, C-1, and C-2 are muddy sandstones that represent relatively continuous deposition from late Oligocene to late Miocene time. Dredge samples from the Navarin continental slope indicate that the time-stratigraphic equivalents of lithologic zones B, C-1, and C-2 are middle Miocene diatomaceous, tuffaceous mudstones, clayey limestones, and diatomaceous sandstones as well as early Miocene sandstones, calcareous diatomites, and tuffaceous mudstones.

CDP seismic reflection data indicate laterally continuous
bedding and vertically continuous deposition within seismic sequence
II. Sequence II sedimentary deposits were the first to extend beyond
the structurally controlled limits of all of the subbasins and
probably joined the distinct marine depositional systems of the three
subbasins in an area-wide marine environment.

A structure-contour map of horizon B displays these trends
(fig. 12). The figure also shows the erosional truncation of Mesozoic
basement highs by horizon B to a common base level. The geometry of
horizon B indicates mostly regional subsidence in response to
crustal cooling. The Pinnacle Island and Pervenets subbasins,
however, were sites of local sediment accumulation in the early
Oligocene. The Pinnacle Island subbasin deepens to more than
11,500 feet, and the Pervenets subbasin deepens to slightly more
than 8,000 feet. Sequence II represents the transition from local
accumulation in subbasins controlled by tectonic movement to uniform
deposition in and between subbasins controlled by regional subsidence.

Seismic Sequence III (late Oligocene)

Seismic sequence III comprises most of the late Oligocene
section. The sequence is bounded by horizons B and C (fig. 7).
At the well, horizon B occurs at 2.20 seconds (or about 7,400 feet
below sea level), and horizon C occurs at 2.94 seconds (or about
11,000 feet below sea level).

At the well and on most of the basin flanks, horizon C is an
indistinct, discontinuous, variable-amplitude reflection. In the
deeper part of the subbasins, however, horizon C is a distinct
seismic sequence boundary recognized as a continuous, large-amplitude
reflection. Along the shelf break, horizon C represents a regressive
event that truncated older Tertiary and Mesozoic rocks (fig. 10).
In the center of the subbasins and at the COST well, it represents,
at most, a depositional hiatus.

Sequence III is a zone of discontinuous, parallel, variable-
amplitude reflections (at the well and in the shallower parts of
the basin) that become larger in amplitude and more continuous
in the deeper parts of the basin. The stratal surfaces of sequence
III are concordant with horizon C except along the Navarin Basin
flanks, where they onlap older rocks. These surfaces may represent
flank deposits derived from Mesozoic basement highs along the
continental shelf break that were eventually truncated by the
regressive horizon B event (fig. 10). In addition, they were
uplifted and intruded by late Miocene shale diapirs in the northern
Navarinsky subbasin. The stratal surfaces of sequence III exhibit
an obvious divergence toward the subbasin centers, indicating
rapid, constant sedimentation.

At the COST well, seismic sequence III is correlated to
lithologic zones D-1 and D-2 (late Oligocene). Zone D-1 is composed

EXPLANATION

_3000 _--STRUCTURE CONTOUR IN FEET, DASHED WHERE INFERRED

D U FAULT, D ON DOWNTHROWN SIDE

(H) STRUCTURALLY HIGH AREA

STRUCTURALLY LOW AREA

COST NO. 1 WELL

N

CONTOUR INTERVAL 500 FEET
SCALE 1:1,267,200
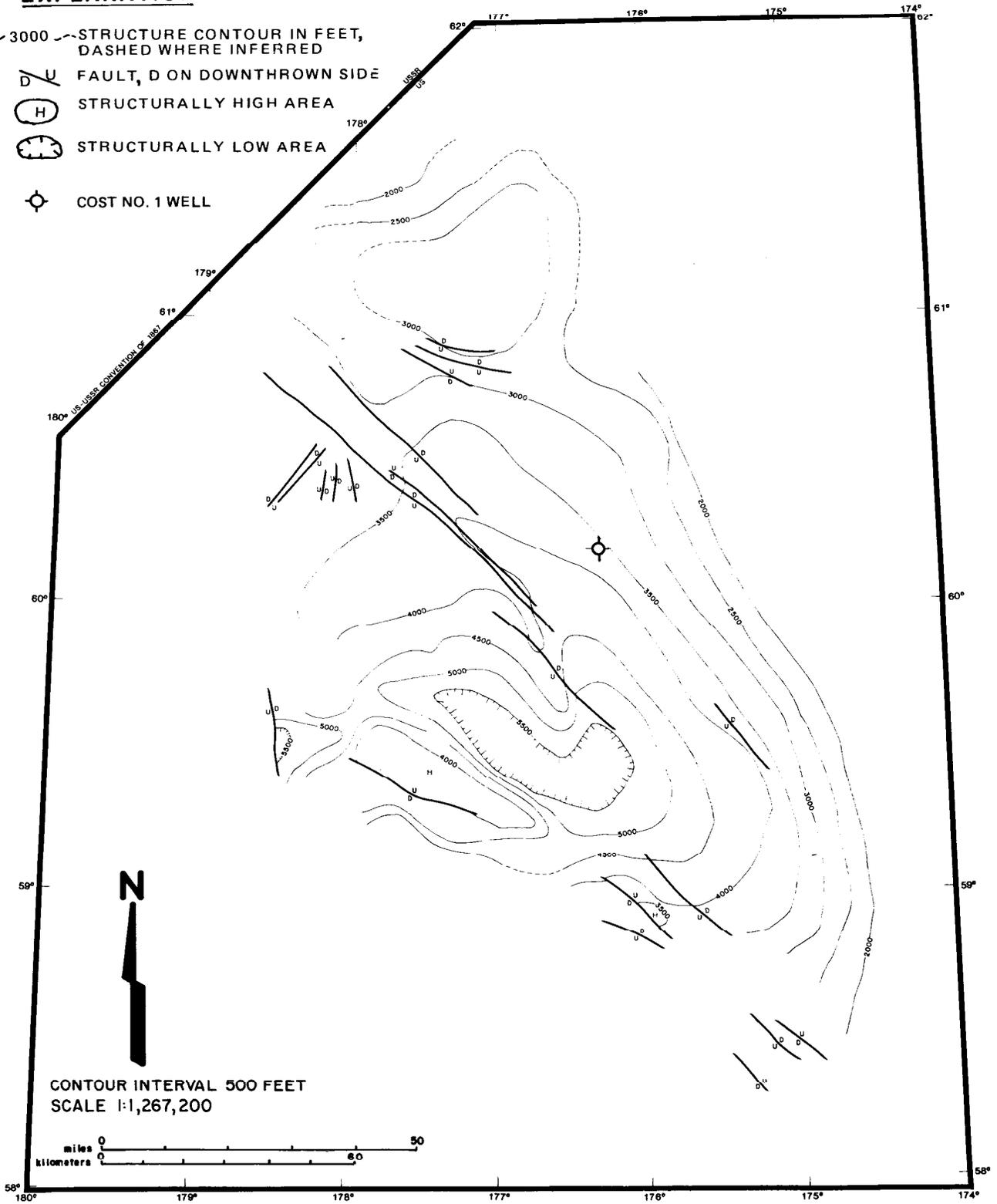
miles 0   50
kilometers 0   60

FIGURE 11. Structure-contour map of horizon A (late Miocene). Based on available U.S. Geological Survey seismic reflection data.

of outer neritic to middle bathyal mudstones and siltstones. Zone D-2 contains middle bathyal mudstone with sandstone interlaminations. Dredge samples from the Navarin continental slope indicate that the time-stratigraphic equivalents of the late Oligocene lithologic zones are tuffaceous sandstones and mudstones.

CDP seismic reflection data indicate that the deposition of most of sequence III was laterally and vertically continuous. However, the sequence grades into what appear to be proximal turbidite deposits flanking local basement highs along the continental shelf break. This interpretation is based on three observations: (1) the onlapping of sequence III stratal surfaces over local structural highs; (2) the presence of coarse-grained material in dredge samples of rocks that are time equivalent to sequence III; and (3) the fact that early Oligocene (sequence IV) and Mesozoic basement rocks were exposed to wave-base erosion in the late Oligocene, which could have provided a local sediment source adjacent to deepwater basins.

Figure 13 is a structure-contour map of horizon C. The post-erosional relief of the horizon represents the syndepositional control of that structure on Oligocene stratigraphy. The Pinnacle Island subbasin (fig. 16) is an asymmetric graben formed by a series of northwest-trending normal faults. The subbasin contains more than 22,000 feet of post-early Oligocene sediment. Neither horizon A (late Miocene), horizon B (late Oligocene), nor horizon C ("mid"-Oligocene) exhibit unconformable relationships throughout the Pinnacle Island subbasin. These horizons, however, may represent periods of nondeposition in the subbasin and are correlative to unconformable surfaces outside the subbasin. This suggests that in the subbasin, there may have been nearly continuous deposition since the early Oligocene. Similar relationships between these horizons and structure are recognized in the Pervenets and Navarinsky subbasins. Nearly continuous deposition since the early Oligocene has filled the Pervenets subbasin with more than 19,000 feet of sediment and the Navarinsky subbasin with more than 29,000 feet of sediment.

Seismic Sequence IV
(early Oligocene, Eocene, and possible Paleocene)

At the well, seismic sequence IV comprises the early Oligocene and Eocene sections. In the deeper parts of the basin, it may also include some Paleocene section. It is bounded by horizons C and D (fig. 7). At the well, horizon C occurs at 2.94 seconds (or about 11,000 feet below sea level), and horizon D occurs at 3.30 seconds (or about 12,700 feet below sea level).

Throughout the basin, horizon D represents a distinct angular unconformity between sequences IV and V. Horizon D is the contact where the discontinuous, variable-amplitude reflections of sequence IV overlie and overlap the discordant, dipping, large-amplitude

EXPLANATION

~10,000~ STRUCTURE CONTOUR IN FEET, DASHED WHERE INFERRED

FAULT, D ON DOWNTHROWN SIDE

(H) STRUCTURALLY HIGH AREA

STRUCTURALLY LOW AREA

MESOZOIC BASEMENT SUBCROP

COST NO. 1 WELL

CONTOUR INTERVAL 500 FEET
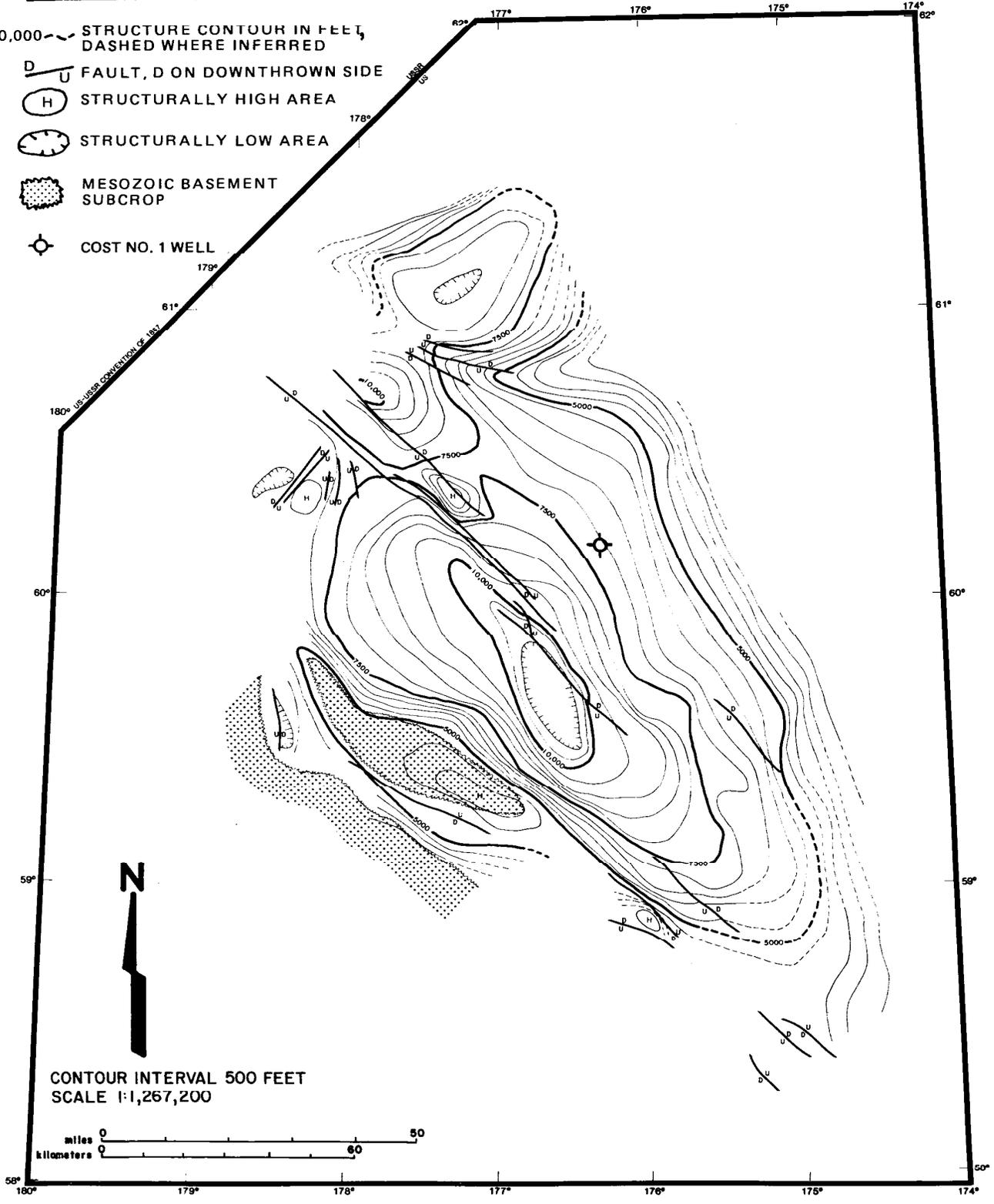SCALE 1:1,267,200

miles 0 _____ 50
kilometers 0 _____ 60

FIGURE 12. Structure-contour map of horizon B (late Oligocene). Based on available U.S. Geological Survey seismic reflection data.

reflections and diffractions that characterize the acoustic basement, sequence V. The stratal surfaces of sequence IV diverge as they deepen into the centers of the subbasins, indicating continuous sedimentation during structural subsidence.

At the well, sequence IV correlates to lithologic zones E and F. There is some well log, geochemical, and paleontological evidence for an unconformity between zones E and F, although the geochemical data indicate that there is little missing section at the well site. Zone E consists of early Oligocene middle bathyal mudstones containing calcite concretions. Dredge samples from the Navarin continental slope indicate that the time-stratigraphic equivalents of zone E are mudstones containing limestone nodules. Zone F consists of late middle to late Eocene, upper bathyal to outer neritic, calcareous and sandy mudstones. Dredge sample equivalents of zone F are middle to late Eocene mudstone and volcanic sandstone (Marlow and others, Description of Samples, 1983). Basalt collected on the Navarin slope was dated as early Eocene by radiometric (K-Ar) methods.

Although no Paleocene rocks were identified in the Navarin COST well, they might be present elsewhere in the basin. Dredge samples from the nearby continental slope contained probable Paleocene volcanic sandstone and limestone, and Paleocene to Eocene brecciated mudstone and conglomerate. The pronounced basinward thickening of seismic sequence IV may be indirect evidence for Eocene and Paleocene rocks in the center of the subbasins. An isopach map of sequence IV (fig. 14) indicates as much as 20,000 feet of sediment present in the Pinnacle Island subbasin. The fact that sequence IV stratal surfaces onlap horizon D in areas which are stratigraphically down-section from the well suggests that the deposition commenced before zone F deposition (middle to late Eocene) and that early Eocene to Paleocene rocks are probably present in the deeper parts of the basin as well as along the shelf break.

Although CDP seismic reflection data suggest vertically continuous deposition of sequence IV, the bedding is laterally discontinuous. Along the continental shelf break, sequence IV, like sequence III, grades into what are inferred to be proximal turbidite deposits flanking local basement highs.

Sequence IV is believed to be the source for the shale diapirs in the northern Navarinsky subbasin. The overall lateral continuity of seismic sequence IV outward from the well indicates that the sequence is made up of fine-grained material throughout the subbasin. These fine-grained materials are believed to be overpressured in the well (Sherwood, 1984). Lithologic zone F, in sequence IV, lies within the oil window and contains kerogen suitable for wet-gas generation. Hedberg (1976) suggested that methane formation in organic-rich shales might enhance their instability. The presence of an unsampled gas plume over the flank of a shale diapir in the

─5000─ STRUCTURE CONTOUR IN FEET

FAULT, D ON DOWNTHROWN SIDE

(H) STRUCTURALLY HIGH AREA

STRUCTURALLY LOW AREA

TRUNCATION DUE
TO EROSION

TRUNCATION DUE
TO SHALE DIAPIR

◇ COST NO. 1 WELL

N

CONTOUR INTERVAL 1000 FEET
SCALE 1:1,267,200

miles 0 ———————— 50
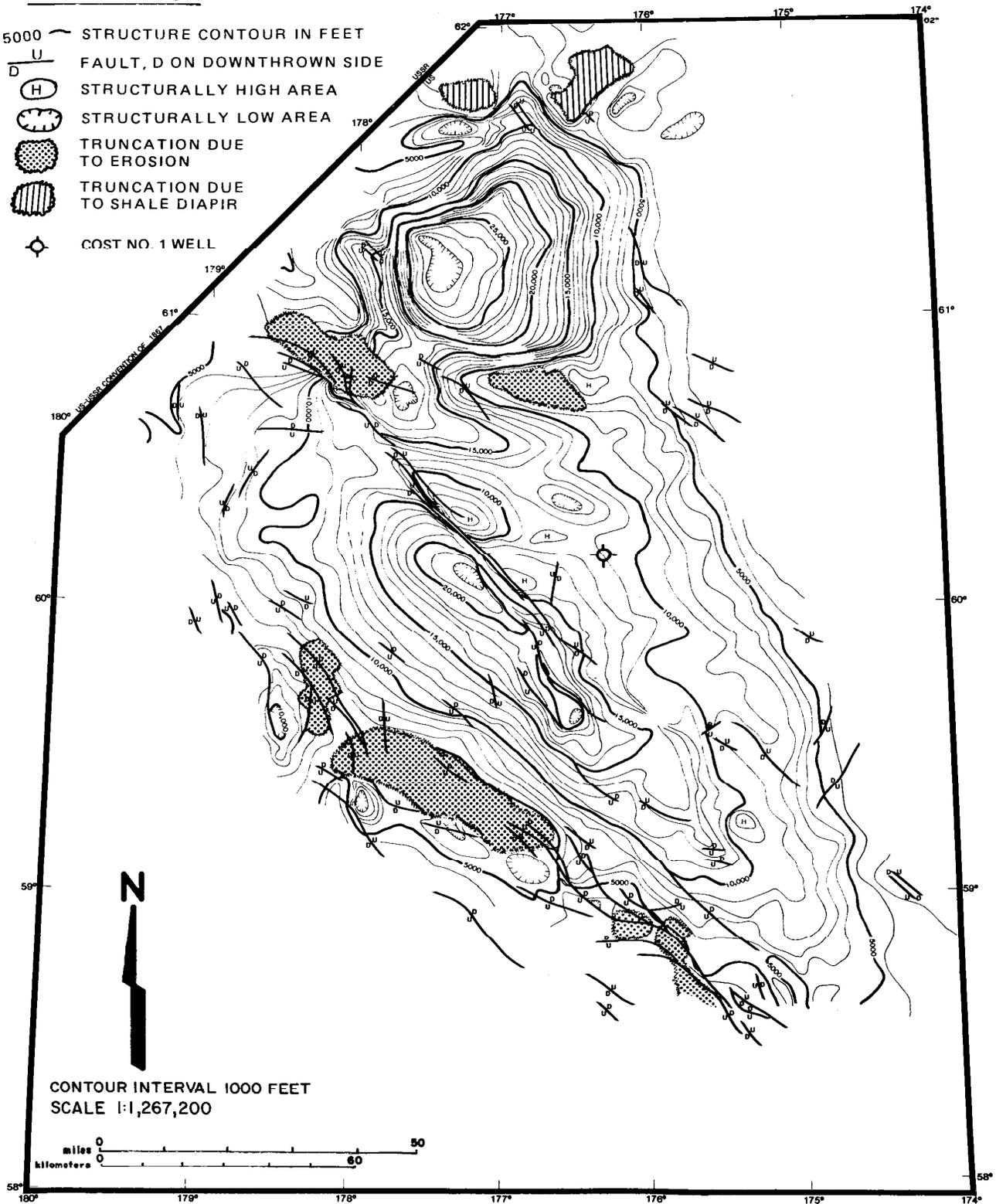kilometers 0 ———————— 60

FIGURE 13. Structure-contour map of horizon C ("mid"-Oligocene). Based on
the 1978, 1980, and 1981 seismic reflection surveys of Western
Geophysical Co.

Navarinsky subbasin (Carlson and Marlow, 1984) may corroborate Hedberg's contention. The diverging stratal surfaces of sequence IV indicate continuous, rapid sedimentation. Rapid sedimentation increases the likelihood of maturation of trapped organic matter by enhancing anoxic conditions near the sea floor and by later decreasing geothermal heat loss at depth (Anstey, 1977). Diapir movement occurred as recently as late Miocene, piercing and disrupting the stratal surfaces of sequences II and III. Eventually, the diapirs were truncated by an erosional surface, horizon A. Emplacement of the diapirs seems to have been controlled by the structural relief of the basement rock, sequence V. A free-air gravity profile of the diapir area (fig. 9) reflects the gradual deepening of the basement rock toward the center of the subbasin. Uneven sediment loading appears to have forced the diapir to rise near the northern flank of the subbasin near the Anadyr Ridge.

An Eocene(?) unconformity was identified near the shelf break at the Pervenets Ridge (fig. 34, point A). This unconformity was not mapped or tied to the well. A tentative Eocene date has been assigned to the unconformity, although a Paleocene age may be just as reasonable. The angular unconformity apparently truncated the basement rock high along the shelf break and in turn was truncated by "mid"-Oligocene (horizon C) and late Oligocene (horizon B) erosional events. This unconformity marks a significant tectonostratigraphic change in the outer-shelf geologic setting in pre-horizon C time and the rejuvenation of a Mesozoic basement high. If this high was exposed to wave-base erosion, then the provenance for the stratal surfaces onlapping the unconformity could include both Mesozoic and sequence IV Tertiary rocks. Reworking of these sediments could generate clean, coarse-grained material of reservoir quality. The presence of coarse-grained sedimentary deposits is suggested by the occurrence of the incoherent, discontinuous reflections commonly associated with coarser grained sediments.

A structure-contour map of horizon D (fig. 15) depicts Mesozoic basement highs separating three structurally distinct subbasins. All three subbasins deepen to greater than 32,000 feet below sea level. The Pinnacle Island and Pervenets subbasins are elongated depressions that parallel the northwest-trending Navarin continental shelf break. The more circular Navarinsky subbasin is bordered by the Anadyr Ridge on the west and lies farthest from the present shelf break.

Seismic Sequence V (early Tertiary and Mesozoic)

Seismic sequence V encompasses possible early Tertiary basin fill and the acoustic basement composed of Mesozoic rocks. At the COST well, the top of sequence V occurs at 3.30 seconds (about 12,700 feet below sea level). The Mesozoic component of sequence V is recognized by its variable-amplitude, discordant reflections, diffractions, and incoherent noise (fig. 7). The possible early Tertiary basin fill occurs as layered deposits in small, isolated, structurally controlled depocenters, and

EXPLANATION

～5000～ ISOPACH CONTOUR IN FEET

FAULT, D ON DOWNTHROWN SIDE

HACHURES ON CONTOUR WITH A
SMALLER VALUE,
INDICATING THINNING

MISSING SECTION DUE TO
EROSION

TRUNCATION DUE TO
SHALE DIAPIR

COST NO. 1 WELL

POOR DATA

N

CONTOUR INTERVAL 1000 FEET
SCALE 1:1,267,200

miles 0   50
kilometers 0   60
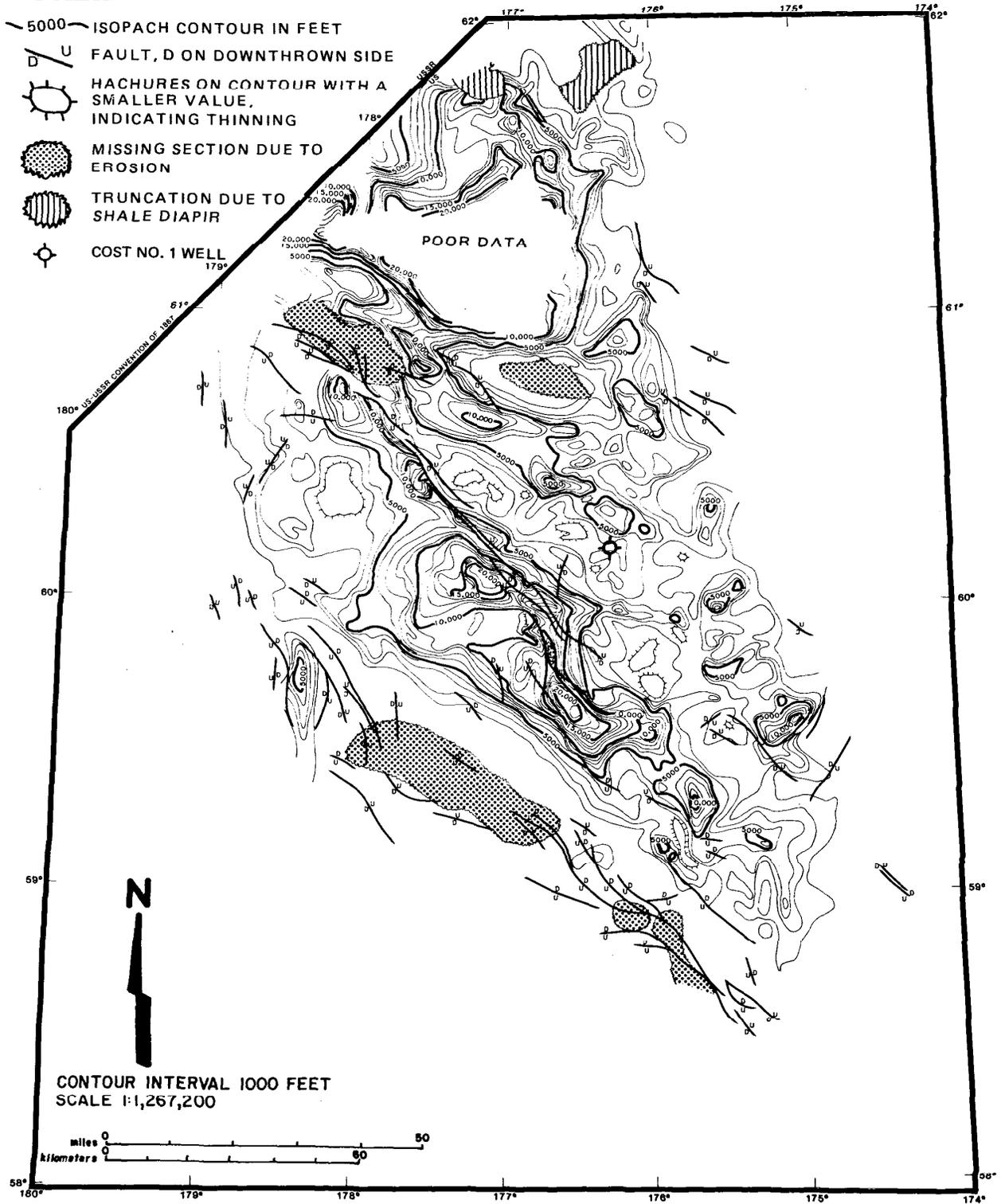
FIGURE 14. Isopach map of seismic sequence IV, between horizon D
(Late Cretaceous-early Tertiary) and horizon C ("mid"-Oligocene).
Based on the 1978, 1980, and 1981 seismic reflection surveys of
Western Geophysical Co.

was apparently sourced from local basement paleohighs. The fill lies
unconformably on the Mesozoic basement and is offset by basement-
controlled faults. The fill, not encountered at the COST well, is
recognized by its concordant, parallel reflections with amplitudes
that increase updip. The reflections show a downlap relationship to
the underlying Mesozoic rock.

Throughout the Navarin Basin, an erosional surface separates
seismic sequence V from the overlying Tertiary section. Horizon
D represents the area-wide degradation of the Bering Sea shelf
before the formation of the Navarin subbasins. Subsequent
erosional events, such as those represented by horizons B and C,
eroded local basement highs that flank the individual subbasins.

In the COST well, sequence V is represented by lithologic
zones G/H and I. Lithologic zone G/H consists of Maastrichtian
mudstone, sandstone, and coal deposited in a nonmarine environment.
Lithologic zone I is probably Campanian or older mudstone deposited
at inner neritic to upper bathyal depths. The lower part of this
zone contains thin volcanic-tuff layers. Dredge samples from the
Navarin continental slope that are time-stratigraphic equivalents
to sequence V are listed in table 1.

Table 1. Lithology and age of dredge samples.

Sample No.	Lithology	Age	
		Steffy (1984b)	Jones and others (1981)
L5-78-(27-1)	Sandy siltstone	Late Cretaceous (Maastrichtian and reworked Albian)	Late Cretaceous (Campanian or Maastrichtian)
L5-78-(27-2)	Sandstone	Late Cretaceous (Cenomanian to Turonian)	Not evaluated
L5-78-(5-5)	Volcanic sandstone	Late to Middle Jurassic (Callovian?)	Late Jurassic (Kimmeridgian)
L5-78-(22-4)	Siltstone	Paleocene (probable Danian)	Late Cretaceous (Campanian or Maastrichtian)

The locations of the sampling sites are plotted on figure 34,
except for sample L5-78-(5-5), which lies southeast of the map area
at lat 56°51.1' N. and long 173°32.7' W. Paleontological similarities
between the Maastrichtian rocks found in the well and the dredge

EXPLANATION
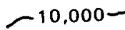
$\frown$ 10,000 $\frown$ STRUCTURE CONTOUR IN FEET

⬚ FAULT, D ON DOWNTHROWN SIDE

Ⓗ STRUCTURALLY HIGH AREA

⬭ STRUCTURALLY LOW AREA

✛ COST NO. 1 WELL

POOR DATA

N

CONTOUR INTERVAL 2000 FEET
SCALE 1:1,267,200

miles 0 _____ 50
kilometers 0 _____ 60
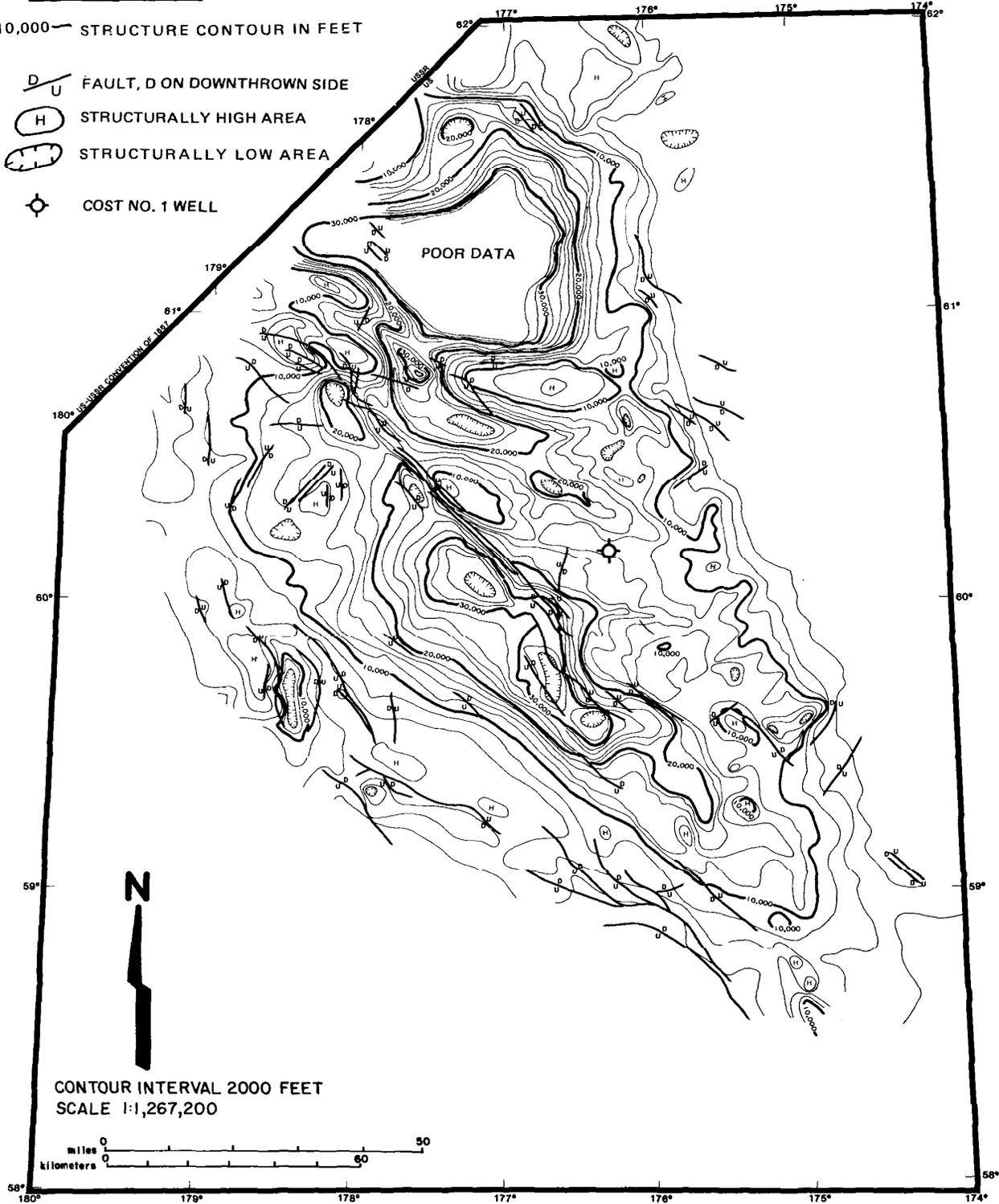
FIGURE 15. Structure-contour map of horizon D (Late Cretaceous-
early Tertiary). Based on the 1978, 1980, and 1981 seismic
reflection surveys of Western Geophysical Co.

samples indicate the presence of Late Cretaceous marine and nonmarine
depositional environments throughout the Navarin continental shelf.
The presence of Maastrichtian coal beds unconformably overlying
probable Campanian upper bathyal rocks suggests that the geologic
history of the Late Cretaceous is relatively complex. McLean (1979a)
and Vallier and others (1980) indicated that the Naknek Formation
(Late Jurassic to Early Cretaceous) extends from the Alaska Peninsula
to the Pribilof Islands. Sample L5-78-(5-5) is a Middle to Late
Jurassic volcanic sandstone dredged from the Zemchug Canyon of the
Navarin continental slope. This suggests that the Naknek Formation
(or a time-stratigraphic equivalent) extends into the Navarin shelf
and supports the contention of Marlow and others (Tectonic Evolution,
1983) that the Mesozoic basement rock in the Navarin Basin and the
outer Beringian shelf is a single, continuous terrane.

Structural Geology

A structure-contour map of the Late Cretaceous-early Tertiary unconformity in the Navarin Basin reveals the axes of three en echelon subbasins that trend generally northwestward and parallel the continental shelf break (fig. 16). These depocenters (informally named the Navarinsky, Pervenets, and Pinnacle Island subbasins) may contain as much as 36,000 feet of Tertiary sediments. The structural framework, depicted by seismic horizon D, is a result of both compressional and tensional stresses imposed on the Beringian margin by interplate motion. The Navarin forearc basin resulted from the Late Cretaceous-early Tertiary collapse of the Beringian margin during oblique subduction or transform motion between the Kula plate and the North American plate (Scholl and others, 1975; Marlow and others, 1976; Marlow and others, 1981; Marlow and others, Tectonic Evolution, 1983; Whitney and Wallace, 1984).

The Pinnacle Island subbasin, the southernmost depocenter, is 45 miles wide and over 170 miles long. It is an asymmetrical graben filled with as much as 36,000 feet of Tertiary sediments. The 16,000-foot structure contour of horizon D depicts the limits of the structurally defined subbasin. Above a depth of 16,000 feet, the Tertiary sedimentary fill extends beyond the basement topography. The axis of the Pinnacle Island subbasin follows a long, dominantly northwesterly trend that is offset by short, more northerly doglegs. A linear zone containing detached and basement-controlled synthetic normal faults and their antithetic-fault complements flanks the subbasin to the northeast. This dominantly Tertiary fault zone is over 70 miles long and up to 5 miles wide. Although it exhibits no shear component, its magnitude, orientation, and location suggest that it may in part be an older shear zone. Such a shear zone (produced by a converging, right-lateral couple) should be present at an obliquely subducting plate boundary (Harding, 1973). An analog to the Beringian margin shearing couple is the Whittier fault section of the Los Angeles Basin (Lowell, 1984). In this analog basin, the basin axis formed parallel to the shearing couple, and the anticlinal axes are at angles of up to 45° to the basin axis. Similar relationships are apparent between the Pinnacle Island subbasin, the flanking fault zone, and surrounding anticlines.

The Pervenets subbasin, a symmetrical graben 75 miles long and 15 miles wide, lies between the Pinnacle Island and the Navarinsky subbasins (fig. 16). The subbasin contains over 34,000 feet of Tertiary sediment. The 26,000-foot structure contour of horizon D defines the limits of the structurally controlled subbasin (fig. 15). Above 26,000 feet, the Tertiary fill extends beyond the basement topography, linking the Pervenets and the Navarinsky subbasins. At a depth of 26,000 feet, the subbasin axis is discontinuous and exhibits the same dogleg trend as the Pinnacle Island subbasin. This configuration apparently reflects compressional and tensional stresses imposed by the obliquely subducting Kula plate.

The Navarinsky subbasin, the northernmost of the three subbasins, is flanked by the Pervenets subbasin to the south, the Anadyr Ridge to the west, and the Okhotsk-Chukotsk volcanic belt to the north and east (fig. 3). The Navarinsky subbasin is less elongated than the other two subbasins, with dimensions of 70 by 50 miles on horizon D (fig. 15). This deepest subbasin is a graben filled with at least 36,000 feet of Tertiary sediment. The 26,000-foot structure contour defines the limits of the structurally controlled subbasin. Above 26,000 feet, the Navarinsky and Pervenets subbasins can no longer be structurally differentiated.

Basement-rock ridges separate the three Navarin subbasins. Many of these features initially formed as compressional folds associated with basement shear during the early stages of basin evolution. These features remained positive tectonic elements until the late Oligocene (horizon B). The basement ridges near the shelf break flank the Pinnacle Island subbasin and have apparently undergone nearly continuous growth since the early Tertiary. This continuous growth is inferred from the sedimentary drape geometry and the increasing anticlinal widths in younger strata lying above the ridges.

Figure 10 is a line interpretation of a Petty-Ray seismic reflection profile of the shelf break at point A (fig. 34). This interpretation depicts the typical shelf-break setting of a fault-bounded basement ridge. Many of these basement-controlled growth faults parallel the shelf break and offset strata as young as late Miocene. The basement ridge remained a positive tectonic feature from the early Tertiary to the late Oligocene. Unconformities in the Eocene(?), "mid"-Oligocene (horizon C), and late Oligocene (horizon B) apparently breached the ridge. If the ridge was exposed to wave-base erosion during these events, it may have been the source for the onlapping, possible turbidite, deposits seen on several seismic profiles. The late Oligocene unconformity was followed by a transgression which allowed marine deposition beyond the structurally controlled subbasins, thus unifying the several Navarin depositional systems. Horizon B also beveled the basement ridges to a common level, now at a depth of about 1.7 seconds, or about 5,100 feet below sea level.

EXPLANATION

—✱— SYNCLINAL AXIS

—✚— ANTICLINAL AXIS

— 8000 — STRUCTURE CONTOUR OF HORIZON D IN FEET

FAULT, HACHURES ON DOWNTHROWN SIDE

--6C0-- BATHYMETRIC CONTOUR IN FEET

✛ COST NO. 1 WELL

SCALE 1:1,267,200
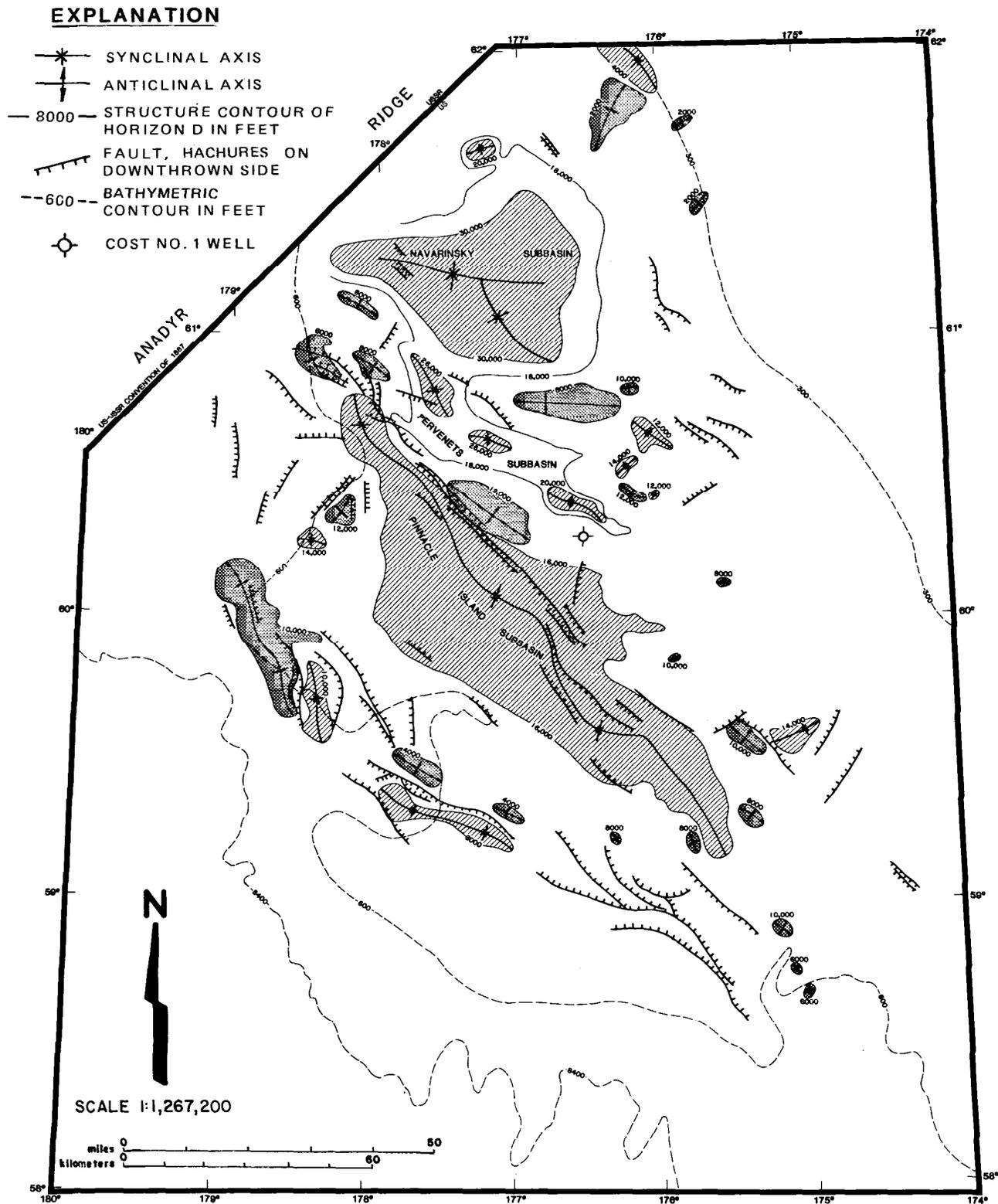
FIGURE 16. Major geologic features of the Mesozoic basement rock represented by horizon D (Late Cretaceous–early Tertiary). Based on the 1978, 1980, and 1981 seismic reflection surveys of Western Geophysical Co.

The basement ridge separating the Pinnacle Island and Pervenets subbasins is a deep, dissected feature which trends northwestward. The ridge is flanked on the southwest by a previously described major fault zone. The northern flank of the ridge is less faulted and exhibits a gradual northwest dip beneath the Pervenets subbasin. This ridge also exhibits nearly continuous growth into the late Miocene. Horizon B (late Oligocene) and horizon A (late Miocene) appear to be conformable over this basement feature, but are unconformable elsewhere in the basin. With the exception of the extreme northwest end of the ridge, where horizon C was truncated by horizon B (fig. 13), neither the ridge nor the overlying strata served as a source for local sediments.

The basement ridge separating the Pervenets and Navarinsky subbasins is a deep, dissected feature which trends northwestward. The top of the ridge ranges from 8,000 to 10,000 feet below sea level. A saddle at a depth of 26,000 feet joins the two subbasins. The saddle separates two large, faulted anticlines with dimensions of 40 by 12 miles and 15 by 4 miles. Growth of these anticlines continued from the early Tertiary into the late Miocene (horizon A, fig. 11).

The onlapping relationship between pre-horizon C stratal surfaces (sequence IV) and the faulted anticlines indicates that the basement rock (sequence V) may have been the source of some Navarin Basin sediments. The truncation of horizon C by horizon B near the tops of these faulted anticlines indicates renewed exposure of the basement rock to erosion (fig. 13). Subsequent deposition of sequences I and II covered the ridge. Deposition continued throughout the remaining Tertiary and into the Quaternary. Anticlinal growth and associated faulting also continued at least through the late Miocene (horizon A).

Both detached growth faulting and basement-controlled faulting appear to be active in the Navarin Basin. High-resolution seismic data reveal fault offsets of sediment as young as Pleistocene near the COST No. 1 well site and along the edges of the individual subbasins, which suggests a basin actively subsiding in response to sedimentary loading and crustal cooling.

Geologic History

The Navarin forearc basin formed in the Late Cretaceous-early Tertiary as a response to oblique subduction or transform motion between the Kula and the North American plates (Scholl and others, 1975; Marlow and others, 1976; Cooper and others, 1976). The initial opening of the Navarin Basin apparently was a response to pull-apart tectonics imposed on the Beringian shelf by this interplate motion. A major shear couple developed from this motion, causing the sudden subsidence of the three fault-bounded subbasins. The shear couple is evidenced by a fault zone located between the Pinnacle Island and Pervenets subbasins, which also display disjointed subbasin axes and compressional folding of the Mesozoic basement rock (fig. 16). The Kula plate moved northwestward past the Beringian shelf and underthrust the Koryak-Kamchatka coast, thus forming a magmatic arc (the Okhotsk-Chukotsk volcanic belt, fig. 3) parallel to the subduction zone (Meyerhoff, 1980) and the Anadyr Basin (Marlow and others, Tectonic Evolution, 1983). The arc extends from eastern Siberia to western Alaska, paralleling the Beringian margin. Exposures of volcanic-arc material are found on western St. Lawrence Island and on St. Matthew, Pribilof, and Nunivak Islands. Arc-type materials dredged from the Navarin outer shelf and upper slope have whole-rock K-Ar dates of late Paleocene or early Eocene. Marlow and Cooper (1984) propose that the perplexing occurrence of arc lithologies on the Beringian margin may represent material either rafted by the Kula plate from the tip of the Alaska Peninsula or emplaced via a "leaky" transform margin.

South of the volcanic belt in eastern Siberia, the Koryak Range was formed by the obduction of allochthonous blocks of melange and olistostrome sequences. Orogenic movement of the range continued into the Paleocene, as evidenced by the folded Paleocene marine rocks found along the southern edge of the range (Aleksandrov and others, 1976; McLean, 1979a; Marlow and others, 1981). There are at least 6,000 feet of Paleocene marine rocks composed of argillite, siltstone, spilite, sandy claystone, shale, andesite, and cherty volcaniclastics present in the Koryak Range (Pichugina and others, 1974). Dredge samples from the Navarin continental slope also contain early Eocene and Paleocene volcanic sandstone, limestone, conglomerate, and brecciated mudstone (Marlow and others, Description of Samples, 1983).

These marine Paleocene and early Eocene rocks, though not present in the COST well, are considered to be present within seismic sequence IV (bounded on the bottom by horizon D, fig. 15). The areawide erosional degradation represented by the horizon D unconformity apparently occurred after early Tertiary deposition commenced in the Navarin Basin.

The Late Cretaceous-early Tertiary erosion of the Navarin shelf is represented by a time-transgressive unconformity (horizon D). This breakup unconformity occurred in the period between the amalgamation of Mesozoic allochthonous basement elements with the Bering Sea continental shelf and postrift collapse and subsequent Tertiary deposition. Paleomagnetic, geologic, and paleontologic data suggest that a Mesozoic basement rock terrane, which encompasses the forearc basin province, was rafted northward and docked against the Bering sea margin (McGeary and Ben-Avraham, 1981; Stone and others, 1982; Keller and others, 1984). Paleomagnetic data from the Navarin COST well suggest that although the Cenozoic section was deposited within 5° of the present well site, the Late Cretaceous section may have been deposited as much as 50° south of the present location. The amalgamation of the Mesozoic basement rock terrane occurred before the formation of the Aleutian Arc in the late Eocene (Whitney and Wallace, 1984). Alternatively, an existing Aleutian Arc subduction zone complex could have migrated northward with the Mesozoic basement rock terrane and docked against the Beringian margin by the late Eocene. In either case, initiation of subduction along the Aleutian Arc at its present position isolated the Kula plate, which now floors the Aleutian Basin (Scholl and others, 1975; Cooper and others, 1976). The Kula plate apparently continued moving northwestward after its isolation in the late Eocene. Blanton (1977) postulates that this motion was a function of the subducting Kula plate's momentum and its density contrast with the asthenosphere. This interplate motion and the resulting stresses caused the rapid structural downdropping of the subbasins. This "event" may be marked by the abrupt change from an outer neritic to an upper bathyal environment indicated by changes in the late Eocene foraminiferal faunas seen in the COST well. This paleobathymetric shift may be correlative with the 42-million-year event postulated by Whitney and Wallace (1984). By the late Oligocene, the Kula plate had reached a state of static equilibrium. Synkinematic deposition continued into the late Oligocene. Normal faulting offsetting the Tertiary fill occurred along planes of weakness established by the shear couple (such as the fault zone located between the Pinnacle Island and Pervenets subbasins).

Paleocene and early Eocene synkinematic marine deposition took place in structurally controlled subbasins separated by growing basement ridges. An isopach map of seismic sequence IV suggests that there may be several thousand feet of sediment present that was derived from adjacent basement highs during horizon D erosional episodes (fig. 15). The diverging reflections of sequence IV suggest

constant clastic deposition in rapidly subsiding subbasins. These strata were isolated from chronostratigraphic equivalents in eastern Siberia by the offshore Anadyr Ridge.

Data from the COST well show that Cenozoic sedimentation within the three subbasins consisted of predominantly marine mudstone and siltstone. Anoxic conditions preserved the abundant kerogen found in the organic-rich, outer neritic and upper bathyal mudstones of zones E and F (early Oligocene and late to late middle Eocene). These potential source rocks are distributed throughout the Navarin Basin and may be several thousand feet thick in the subbasin centers. Local unconformities, such as the unmapped Eocene(?) events along the shelf break, may have supplied some coarser grained sediment to the basement-high flank deposits adjacent to these deepwater subbasins. A regional regressive event (horizon C) in the middle Oligocene exposed older Tertiary and Mesozoic basement highs to wave-base erosion, which may have generated additional aprons of coarser grained detritus along the subbasin flanks. In both instances, the coarse-grained material may have formed proximal turbidite deposits in the upper and middle bathyal environment of the adjacent subbasins. These turbidite deposits may be reservoirs in hydrodynamic contact with Eocene source rock.

At the COST well site, the environment "shoaled" from middle bathyal to middle neritic water depths during Oligocene time. Mudstone dominates the early and late Oligocene section beneath the diachronous horizon B. The arc-type material of the Okhotsk-Chukotsk volcanic belt and the metamorphic rock of the miogeoclinal belt were the probable source terranes for most of the Oligocene section.

A sea level drop during the late Oligocene (horizon B) exposed local subbasin highs to wave-base erosion and reduced them to a common base level. Locally sourced shelf sands were then deposited, probably throughout much of the basin, by an areawide shelf depositional system which persisted into the late Miocene. At the COST well, this deposition is reflected by a predominantly sandstone sequence. The lower half of this sandstone section is a generally regressive sequence; the upper half is largely transgressive. The regressive sequence contains the thickest and cleanest potential reservoir sands, which are considered to represent offshore bar deposits. These shelf sands may grade into deeper water lithofacies in the subbasin centers.

The cessation of interplate motion initiated a regional subsidence controlled primarily by crustal cooling. This subsidence was subsequent to the regional degradation of horizon B. Erosional truncation of subbasin highs to a common base level allowed an areawide unification of the three subbasin depositional systems.

At the COST well, early Miocene basaltic sills intruded the nonmarine, Late Cretaceous section. This igneous activity may be attributable to crustal thinning and deepening.

A late Miocene angular unconformity (horizon A) is present in the northwest area of the basin. Stratal surfaces older than horizon A were uplifted by shale diapirism and truncated by the erosional surface represented by horizon A. At the COST well, horizon A may represent a depositional hiatus. Similarities between COST well lithologies and dredge samples indicate relatively uniform, regional deposition since horizon A time. A prograding wedge of Miocene-Pliocene sediment along the Pervenets Ridge, however, indicates a change in the rate of sea level rise or of basin subsidence since horizon A time.

Both detached growth faulting and basement-controlled faulting offset strata as young as Pleistocene throughout the margins of the individual subbasins. Many of these faults are associated with basement ridges that have displayed continual growth since the early Tertiary.

II. Petroleum Geology

Exploration History

The earliest petroleum exploration in shelf basins of the western Bering Sea was initiated by the Soviet Union in 1959 in the onshore portions of the Anadyr and Khatyrka Basins (McLean, 1979a). The Navarin Basin lies south and west of these two basins (fig. 3). The Anadyr and Navarin are both forearc basins flanked by the Okhotsk-Chukotsk volcanic arc. Although the basins are separate and structurally distinct, the seismic velocity profile of each basin suggests that their depositional histories were similar (Marlow and others, 1981). Because the three basins are geographically close and geologically similar, petroleum exploration data from the Anadyr and Khatyrka Basins are useful in evaluating the hydrocarbon potential of the Navarin Basin.

Between 1963 and 1978 the Soviet Union drilled over 30 onshore exploratory and stratigraphic test wells, most of them in the larger Anadyr Basin. Exploratory results were discouraging, and both reservoir rock distribution and timing of trap formation appeared to be major problems. Gas shows were reported in Miocene sandstones, and oil and gas shows were reported in Eocene and Oligocene strata. One well produced excellent initial gas shows from at least 10 middle to upper Miocene sandstones with an aggregate thickness of 260 feet. These sandstones had porosities over 20 percent and permeabilities from 92 to 560 millidarcies. However, reservoir pressures declined rapidly with further testing, which suggests that the sandstones were small-volume, lenticular bodies (McLean, 1979a). Although the most prospective reservoir rocks were encountered in Cretaceous and upper to middle Miocene sandstones, the interbedded source shales contained mostly gas-prone humic organic matter. The more oil-prone Eocene, Oligocene, and lower Miocene sections contained only tight sandstones (McLean, 1979a).

Exploratory drilling since 1978 has yielded more encouraging results. In 1981 an oil discovery was reported. This discovery, although not a commercial find, stimulated further drilling. To date, commercial accumulations of both oil and gas condensate have been reported from the Anadyr lowlands of the Anadyr Basin (Oil and Gas Journal, 1984). Specific data on reservoir horizons or flow volumes were not disclosed.

Private industry has conducted seismic surveys in the Navarin Basin since 1971. From 1971 through 1984 industry collected a total of 90,653 trackline miles of deep-penetration, multichannel seismic reflection data. In addition, a total of 9,942 trackline miles of single-channel, high-resolution seismic reflection data have been collected by industry since 1982. There was a noticeable increase in seismic activity leading up to Sale 83, the first oil-and-gas lease sale in the Navarin Basin. The rapid increase in seismic exploration activity between 1976 and 1983 reflected the petroleum industry's need for adequate coverage over prospective areas in the basin.

Government and academic seismic surveys of the Navarin Basin have been conducted since the mid-1960's. These regional framework surveys were mostly uncoordinated reconnaissance-mapping efforts. The exact amount of data collected is unknown, but is much less than that obtained by private industry.

Dredge and gravity core sampling along the Bering Sea continental slope west and southeast of the Navarin Basin (from 1977 to 1983) provided the only lithologic data before the drilling of the Navarin COST well in 1983. Geological information from the well, released by MMS shortly after Sale 83, represents the first nonproprietary subsurface data available from the Navarin Basin (Turner and others, 1984).

Just before Sale 83, Carlson and Marlow (1984) reported a probable plume of gas escaping from the sea floor in the northern Navarinsky subbasin. The plume was detected on high-resolution reflection records and is apparently escaping from the crest of an eroded shale diapir. Numerous shallow seismic anomalies in the northern half of the basin had previously been attributed to gas-charged sediment (Carlson and others, 1982), and light alkanes and alkenes had been detected in sediment samples (Vogel and Kvenvolden, 1981; Golan-Bac and Kvenvolden, 1984a, 1984b). However, the plume, if composed of thermogenic gas, is the first evidence in the basin of hydrocarbons leaking from an anticlinal structure (Carlson and Marlow, 1984).

Sale 83 was held by the MMS in April 1984. A total of 5,036 lease blocks covering about 28 million acres were offered. Despite the remoteness of the area and the water depths, 186 blocks covering about 1 million acres received $1.148 billion in total bids. High bids totaled over $631 million. The highest bid was over $39 million for a block on a large structure in the central part of the basin (approximately 25 miles northwest of the COST well). The first exploratory drilling is expected to take place in 1985.

Geothermal Gradient

The geothermal gradient measured in the COST well has been used as an approximation for calculations and interpretations throughout the basin. Because this gradient is so important in understanding the petroleum potential of the basin, the derivation is given in its entirety. The geothermal gradient greatly controls organic maturation and several temperature-dependent diagenetic processes and genetically related geophysical phenomena such as the alteration of biogenic silica and smectitic clay (fig. 17). For instance, thermally activated smectite dehydration is a critical factor in the timing and availability of water as a vehicle for hydrocarbon migration. Smectite diagenesis is also a critical factor in the occurrence of abnormal formation pressure, which probably plays a fundamental role in both the development of some potential traps and the preservation or enhancement of reservoir quality with depth (Bruce, 1984; Surdam and others, 1984). The relatively shallow zone of biogenic silica diagenesis may act as a local or regional sealing horizon.

The thermal gradient for the Navarin Basin COST No. 1 well was determined by using the High Resolution Thermometer (HRT) log, bottom hole temperatures (BHT) from the logging runs, and formation fluid temperatures from the drill stem test (DST) and from the Repeat Formation Tester (RFT) log. True formation temperatures were estimated from each logging run by extrapolating BHT measurements obtained from successive log suites to a static formation temperature.

The analytical extrapolation technique consists of a linear regression applied to the suite of BHT measurements versus the logarithm of the expression:

$$\frac{dt}{t + dt}$$

where for each measurement, dt = time after circulation stopped (hours) and t = circulating time (hours). The extrapolation of the obtained line to the temperature reached when

$$\frac{dt}{t + dt} = 1$$

should define true static formation temperature (fig. 18).
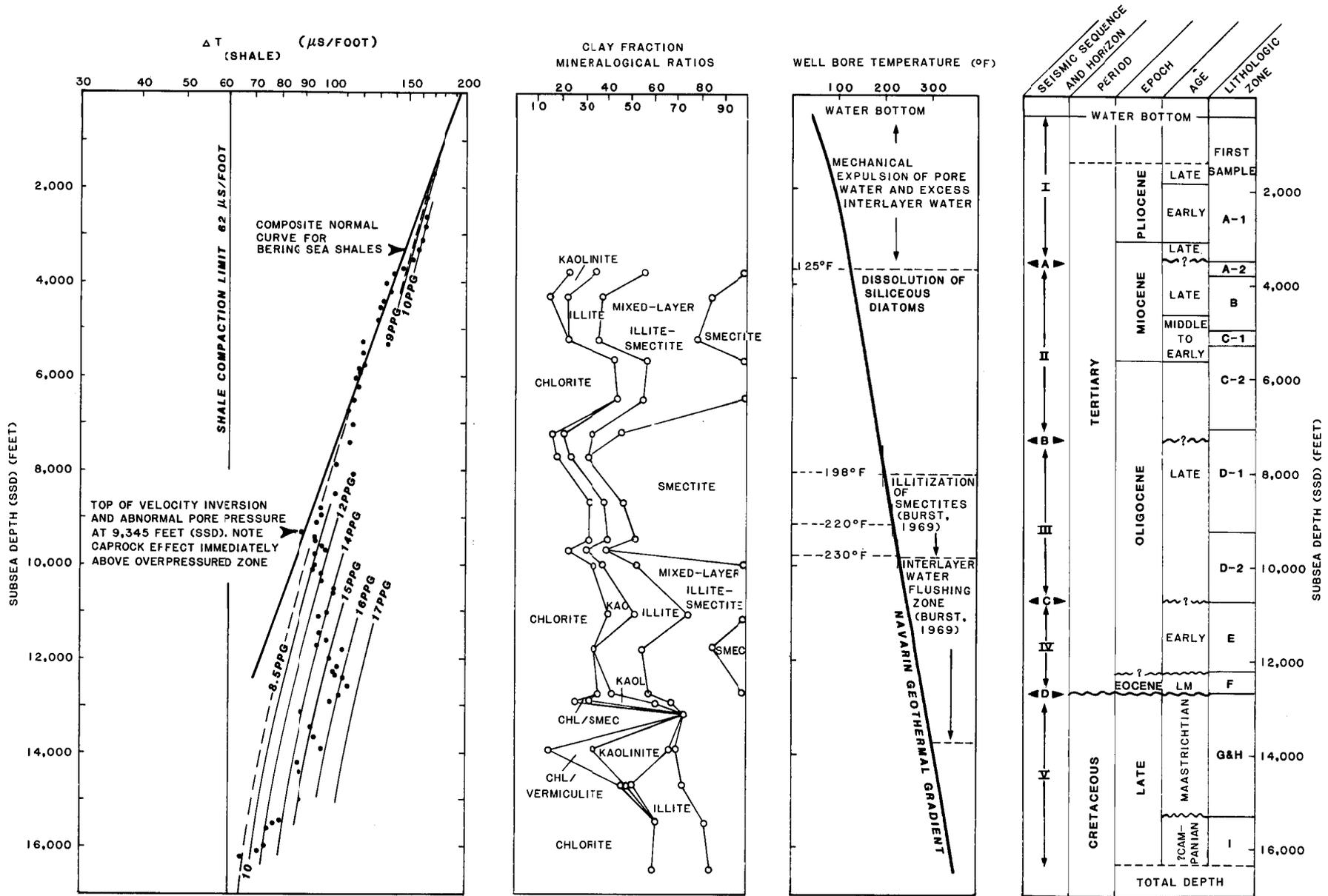
FIGURE 17. Geothermal gradient of the Navarin Basin COST No. 1 well, and temperature-related diagenetic effects on sediment mineralogy, compaction and abnormal pressure. (Modified from Sherwood, 1984).

This technique is based on the observation that temperature rise after circulation has stopped is similar to static pressure buildup and thus may be analyzed in a similar manner (Fertl and Wichmann, 1977). In practice, this technique yields accurate estimates of true static formation temperature except when circulation times are in excess of 24 hours.

After static BHT was calculated from each logging run, a plot of temperature versus depth was constructed by using all available temperature data (fig. 19). After comparing the various data and noting the characteristics of heat transfer between drilling fluids and formation lithology and fluids, it was determined that the true thermal gradient was best approximated by the static BHT and DST data.

The thermal gradient obtained from the HRT log is anomalously high. This log was run through the cased section of the hole (from the sea floor to 12,834 feet) after total depth had been reached. Drilling mud heated by the higher temperatures at the bottom of the hole was circulated past the well casing string for 63 days before reaching total depth. This heat was readily conducted from the mud through the casing and heated the upper borehole above true formation temperature. Theoretically, this effect should increase uphole and probably accounts for the progressive divergence upward of the HRT thermal gradient from the estimated true geothermal gradient in figure 19.

The RFT temperature data were also found to be generally unsatisfactory for calculating the true geothermal gradient. This is probably a function of the small amount of formation fluid sampled in an RFT test and the resulting susceptibility of this test to near-borehole thermal modification. RFT data were apparently affected by a process similar to the one that affected the HRT data; that is, the heat transfer in the upper sections of the borehole was from the mud to the formation (warming the formation), but the heat transfer in the lower sections of the borehole was from the formation to the mud (chilling the formation). This process of thermal modification may account for the slight positive uphole divergence of the RFT temperatures in logging run 1 from the calculated true geothermal gradient.

Thermal modification also probably accounts for the low RFT temperatures obtained in runs 2 and 3. These low temperatures were obtained from relatively deeper sections of the well at the time logging runs 2 and 3 were recorded and are due to the relatively cool circulating mud chilling the formation adjacent to the borehole. RFT temperatures in the extensively sampled sandy interval from 5,000 to 7,000 feet approximate the flowline mud temperatures recorded during drilling. This suggests thermal equilibration (cooling) of the formation with the well bore through contact with the relatively cool circulating mud. RFT temperatures in this sandy

Static Bottom
Hole Temperature
(BHT) at 11,060 Feet →

Bottom Hole
Temperature
(°F)

$$\frac{dT}{T + dT}$$
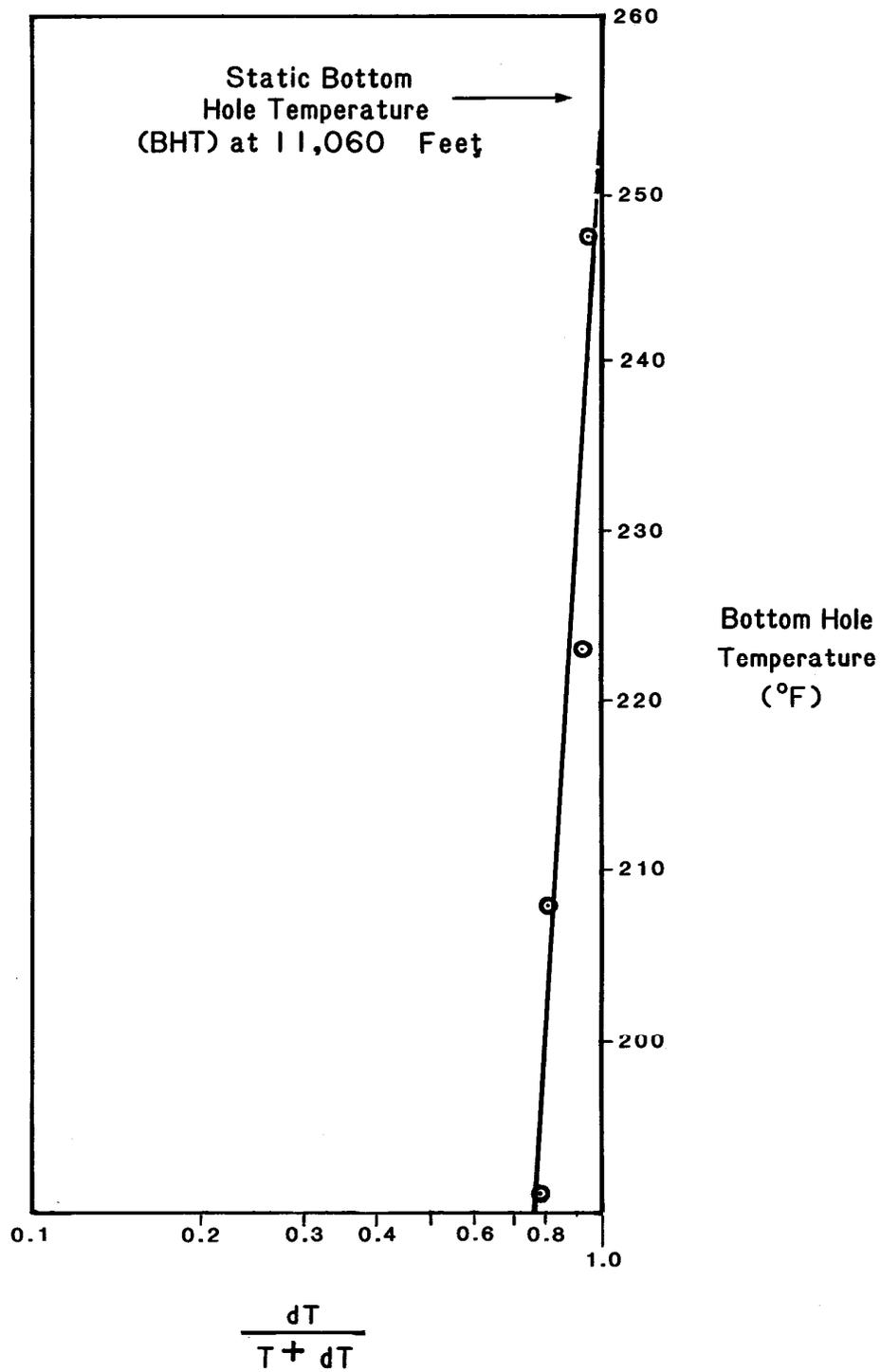
T equals circulating time in hours and
dT equals elapsed time after circulation stopped.

FIGURE 18. Extrapolation of bottom hole temperatures (BHT) to determine static BHT for logging run 2, Navarin Basin Cost No. 1 well.
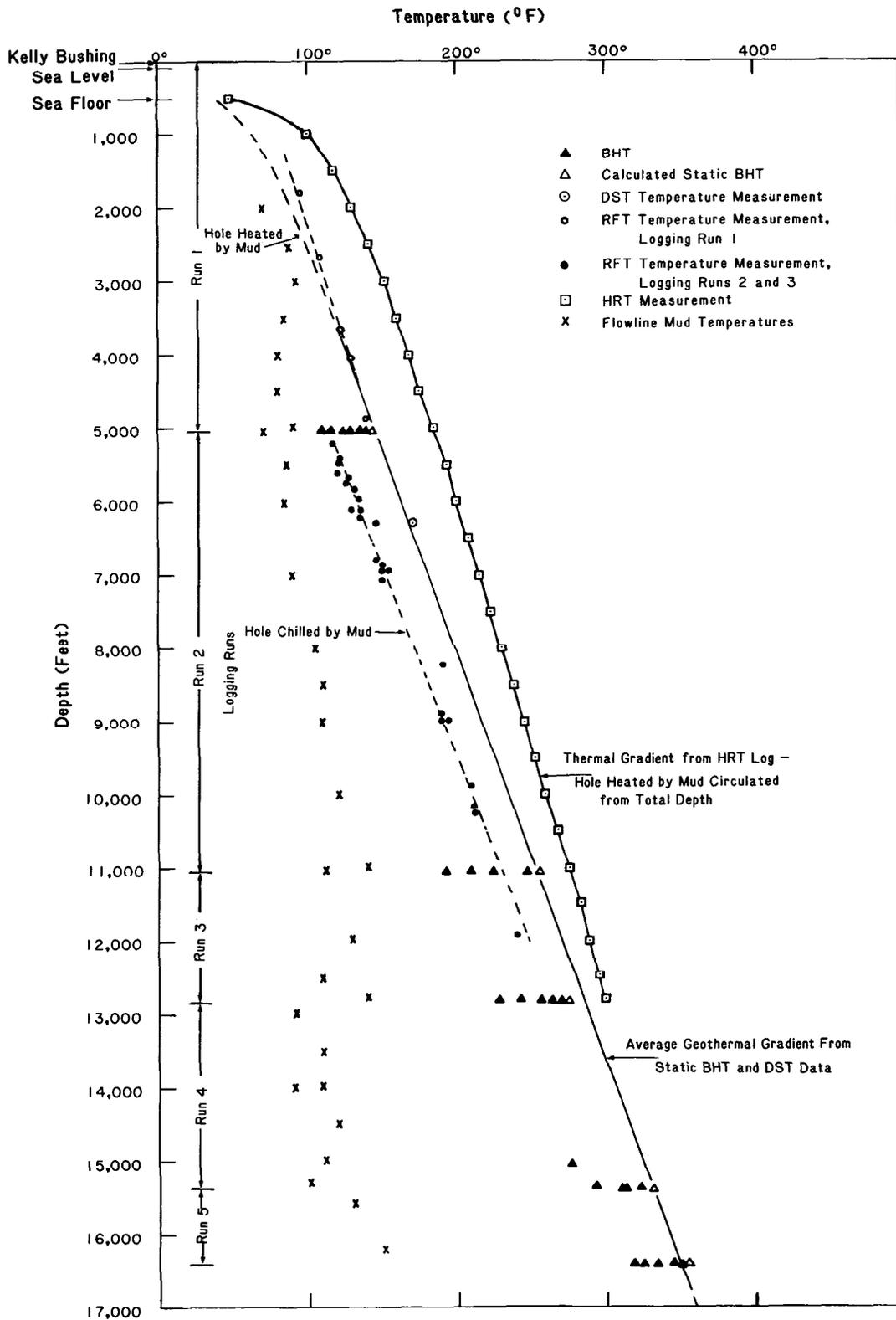
FIGURE 19. Thermal gradient for the Navarin Basin COST No. 1 well.

interval are farther displaced from the calculated geothermal gradient than those measured in the underlying mudstone interval (7,000 to 10,300 feet). This is probably due to the inherently greater thermal conductivities of the sandstones.

The single DST temperature was assumed to represent in situ formation temperature because the DST extracted a large volume (55 barrels) of formation fluid and thus sampled fluid a sufficient distance from the borehole. The DST temperature falls very close to the geothermal gradient calculated from the BHT data.

Linear regression (least squares) was applied to the static BHT and DST data to determine the average geothermal gradient shown in figure 19. This yielded a gradient of 1.78 °F per 100 feet from total depth (16,400 feet) to about 3,800 feet. Above 3,800 feet, the gradient is higher and is estimated to be 2.5 °F per 100 feet, on the basis of an assumed sea-floor temperature of 40 °F. This higher gradient is attributed to the change in lithology and degree of compaction at 3,800 feet. The unconsolidated, undercompacted diatomaceous sediments above 3,800 feet appear to be overpressured (Sherwood, 1984) and have an excessively high fluid content. Because of the overpressuring and because water has a lower thermal conductivity than sediment, this interval has a lower average thermal conductivity than the more compacted rocks below 3,800 feet. This effect has apparently produced the characteristic higher geothermal gradient observed in the well.

Organic Geochemistry, Source Rocks, and Thermal Maturity

Geochemical sampling programs have been conducted in the Navarin Basin since about 1977. Most of these studies were performed by the petroleum industry and are proprietary. Since 1980 the USGS has exhibited a mounting interest in the occurrence of hydrocarbon gases in the Bering Sea shelf province (Carlson and others, 1985; Carlson and Marlow, 1984; Golan-Bac and Kvenvolden, 1984a, 1984b; Vogel and Kvenvolden, 1981; Kvenvolden and Redden, 1980). Detailed subsurface organic-geochemical analyses, thermal maturity, source rock potential, and temperature observations became available with the drilling of the first Navarin Basin COST well in 1983 (Turner and others, 1984).

SOURCE ROCK POTENTIAL

The COST well penetrated three intervals with source rock potential: the Late Cretaceous interval, the Eocene-early Oligocene interval, and the late Oligocene interval. Geochemical data from the well showing organic richness and source potential are presented in plate 2 and figures 20 and 21.

Late Cretaceous Interval

The deepest potential source rock interval occurs between 15,300 and 16,400 feet in the COST well (lithologic zone I, pl. 1). It is a Late Cretaceous sequence of claystone, siltstone, mudstone, and tuff deposited in inner neritic to upper bathyal marine environments. The total organic carbon content (TOC) is low, generally around 0.5 percent. A few cuttings samples yielded higher TOC values, but these appear to be due to coal contamination from overlying horizons. Cores 19 and 20 were cut from this interval. Core 19 contains modest amounts of $C_{15}+$ hydrocarbons and plots between the gray shales and carbonates on figure 21. It is a clastic sediment containing largely vitrinitic kerogen (pl. 2). It is very mature. Random vitrinite reflectance (R_0) is in excess of 1.3 percent.

This interval is not a likely source rock at the COST well. The deposition of a more hydrogen-rich kerogen plus a fortuitous

facies change that preserved more organic carbon would be necessary for these rocks to constitute source material at this location. Although this horizon does occur within the wet-gas generative zone in the COST well, the migration of hydrocarbons to a cooler environment would probably be necessary to ensure their preservation elsewhere in the basin.

Eocene-Early Oligocene Interval

The most favorable lithology with source rock potential occurs between approximately 11,700 and 12,780 feet (lithologic zone F and the lower part of zone E). These early Oligocene to Eocene rocks consist of gray claystone and organic-rich claystone with local limestone lenses and calcite-filled fractures. The sequence was deposited in outer neritic to middle bathyal environments. The base of this section is marked by an angular unconformity which separates it from coal-bearing, nonmarine sediments of Cretaceous age. The possible unconformity at the top of the Eocene lithology is marked by a decrease in the wetness of the light hydrocarbons, a decrease in the content of $C_{15}+$ hydrocarbons and bitumen, and a brief increase in the vitrinite content of cuttings samples. There is no apparent change in TOC or in the response of pyrolysis analyses of kerogen. Total organic carbon content in this section is generally between 1.0 and 2.0 percent from a mixture of types II and III kerogen. The sum of amorphous plus exinitic kerogens is generally greater than 65 percent (pl. 2).

Core 14 (12,715 to 12,743 feet) has organic carbon contents that range from 1.31 to 1.89 percent. Hydrogen indices from this core are between 286 and 362 milligrams of hydrocarbons per gram of organic carbon, which when plotted on a modified Van Krevelen diagram in the context of the rest of the geochemistry, indicate a type II kerogen (fig. 20). The amount of $C_{15}+$ extractable hydrocarbons from this core sample approaches the amount observed in known reservoir rocks (fig. 21), which combined with the low oxygen indices might indicate contamination.

This early Oligocene to Eocene lithology in the COST well falls within the catagenetic zone, as defined by Hunt (1979) and Tissot and Welte (1984), where microbial activity ceases and increased temperatures promote the thermally driven reactions responsible for the formation of petroleum. Random vitrinite reflectance (R_0) reaches 0.6 percent at approximately 9,400 feet and 1.3 percent by about 15,000 feet. Abnormally high pore pressures occur between 9,430 and 15,300 feet, which could facilitate the liberation of hydrocarbons from these sediments.

Late Oligocene Interval

The third zone which could contain source rocks extends from about 7,400 to 11,700 feet (lithologic zones D-1, D-2, and the upper part of E). These sediments are composed largely of sandy
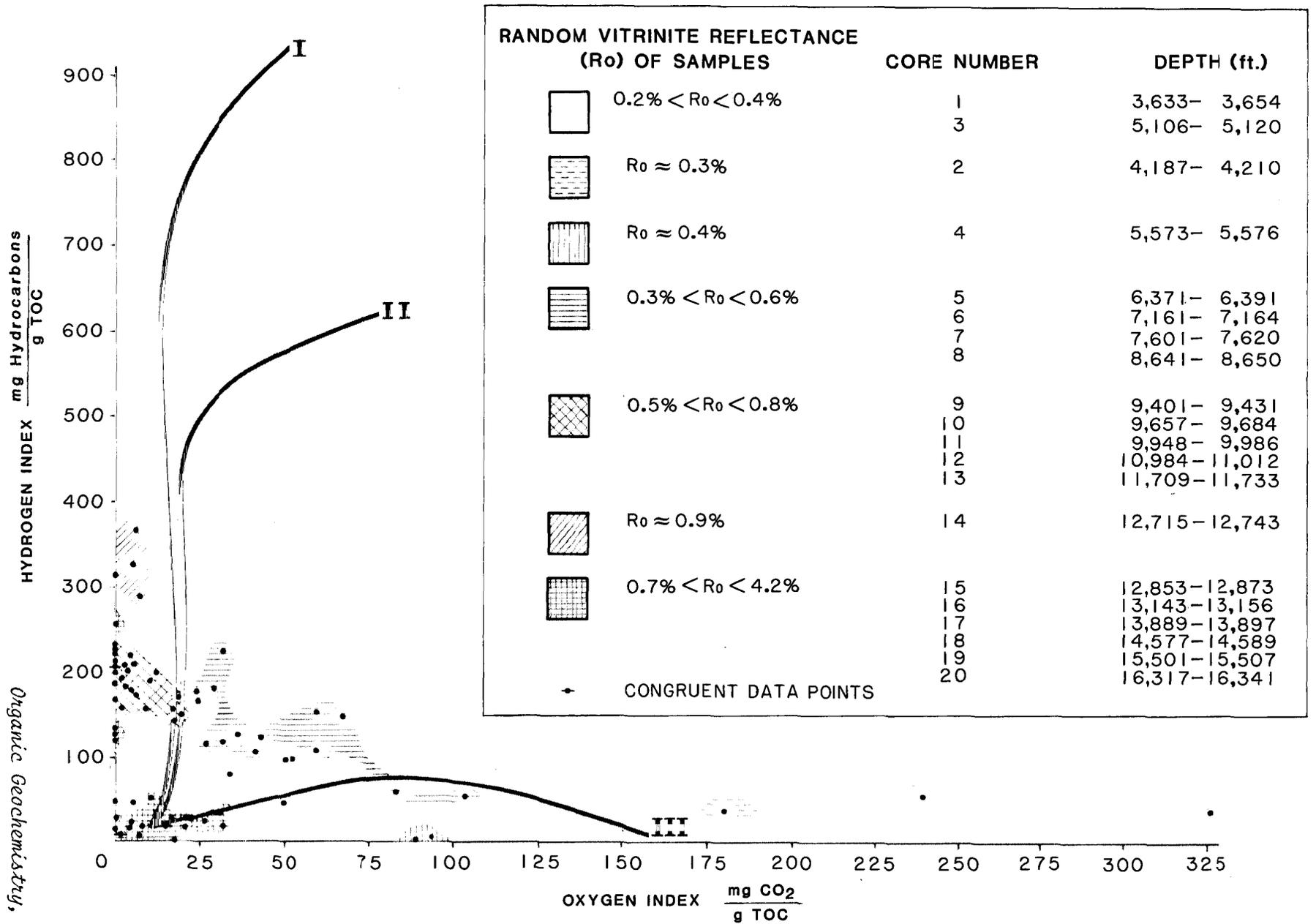
FIGURE 20. Modified Van Krevelen diagram from conventional cores, COST No. 1 well.

mudstone, fine-grained muddy sandstone, and claystone, with rare lenses of siltstone and sandy carbonate. The section was deposited in environments that ranged from outer neritic to middle bathyal. The total organic carbon content is relatively low, ranging from less than 0.5 to just under 1.0 percent. Relative amounts of sapropelic kerogen exceed 65 percent in isolated instances. The hydrogen index peaks just above 200 milligrams of hydrocarbons per gram of TOC in a similarly sporadic manner (pl. 2). On the modified Van Krevelen diagram (fig. 20), data from this interval appear to be distributed between type II and type III kerogen. All of this suggests an intermingling of kerogen from both marine and terrestrial sources. Except for the bottom of the interval, these sediments are immature, entering the catagenetic stage at about 9,400 feet. Although the source potential of this lithologic sequence is limited at this location, it is organically rich enough and sufficiently mature to produce hydrocarbons with only a modest facies change and slightly greater depths of burial. This lithology may, therefore, constitute source rock elsewhere in the Navarin Basin.

In summary, the most promising source rocks seen in the COST well occur between seismic horizons B and D, at approximately 7,400 and 12,700 feet, respectively (lithologic zones D-1, D-2, E, and F). The richest organic material is immediately above the Cretaceous-Tertiary unconformity within lithologic zone F and the lower 80 feet of lithologic zone E.

The COST well is situated on the eastern edge of the Navarin Basin, and seismically recognized lithologic sequences thicken in nearly every direction away from the well. It is possible, therefore, that the total thickness of potential source beds also increases away from the well. Although the effects of facies changes are as yet unknown, it is possible to estimate the effect the geometry of the sedimentary basin may have upon the relative level of maturity of a given lithology if certain assumptions are made.

THERMAL MATURITY

Various models have been developed to predict the relative level of thermal maturity of organic material within buried sediments in response to the thermal gradient. Lopatin (1971) suggested a method for applying the Arrhenius equation to calculate a coefficient he called the time-temperature index (TTI), which serves as a measure of thermal maturity, corresponding to random vitrinite reflectance (R_0) or Staplin's thermal alteration index (TAI). This model has recently been successfully used by a number of authors because of its flexibility in situations where both the quantity and quality of available data are not completely adequate (Zieglar and Spotts, 1978; Macmillan, 1980; Magoon and Claypool, 1983; Issler, 1984).
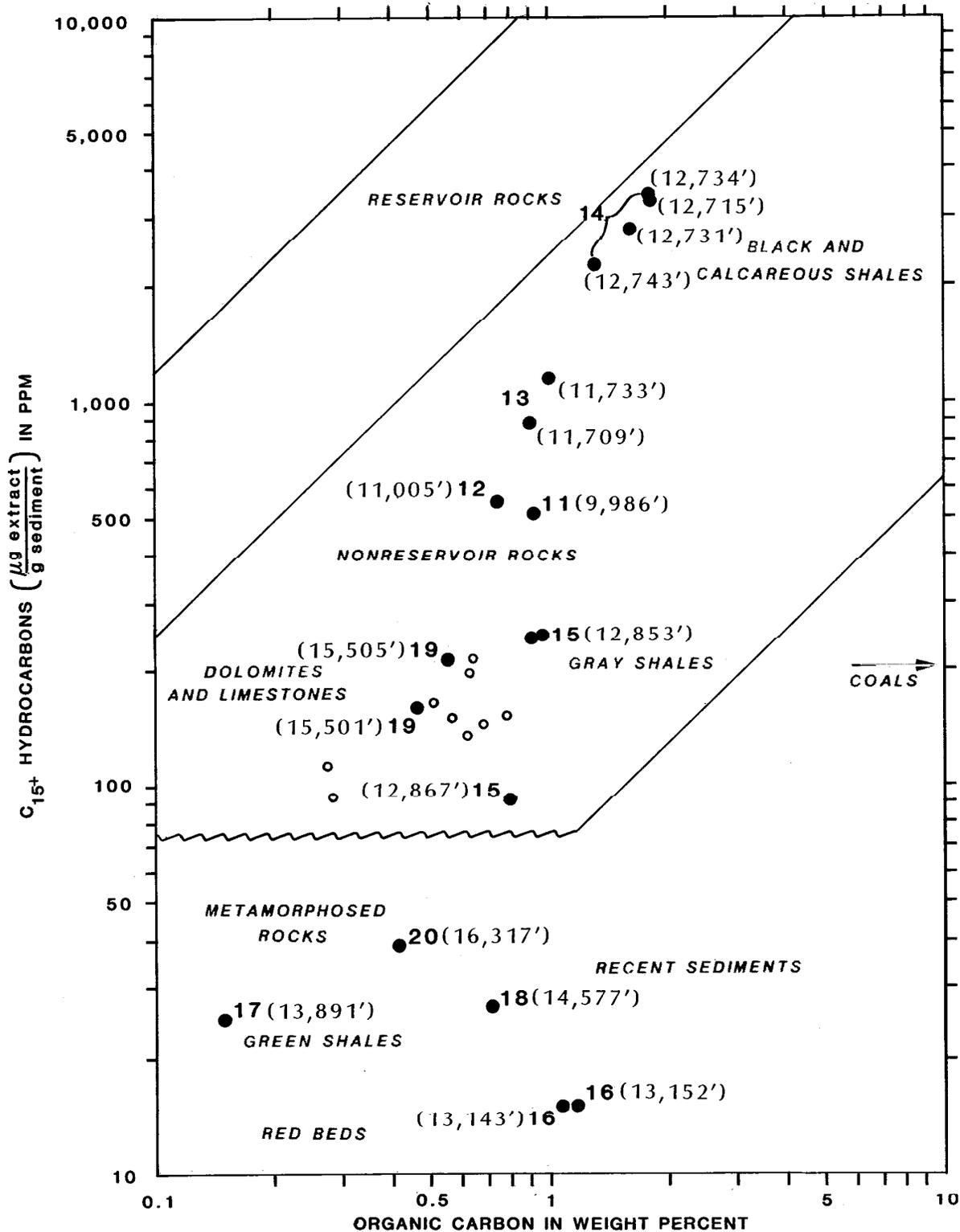
FIGURE 21. Total organic carbon and extractable C_{15}^+ hydrocarbons, COST No. 1 well. Analyzed by Robertson Research (US) Inc.

It can be demonstrated from the Arrhenius equation that the rate of a chemical reaction doubles for every 10 °C increase in temperature if the activation energy and the temperature of the reaction are relatively low (Tissot and Welte, 1984). Upon burial, sediments become progressively hotter, and one can, therefore, calculate an interval maturity by multiplying the time of residence ΔT in a temperature interval of 10 °C by a factor of 2^n, which changes to 2^{n+1}, 2^{n+2}...$2^{n_{max}}$ every 10 °C. Lopatin arbitrarily assigned a value of 0 to n for the temperature interval from 100 to 110 °C. The total sum of the interval maturities is termed the time-temperature index, or TTI.

$$TTI = \sum_{n_{min}}^{n_{max}} 2^n (\Delta T_n)$$

Tissot and Welte (1984) feel that this model does not adequately take into account the consequences of the higher temperatures and greater activation energies that are believed to be involved after the peak of oil generation has been reached, where thermal cracking becomes the predominant reaction. However, uncertainties in frontier areas regarding temperature gradients, the absolute ages of sediments, the composition of organic material, the timing and amount of tectonic activity, and the possibility that temperature gradients have changed through time probably represent much more formidable problems than chemical kinetics. Frequently, for example, there is no adequate drilling history from which a correction can be computed for raw temperature data taken from a drill hole, and often only a single bottom hole observation is available, necessitating a rough estimate of the surface temperature and the consequent temperature gradient.

Despite these difficulties, Waples (1980) correlated TTI values with R_o values using several reaction rates for 402 samples from 31 wells worldwide. He concluded that the 2^n factor originally proposed by Lopatin was satisfactory. Issler (1984) correlated TTI values and R_o measurements from offshore eastern Canada and compared them with Waples' values. These TTI values and R_o measurements fell within the statistical variation of Waples' data. The TTI and analogous R_o values from the Navarin Basin also fall within these limits.

To apply the Lopatin model, it is necessary to reconstruct the depositional and tectonic history for the sediments being studied. This has been done for seismic horizons A, B, C, and D, plus a hypothetical Cretaceous horizon K, at the COST well (pl. 3). These horizons were selected because they represent the boundaries of seismic sequences that are regionally traceable. Horizon K, within the Mesozoic "basement," has been included in order to project TTI values to greater depths and to facilitate an estimate of the maximum amount of erosion at the Cretaceous-Tertiary

unconformity that will satisfy the thermal constraints imposed by
the model. Approximate ages (in millions of years before present)
and depths for the seismic horizons are given in table 2.

Table 2. Depths and absolute ages of seismic horizons in the
Navarin Basin COST No. 1 well used in Lopatin computation.

Horizon	Depth (feet)	Age (m.y.)
A	3,560	7
B	7,400	24
C	11,000	30
D	12,700	40
K	15,000	70

Waples (1984) considers the greatest source of error in time-
temperature modeling to be poor temperature data. Because drilling
fluids alter the ambient rock temperature, a correction must be made
for observed temperature measurements. Bottom hole temperatures
taken at the end of each drilling run were corrected using a method
by Fertl and Wichmann (1977) which yielded a temperature gradient of
1.78 °F per 100 feet (0.989 °C per 100 feet) below 3,800 feet. This
gradient agrees favorably with a drill stem test, several observations
from the repeat formation tester, and temperature estimates from
probable silica phase changes. Above 3,800 feet, the temperature
gradient is curvilinear and individual measurements are erratic,
probably due to inhomogeneities in the uncompacted sediments. A
reasonable estimate of average sediment temperature near the sea
floor is 40 °F. However, conjectures concerning the temperatures
at less than 3,800 feet are rather academic, because these
temperatures are no greater than about 50 °C, with the result
that 2^n is less than 0.03, a value which yields TTI values less
than 0.05 in the COST well. For the Lopatin model used to estimate
levels of thermal maturity in the Navarin Basin, it is assumed that
the temperature gradient is constant throughout the basin and that
it has not changed appreciably for the last 70 million years. This
assumption produces TTI values that agree favorably with R_0 values
worldwide (Waples, 1980) and with observations from the COST well
(fig. 22).

The main zone of oil generation, also termed the oil generation
window, has been identified by various authors using random vitrinite
reflectance (R_0) (table 3).

Table 3. R_0 values for the oil generation zone.

Author	R_0 Range
Dow, 1977	0.6 to 1.35%
Hunt, 1979	0.6 to 1.35%
Tissot and Welte, 1984	0.5 to 0.7% < R_0 < ca. 1.3%
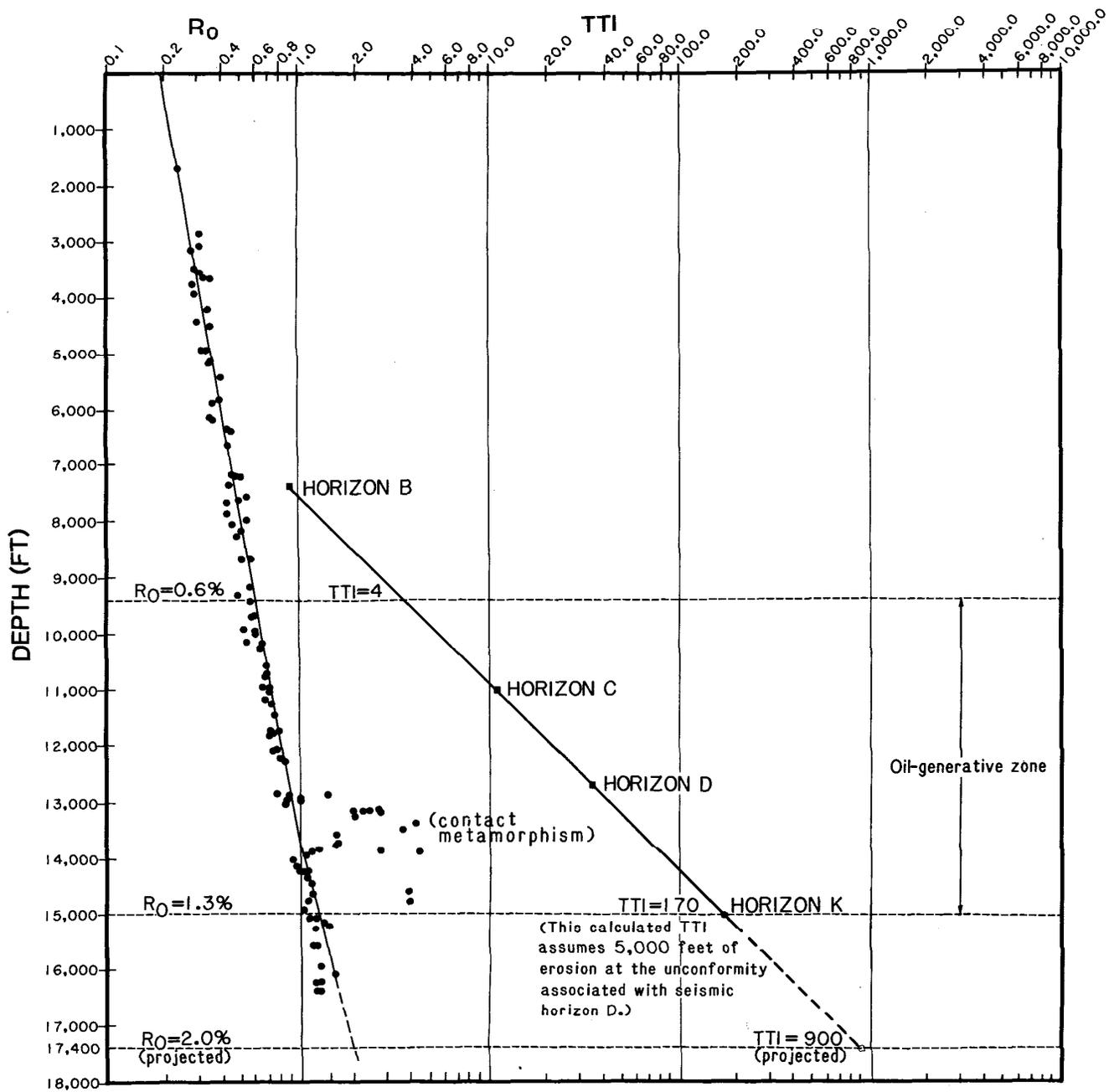
FIGURE 2.2. Correlation of R_O and present–day TTI values for COST No. 1 well.

Although the limits for the oil generation zone vary slightly, there is good general agreement that the lower threshold is about 0.5 to 0.6 percent, or perhaps slightly lower if certain less common kerogens are present (Snowdon and Powell, 1982). The upper limit of the oil generation window is generally considered to be about 1.3 or 1.35 percent.

From an R_0 of about 1.3 to 2.0 percent, the generally recognized upper limit of the catagenetic zone, liquid hydrocarbons deteriorate to gaseous hydrocarbons at a significant rate. Wet gas occurs in this range if the unaltered kerogens originally possessed sufficient hydrogen.

When R_0 values exceed 2.0 percent, only dry gas can be anticipated. It has not been precisely established to what depths dry gas can occur, but the amount of methane and other light hydrocarbons present in fine-grained source rocks decreases to low values in deep, high-temperature (>200 °C) sediments. No economic accumulation of gas has been found at depths greater than about 27,000 feet (Hunt, 1984).

Lopatin (1971) originally proposed that specific TTI values correspond to the various stages in the process of hydrocarbon generation. Waples (1980, 1984) modified these threshold values. Table 4 is a compilation of some of Waples' (1984) computations from worldwide geologic reconstructions plus several TTI values from the Navarin Basin.

Although there are minor discrepancies between the data sets, they do not appear to be serious, given the normal variation in such correlations. Waples (1980) suggested that this scatter was due to error in R_0 measurements and in the geologic models used to compute TTI values, as well as to uncertainties about the true threshold for oil generation.

Seismic data were used to construct depositional-tectonic models for nearly 100 sites across the Navarin Basin. Lopatin's TTI values were then computed by using the temperature gradient observed in the COST well. The relationships listed in table 4 were used to interpret the TTI values. Because the most favorable potential source rock encountered occurs between seismic horizons C and D, the relative levels of maturity were contoured on these horizons and the catagenetic zone was mapped on each of them. It should be understood that these seismic "horizons" are actually complex surfaces, generally concave upward, not parallel to the surface, and probably not strictly synchronous in time, although that assumption is implicit for this model. The results are plotted on figures 23 and 24. Figure 25 shows the relationship of the seismic horizons to the predicted catagenetic zone in cross section.

IMMATURE (TTI < 4)
OIL (4 ≤ TTI < 170)
WET GAS (170 ≤ TTI < 900)
DRY GAS (900 ≤ TTI)
COST NO. I WELL
SHALLOW SEDIMENTS
● PROBABLE THERMOGENIC GAS
(SEDIMENT CORE SAMPLES, USGS)
+ GAS PLUME
(H.R. SEISMIC DATA, USGS)

SCALE 1:1,267,200
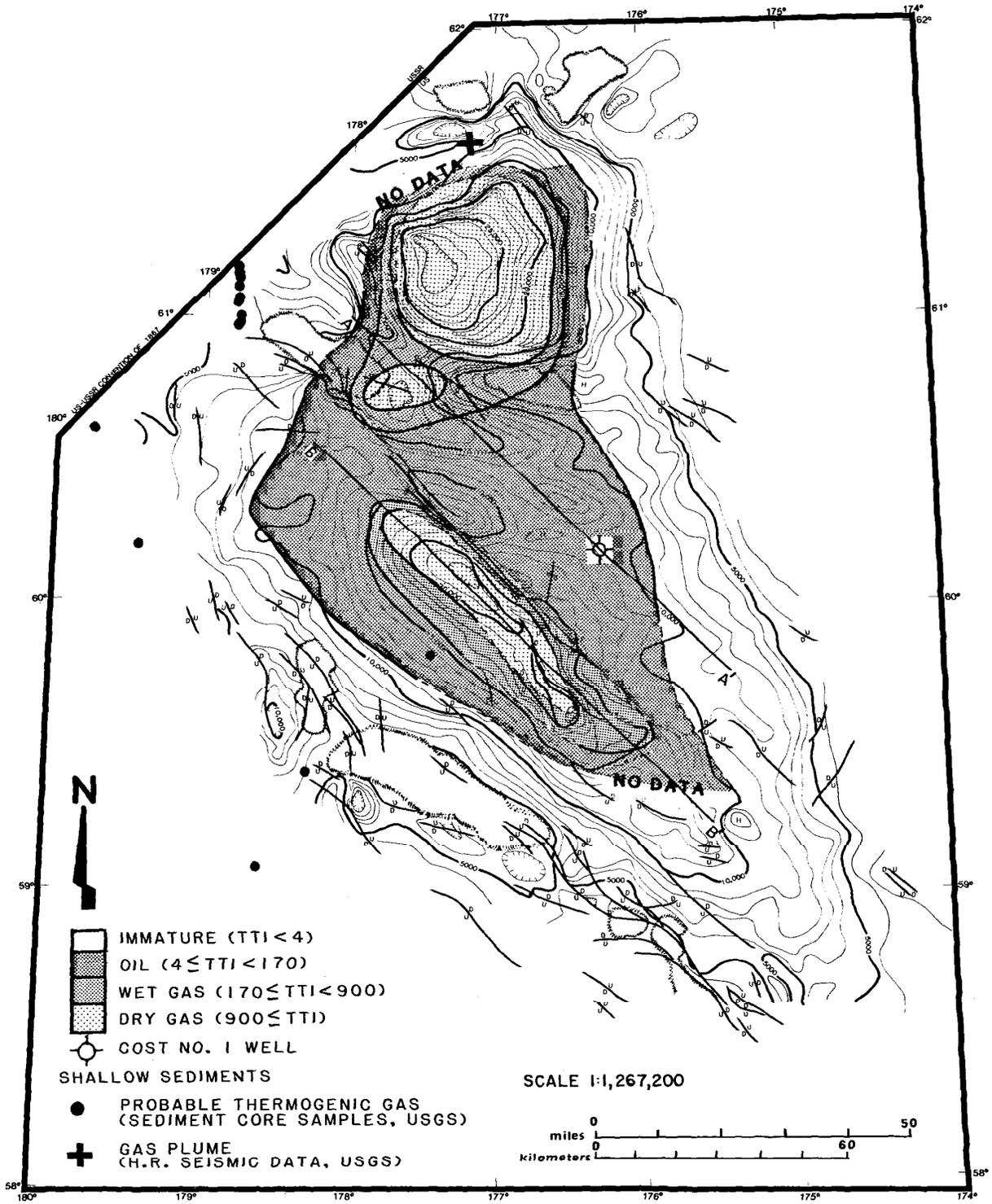
FIGURE 23. Thermal maturity predicted by preliminary Lopatin model superimposed upon structure-contour map of seismic horizon C.

FIGURE 24. Thermal maturity predicted by preliminary Lopatin model superimposed upon structure-contour map of seismic horizon D.

Table 4. Relationship of TTI values to hydrocarbon generation. Adapted from Waples (1984).

TTI	R_O (%) Waples, 1984	R_O (%) Navarin Basin COST Well	Stages of Hydrocarbon Generation
0.05		0.03	
1	0.4		Condensate From Resinite
— 3	0.5		From Sulphur-Rich Kerogen
4		0.6	Early
10	0.6		
34		0.9	Oil Peak
--170		1.3	Late
--180	1.35		
—900*	2.0	2.0*	Wet Gas
			Dry Gas

*Extrapolated values.

It is important to recognize that these maps and diagrams cannot be taken completely literally. Tectonic activity could introduce uncertainties in some instances. Faulted rocks that have dropped relative to the surface of the earth have probably adjusted to the increased temperature of their new environments, but blocks that have moved upward almost certainly have calculated TTI values that are too low to be representative of the true thermal maturity of the sediments. For this reason the cross sections were drawn parallel to regional structure on the downthrown side of faulted blocks. This deficiency does not seriously reduce the applicability of the model at the scale of these illustrations. If the parameters used to construct the model were reasonably accurate, most error, when it occurs, will simply lead to an evaluation of thermal maturity that is slightly low. A further consideration is that seismic horizons A, B, and possibly C represent unconformable surfaces reflecting both regional and local tectonism and perhaps some worldwide eustatic events. There is another possible unconformity between the Eocene and the Oligocene at the well and several unmapped unconformities

FIGURE 25. Cross sections depicting the relationship of the seismic horizons to thermal maturity predicted by a preliminary Lopatin model. Locations of the cross sections are shown on Figures 23 and 24.
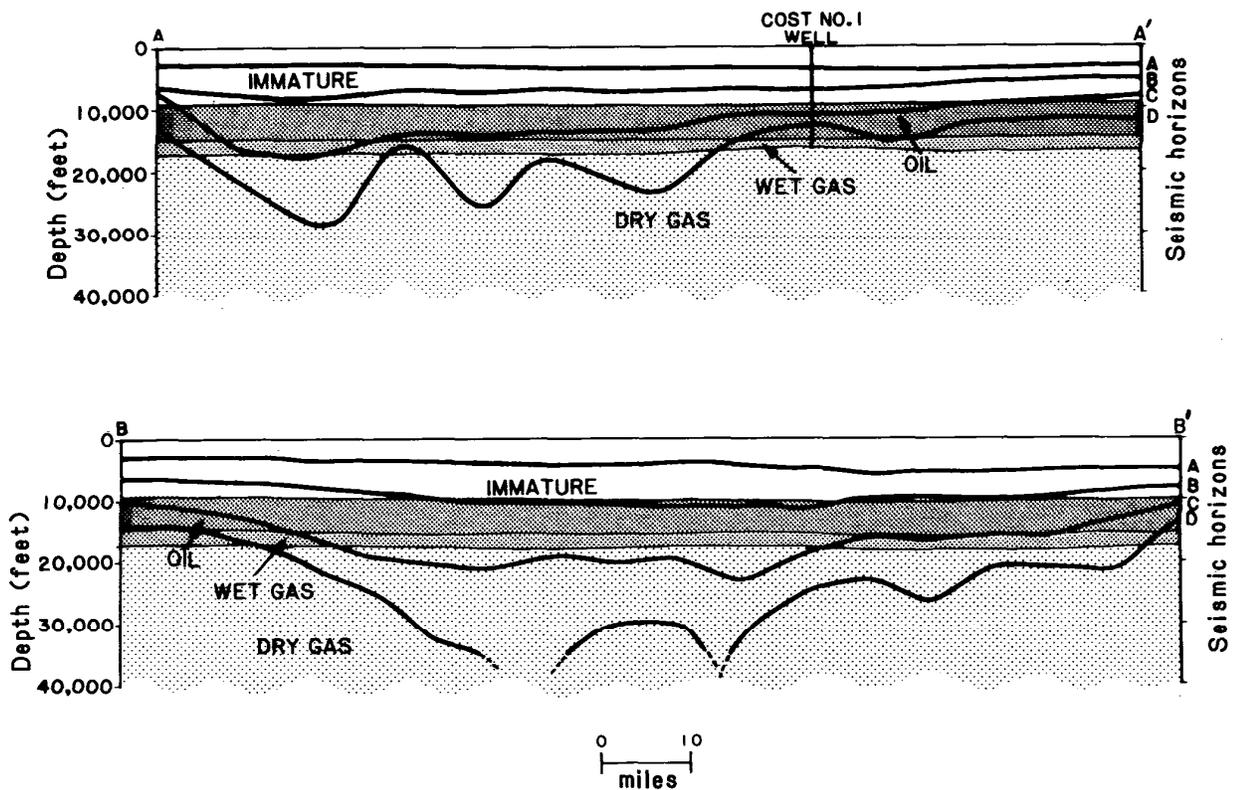
TTI VALUES (CALCULATED)	R_O VALUES (COST NO.1 WELL)	INTERPRETATION	SYMBOLS
TTI < 4	$R_O < 0.6\%$	IMMATURE	
$4 \leq TTI < 170$	$0.6\% \leq R_O < 1.3\%$	OIL	
$170 \leq TTI < 900$	$1.3\% \leq R_O < 2.0\%$	WET GAS	
$900 \leq TTI$	$2.0\% \leq R_O$	DRY GAS	

within the Eocene elsewhere in the basin. For simplicity's sake, as well as for lack of data, these added complexities were not taken into consideration during the construction of the model. Preliminary calculations with hypothetical nondepositional periods or periods of minor uplift suggest that at the depths at which these seismic horizons were buried during the events, the contribution to or change in the TTI values would be negligible at the COST well.

The maps indicate that significant volumes of potential source rock occur within the current oil generation window. Rocks within the dry-gas zone were at one time within the oil generation window, and if these rocks generated oil which escaped from deep, hot areas as the basin subsided, some of it may also have been preserved. To date, no exploratory drilling has occurred in the Navarin Basin, but several lines of evidence imply that hydrocarbons have been generated. This evidence falls into three general categories: data from the COST well, surface samples, and seismic evidence.

EVIDENCE SUGGESTING THE GENERATION OF PETROLEUM

In the COST well, the wetness ratio $\dfrac{C_2 + C_3 + C_4}{C_1 + C_2 + C_3 + C_4}$ [100]
increases from near 0 at 6,000 feet to 91 percent at about 11,910 feet, and remains high down to the Cretaceous-Tertiary unconformity at 12,780 feet (pl. 3). Between 12,440 and 12,780 feet, solvent cuts described on the mud log exhibited "dull brown to gold fluorescence with slow to moderate, dull to strong yellow cuts." In conventional core 14 (12,715 to 12,743 feet), the $C_{15}+$ bitumen content is abnormally high, in excess of 200 milligrams per gram of organic carbon (fig. 21 and pl. 3), a value high enough to have been caused by nonindigenous hydrocarbons (Tissot and Welte, 1984). The $C_{15}+$ hydrocarbon content of this core (fig. 21) is nearly as high as that observed in hydrocarbon reservoirs (Hunt, 1979).

The USGS conducted three cruises to study the Navarin Basin from 1980 to 1981 (Carlson and others, 1985). Gravity cores were taken at 141 sites from all regions of the basin, but most emphasis was placed upon the shelf, where water depths are less than about 500 feet. The authors of this study used the ratios of methane to ethane plus propane (C_1/C_2+C_3) and of ethane to ethene $(C_2/C_2=)$, as described by Bernard and others (1977), to discriminate between the probable sources of the gas mixture, that is, a thermogenic versus a biogenic origin. No carbon isotope ratios were measured because of the volume of gas needed for this kind of analysis and because of possible isotopic fractionation in near-surface sediments (Keith Kvenvolden, oral commun., 1985). Seventeen of the gravity cores had hydrocarbon gas compositions that suggest the presence of thermogenic gas, although this interpretation is, in the words of Kvenvolden, "somewhat equivocal." These cores were obtained largely from slope sediments where water depths are greater than 500 feet. The approximate

surface locations of these anomalous samples are given on figures
23 and 24, although both diagrams depict subsurface features.

Seismic anomalies in this study did not correlate well with
hydrocarbon anomalies from core samples. This discrepancy was
attributed to the shallow penetration of the gravity corer and
possibly to the erratic nature of the gas distribution in the
sediments. The most significant seismic anomaly was reported as a
gas plume located at lat 61°37' N. and long 177°10' W. (Carlson and
Marlow, 1984). This anomaly was identified on high-resolution
reflection records after the last USGS cruise and was not sampled
for chemical analysis. The location of the gas plume is also shown
on figures 23 and 24.

Favorable potential source material in the 1,000-foot interval
above the Cretaceous-Tertiary unconformity in the COST well, evidence
of thermogenic hydrocarbons within the COST well and in sediments
flanking the basin, and theoretically large volumes of thermally
mature sediment, which were sampled in the COST well, all suggest
that significant amounts of oil and gas could have been generated
in the Navarin Basin. This conclusion is based on a single location
from which detailed subsurface data were obtained. Additional
sampling and, ultimately, exploration of specific targets by the
petroleum industry is necessary before the true hydrocarbon potential
of the Navarin Basin will be known.

Reservoir Rocks

RESERVOIR STRATIGRAPHY

Sandstones in lithologic zones C-1 and C-2 (early to middle Miocene to late Oligocene) represent the only significant potential reservoirs encountered in the Navarin COST well. These marine sandstones occur in a vertical, largely regressive megasequence (pl. 1). A total aggregate sand count of 1,425 feet is present in a stratigraphic interval 2,120 feet thick. The net sand (here defined as the sum of intervals with Spontaneous Potential (SP) log curve deflections of at least 10 millivolts) totals 1,070 feet, or about half of the stratigraphic interval. The sandstones discussed are defined by both well log and observed lithologic criteria. Figure 27 illustrates the electric log facies referred to in the text.

The C-1 and C-2 sandstones, as well as most of the other sandstones in the well, chiefly fall within the feldspathic litharenite category of Folk's (1974) classification (fig. 26). The framework clasts are predominantly lithic grains and feldspars (chiefly plagioclase), with quartz grains generally amounting to less than 40 percent. The source terranes were volcanic or volcaniclastic, with some minor input from a low-grade quartz-mica-schist metamorphic terrane (fig. 26). The primary provenance seems to have been remarkably consistent throughout the sedimentary history seen in the COST well.

The sandstone megasequence is characterized on the SP and resistivity logs by three different log facies. In the lower part of zone C-2, the logs show a series of relatively smooth, funnel-shaped curves that indicate coarsening-upward sandstone sequences (fig. 27, part A). In the upper part of zone C-2, the logs show a mix of funnel shapes (coarsening upward), bell shapes (fining upward), and blocky shapes (vertically homogeneous grain size distribution) (fig. 27, part B). Here the sandstones make up a stacked sequence of beds which are amalgamated or separated by thin mudstone interbeds. Overlying these two log facies is the thin-bedded, stacked sandstone facies of zone C-1 (fig. 27, part C).

TERTIARY ROCKS
ZONES A-E

CRETACEOUS ROCKS
ZONES G-I
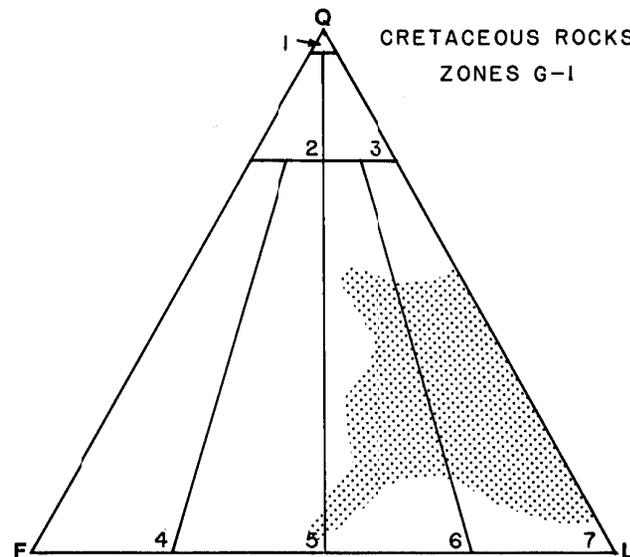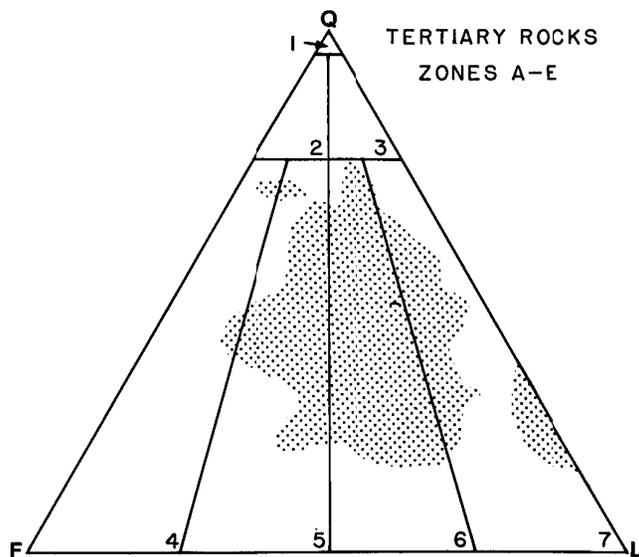
SANDSTONE CLASSIFICATION
(after Folk, 1974)

1. QUARTZARENITE
2. SUBARKOSE
3. SUBLITHARENITE
4. ARKOSE
5. LITHIC ARKOSE
6. FELDSPATHIC LITHARENITE
7. LITHARENITE

Q-QUARTZ
F-FELDSPARS
L-LITHICS

TERTIARY ROCKS
ZONES A-E

CRETACEOUS ROCKS
ZONES G AND H
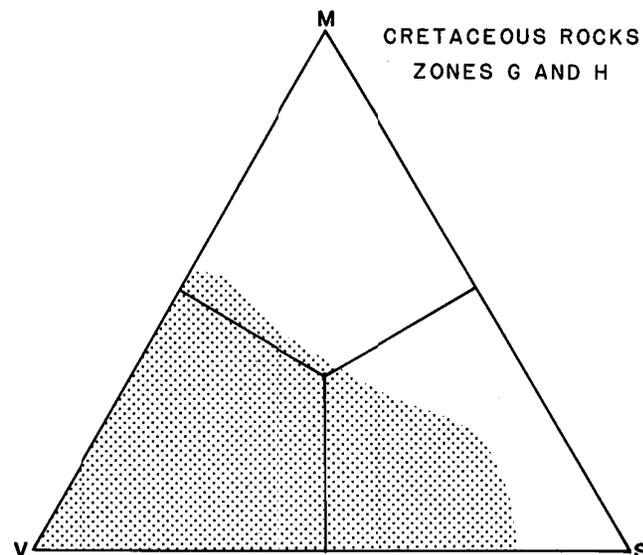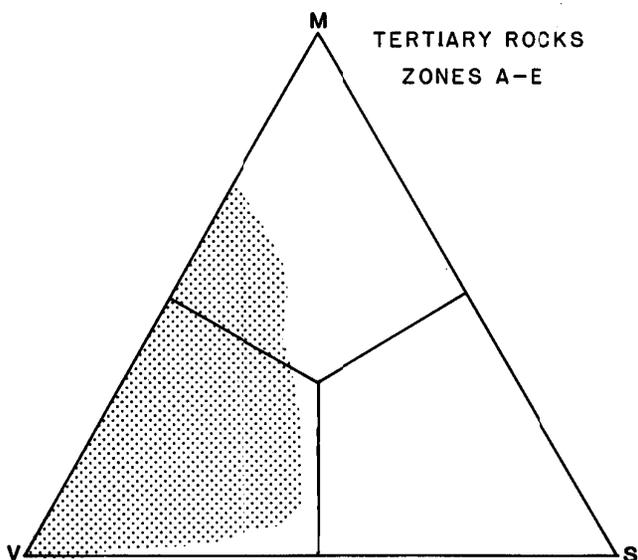
V-VOLCANIC
M-METAMORPHIC
S-SEDIMENTARY

FIGURE 26. Ternary diagrams showing the range of quartz, feldspar, and lithics and volcanic, metamorphic, and sedimentary values found in conventional and sidewall core samples from Tertiary and Cretaceous rocks in the Navarin Basin Cost No. 1 well. (Modified from AGAT Consultants, Inc.)

SP CURVE   RESISTIVITY
               CURVE

SP CURVE   RESISTIVITY
               CURVE

SP CURVE   RESISTIVITY
               CURVE
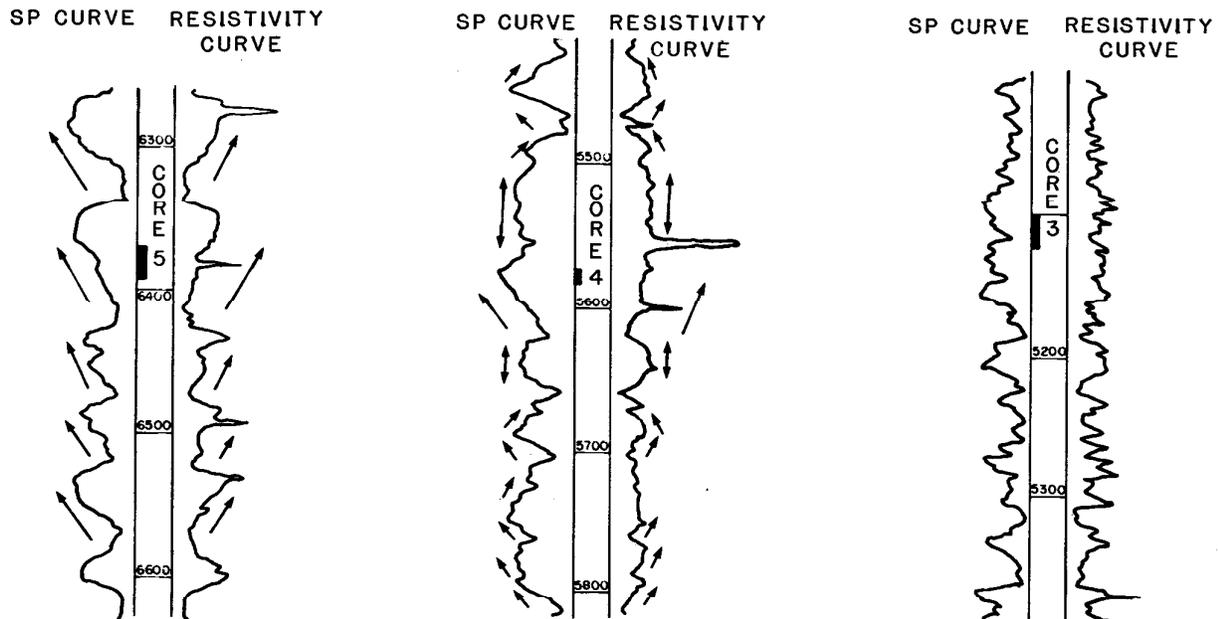
A. Lithologic zone C-2, lower part.
Funnel-shaped log facies.
Coarsening-upward shoaling cycle,
offshore bars. Overall regressive
middle- to outer-shelf sequence.

B. Lithologic zone C-2, upper
part. Mixed log facies: funnel,
bell, and blocky shapes.
Offshore-bar coarsening-upward
sands, and storm-tidal channel(?)
blocky- to bell-shaped sands.
Regressive middle- to inner-shelf
sequence.

C. Lithologic zone C-1. Serrate,
highly active log facies.
Bioturbated middle-shelf sands.
Transgressive sequence.

BED CYCLE PATTERN

\ / FUNNEL-SHAPED

/ \ BELL-SHAPED

↕ BLOCKY-SHAPED

FIGURE 27.   Electric log facies of the late Oligocene to middle Miocene
sandstone megasequence, Navarin Basin COST No. 1 well. Depositional
environments inferred from litho- and biofacies in cores and drill cuttings,
and bed-cycle patterns from SP and resistivity logs.

94

In zone C-2, core 5 sampled 23 feet of the lower part of one of the coarsening-upward sandstone sequences from the funnel-shaped log facies. The sandstone was extensively bioturbated, glauconitic, and contained small amounts of broken, thin-shelled molluscs and volcanic pebbles. The burrows are horizontal to oblique, and some of the smaller horizontal burrows resemble traces ascribable to the ichnogenus Terebellina. This interval contained an outer neritic microfossil assemblage. The core was sedimentologically characterized by wavy to horizontally interlaminated and interbedded very fine grained sandstone and claystone that graded upward into very fine grained sandstone. Sidewall core and cuttings data suggest that core 5 is representative of much of zone C-2.

Coarsening-upward sand sequences characterized by smooth funnel shapes are typical of several different depositional environments: wave-dominated delta front sands, prograding shoreface sands, barrier bars, offshore submarine bars, and perhaps others (Scholle and Spearing, 1982; Harms and others, 1975). Although the sedimentary features described in core 5 bear similarities to both shoreline and offshore bar deposits, the coarsening-upward sequences are here interpreted as offshore submarine bars, based on criteria used by Spearing (1976) and Brenner and Davies (1974) in identifying the Shannon and Sussex sandstones (Late Cretaceous, Powder River Basin, Wyoming) as offshore bars.

The coarsening-upward sands are interbedded with light- to medium-gray bioturbated shales containing marine micro- and macrofaunas and floras. No fluvial features or dark-colored prodelta or lagoonal shales and siltstones indicative of shoreline facies are present. Glauconite, which is common throughout the sandstone megasequence, is not normally present in shoreline settings. Similarly, the abundant soft lithic grains and suspension-deposited clay and clay laminae present are not typical of most shoreface environments. These stacked, repetitive, coarsening-upward sand sequences probably represent offshore submarine bars formed during shoaling cycles by a combination of storm-generated waves and currents, tides, and oceanic currents. Storm action was probably the dominant depositional mechanism as evidenced by the pebbles and broken shells seen in cores and cuttings.

The upper log facies of lithologic zone C-2 apparently represents more than one depositional environment. Core 4 sampled the upper part of a funnel-shaped sand (fig. 27, part B), which was composed of well-sorted, fine-grained, sparsely burrowed sandstone and contained broken and whole, randomly oriented mollusc shells. No sedimentary structures were apparent in the core, perhaps owing to both the mechanical fragmentation of the friable portion of the sandstone during coring and the pervasive masking effects of calcite cementation. Drill cuttings and sidewall cores taken from zone C-2 contained glauconite, shell fragments, fine- to very fine-grained sandstone and muddy sandstone, and light- to medium-gray mudstone. Microfossil

assemblages indicate deposition in a middle neritic environment, or possibly shallower, as there is some very tenuous microfossil evidence suggesting brackish conditions and a minor freshwater influence. (Further information is given in the Biostratigraphy chapter.)

The lack of core data on sedimentary structures in the different types of sand beds in this facies makes interpretation difficult. The microfossil evidence, high sand/shale ratio, and complex mix of bedding sequences suggest relatively shallow-water, high-energy deposition. Blocky and bell-shaped log signatures tend to suggest fluvial channeling processes, but evidence of emergence, such as coal or coaly detritus, freshwater fossils, and associated fine-grained fluvial levee and overbank facies, is lacking. The high resistivity spikes apparent on the logs (fig. 27, part B) are tight, calcite-cemented zones, not coal beds. These channel-like log facies patterns probably reflect marine processes such as storm surge and/or tidal channeling, with associated tidal deltas and washover fans. It is possible that the coarsening-upward sandstones in this facies may not consist exclusively of submarine bars but may contain barrier bar sands. This appears unlikely, however, considering the abundance of soft lithic clasts, which are commonly destroyed in high-energy surf zones.

Core 3, from the thin-bedded sandstone facies of zone C-1 (fig. 27, part C), consists of mottled, extensively bioturbated, poorly to well-sorted, fine- to very fine-grained sandstone. Broken and whole, randomly oriented mollusc fragments and several large volcanic pebbles are also present. Wavy, continuous and discontinuous laminae are present where not obscured by bioturbation. Drill cuttings and sidewall cores are similar to those in zone C-2. Microfossil evidence indicates that deposition took place in middle neritic water depths. Zone C-1 is represented by a serrate log pattern (fig. 27, part C) that represents thin interbeds of sandstone, siltstone, and mudstone that were probably deposited in an environment characterized by variable energy. This log pattern suggests a largely transgressive shelf sequence deposited in a setting that was transitional between the high-energy environments of the upper part of zone C-2 and the deeper water shelf environments of zones A and B. These sands may reflect storm deposits that were extensively reworked by marine organisms during quiet-water periods.

The C-2 sandstone package may be a large-scale analog of the Plio-Pleistocene progradational shelf-slope sequence described by Harms and others (1982) from the Makran Coast, western Pakistan. Sand in this area was moved offshore across a shelf in prograding sequences which were never subaerially exposed. The Makran facies cycles are commonly stacked in thick, repetitive sequences, representing a long-term regression where inner-shelf facies gradually advanced over belts previously occupied by middle- and outer-shelf facies. These large-scale progradational megasequences range from 3,000 to 9,000 feet in thickness and in many instances represent 20 to 60 individual shoaling cycles.

Overall, the model of Harms and others (1982) compares well with the pattern observed in the Miocene to Oligocene sand sequence in the Navarin Basin COST well. The Navarin megasequence contains over 20 shoal cycles composing a regressive sequence about 1,000 feet thick that appears to have never been subaerially exposed. The sparse core data from the COST well make comparisons with detailed descriptions of sedimentary structures from the various facies of the Makran deposits rather difficult. Many of the structures observed in the Makran sequences (and in the Shannon and Sussex sandstones), such as trough and hummocky cross-stratification and coquina storm lag deposits, were not sampled by cores in the Navarin COST well. However, shells and shell fragments were present in all of the cores, and it is possible that some of the highly cemented calcareous zones displayed as spikes or "hard streaks" on the resistivity logs may represent altered coquina deposits. Some cuttings samples also appeared to represent coquinoid layers. Although there is no apparent cross-stratification in the cores, dip patterns displayed on arrowplots from dipmeter logs exhibit the "blue patterns" (dips increasing in magnitude upward within bedding units) typical of current cross-bedding (Schlumberger, 1981, p. 31).

In the absence of three-dimensional control, sand body geometry and dimensions must be inferred from analogous depositional systems where such control is available. In the Makran area, the Plio-Pleistocene sands thin and "shale out" over distances of 6 to 12 miles (Harms and others, 1982). Investigations of shelf sand-ridge deposits from the Cretaceous Western Interior Seaway by various investigators (Slatt, 1984, among others) indicate that these bars are elliptical to linear in plan view and parallel or subparallel to paleoshorelines. Bar dimensions vary from less than 1 mile to 50 miles in width and from 3 to 72 miles in length. Assuming that these represent reasonable analogs to the Navarin offshore bar sands, they also suggest a range of reservoir dimensions for the basin.

RESERVOIR HABITAT AND PETROPHYSICS

The best reservoir potential tends to be in the upper parts of the Miocene-late Oligocene shelf sand-ridge bodies. An analysis of the wireline log suite from the Navarin COST well (Martin, 1984) shows that the potential net reservoir sand in a given sandstone varies in thickness from 10 feet in some of the thinner bar sands to as much as 100 feet in the stacked multiple bar-channel sands (upper log facies, zone C-2).

The total porosities in net sand intervals in the Navarin COST well (determined from conventional core measurements and density log calculations) ranged from about 25 to 35 percent. Permeabilities, however, were much lower than anticipated for this porosity range. Permeability measurements taken from conventional cores were generally less than 10 millidarcies, with a few measurements in the 20- to 120-millidarcy range (fig. 28). These anomalously low permeabilities
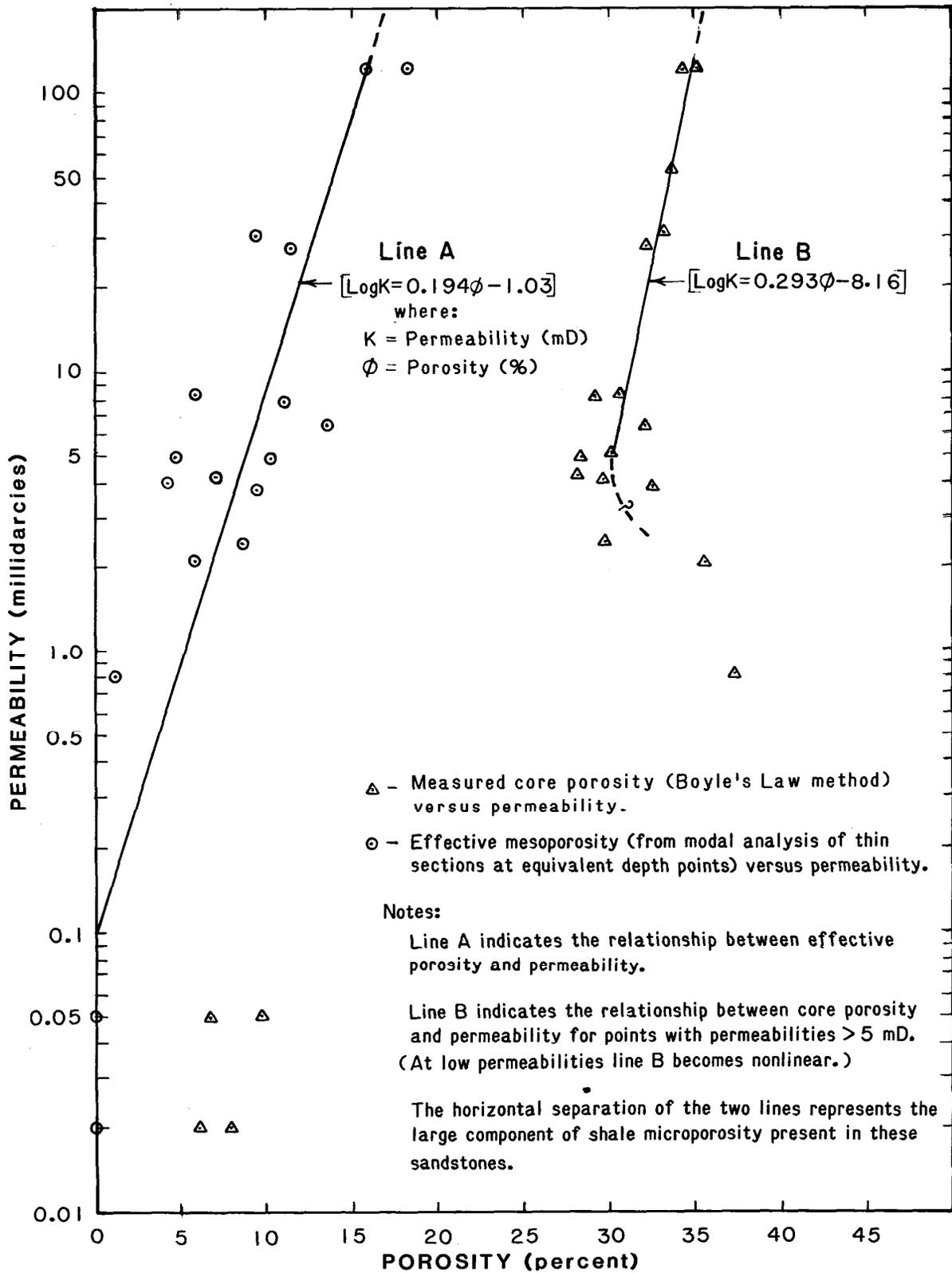
FIGURE 28. Porosity versus permeability for Tertiary sandstones (conventional cores 2 through 5), Navarin Basin Cost No. 1 well.

are the result of a combination of factors, including grain size, clay content, and diagenesis.

Only one of the four cores (core 4) that sampled the Miocene to Oligocene sandstones in the COST well was taken in the upper part of a coarsening-upward bar sequence, the type of lithology with the best reservoir potential. Unfortunately, the friable sandstone recovered was badly broken during coring, and the only measurements obtained were from a tight, highly cemented calcareous zone. As a consequence, the conventional core measurements from the COST well are not entirely representative of typical reservoir zones in the well or elsewhere in the basin. The very fine to fine grain size of these sandstones is in part responsible for their low permeabilities; however, the most important factor is the high content of ductile, clay-rich, lithic framework grains and the high surface area of intergranular smectitic clays.

Effective porosities (estimated by petrographic analysis of core samples and calculated from neutron-density log crossplots) range from 5 to 20 percent (Martin, 1984). This porosity range is more in line with observed permeabilities and suggests that much of the total porosity is in the form of shale microporosity within lithic grains and in intergranular clays.

Sidewall cores taken in lithologic zone C-2 sampled more of the better potential reservoir zones than did conventional cores. Unfortunately, the sidewall-coring process tends to fracture and disrupt rock fabrics and thereby create measurable porosity and permeability beyond that actually present in the undisturbed rock. Because of this, sidewall-core porosity and permeability data are often discounted. These well-documented deleterious effects are most disruptive in older, more brittle rocks. In younger, less consolidated sediments (such as the Cenozoic sandstones in the Navarin COST well), the disruptive effects are far less pronounced, and sidewall core permeability measurements are often found to be only slightly higher than those from conventional cores (Helander, 1983, p. 18). This appears to be the case in zone C-2. The porosity and permeability measurements obtained from both sidewall and conventional cores from the same interval (core 5) are in reasonably close agreement (Lynch, 1984, table 2, p. 76). The more numerous, and probably valid, sidewall core measurements (Lynch, 1984, table 2, p. 74-76) indicate that permeabilities in the better potential reservoir sands in the well probably fall within the upper grouping of points plotted in figure 28. On this basis, permeabilities in Navarin Basin sandstones present at depths of 5,000 to 7,000 feet should range from 20 to 150 millidarcies, which would place many of them in the fair-to-good reservoir category. Crossplots of neutron-density porosity in zone C-2 indicate that there is probably about 200 aggregate feet of good reservoir and 375 aggregate feet of fair reservoir present in the well (Martin, 1984).

INCREASING BURIAL DEPTH

IMMATURE

SEMI-MATURE

MATURE

SUPER MATURE

QUARTZ
ARENITE

DECREASING
MINERALOGICAL
STABILITY
OF SANDSTONES

VOLCANIC
LITHARENITE

IMMATURE STAGE
MAINLY MECHANICAL REDUCTION OF PRIMARY POROSITY
SEMI-MATURE STAGE
MAINLY CHEMICAL REDUCTION OF PRIMARY POROSITY
MATURE STAGE
PRIMARY POROSITY AT IRREDUCIBLE LEVELS; SECONDARY POROSITY MAY EXIST
SUPER MATURE STAGE
PRIMARY AND SECONDARY POROSITY AT IRREDUCIBLE LEVELS

VOLUME %

40   0 40   0

PRIMARY
POROSITY

SECONDARY
POROSITY
(IF PRESENT)

FIGURE 29. Textural stages of sandstone burial diagenesis and reduction of porosity.
(After Schmidt, 1984)

Elsewhere in the Navarin Basin where sands like these, with high volcaniclastic contents, occur at increasing burial depths, a rapid loss of reservoir quality can be expected. Mineralogically unstable sandstones reach a stage of textural maturity, where primary porosity is at an irreducible low level, at shallower burial depths than do more quartzose sandstones (fig. 29 and Schmidt, 1984). Figure 30 is a plot of total porosity from core measurements versus depth in the COST well. Despite a relatively wide scatter of plotted points, the general trend of porosity reduction with depth is apparent. Most of the porosity loss is probably due to compaction and chemical alteration of the ductile and mineralogically unstable volcaniclastic grains.

A comparison of the relationship between total and effective porosity (fig. 28) and total porosity versus depth (fig. 30) allows the prediction of a limiting depth for the occurrence of reservoir quality sandstone. It is evident from the total and effective porosity curves of figure 28 that about 15 to 20 percentage points of the total porosity represent shale or clay microporosity. This suggests that at depths where total porosity falls much below 20 percent, effective porosity and permeability would be very low. Figure 30 indicates that this condition probably occurs below 9,000 feet in the Navarin Basin. This predicted limiting depth for the preservation of reservoir quality is tentatively borne out by petrographic analysis of thin sections from cores. The lowest occurrence of primary mesoporosity (primary effective porosity) in the Navarin Basin COST well is at 9,333 feet (AGAT, 1983, D-423-I).

Reservoir quality sandstone might occur at burial depths greater than 9,000 to 10,000 feet elsewhere in the basin if one or more of the following conditions are met: (1) compositionally mature quartzose sandstones are present; (2) abnormal formation pressures are present and sufficient to preserve porosity; and (3) permeability was significantly enhanced by the development of secondary porosity.

Of these conditions, the latter two (abnormal pressure and secondary porosity) are most likely to play major roles in reservoir development in the Navarin Basin. The apparent ubiquity of volcanic and volcaniclastic source terranes in the Navarin Basin suggests that quartzose sandstones are probably rare in the basin. If barrier bar and/or shoreface deposits are preserved along the basin margins, however, quartzose sandstones may well be present, as these high-energy paralic environments tend to chemically and physically winnow out soft and/or mineralogically unstable grains. There is also a fair possibility that quartzose sediment was carried into the basin from eroding Mesozoic igneous, metamorphic, and sedimentary rocks in the Koryak Highlands of eastern Siberia. These more mineralogically mature sandstones would not be subject to the same depth and diagenetic constraints as the more common volcaniclastic sandstones.

The deeper preservation of reservoir quality sandstone because of overpressuring is also possible. In the Navarin COST well, sediments are significantly overpressured below about 9,400 feet (fig. 17 and Sherwood, 1984). Tertiary sandstone present in this geopressured section would probably retain some original reservoir quality. The occurrence of shale diapirs in the Navarinsky subbasin suggests that abnormal formation pressure may be ubiquitous throughout the basin.

The development of significant secondary porosity is quite possible because of the mineralogical character of the sandstones in the basin. Dissolution of unstable, volcaniclastic grains is common in the COST well sediments, particularly in zones that exhibit good depositional sorting. In core 5, for instance, dissolution has significantly enhanced both porosity and permeability. Sandstones of the Sterling Formation in the Cook Inlet Basin (which have a similar volcano-plutonic provenance) commonly display secondary porosities as high as 30 to 40 percent (Hayes and others, 1976, p. J15) and permeabilities that may exceed 10,000 millidarcies (Alaska Geological Society, 1975, p. 29). Although the diagenesis of volcaniclastic sandstone often results in reservoir degradation due to zeolitization, the Sterling Formation illustrates the potential for reservoir enhancement by diagenetic processes in volcanogenic sandstones.

It is likely that the development of secondary porosity may be genetically related to geopressure phenomena. The upper levels of geopressured zones are known to be favorable locations for secondary porosity enhancement (Schmidt, 1984, p. 9). The rapid rise in fluid pressure near the top of geopressured zones is thought to cause shifts in equilibrium boundaries between hydrous and anhydrous mineral phases, which apparently facilitates dissolution (Boles, 1984, p. 17-22). In addition, high fluid pressures keep lithostatic pressure from compacting and crushing grains, which aids in the development of large secondary pores.

A model proposed by Surdam and others (1984) relating organic and inorganic diagenesis to the development of secondary porosity suggests another relationship between secondary porosity and geopressure. During the progressive thermal maturation of kerogen with burial, decarboxylation and organic-acid generation culminate just before the main phase of liquid hydrocarbon generation. The peak of highly soluble organic-acid generation also coincides in time, temperature, and space with smectite/illite diagenesis. The diagenesis of smectite/illite generates excess pore water by the expulsion of interlayer-bound water, which results in abnormal pore-fluid pressures (McClure, 1977, p. I-7).

The above conditions are ideal for the dissolution of aluminosilicate minerals (chiefly clays and feldspar) in Navarin Basin volcanogenic sandstones. Better yet, this dissolution occurs
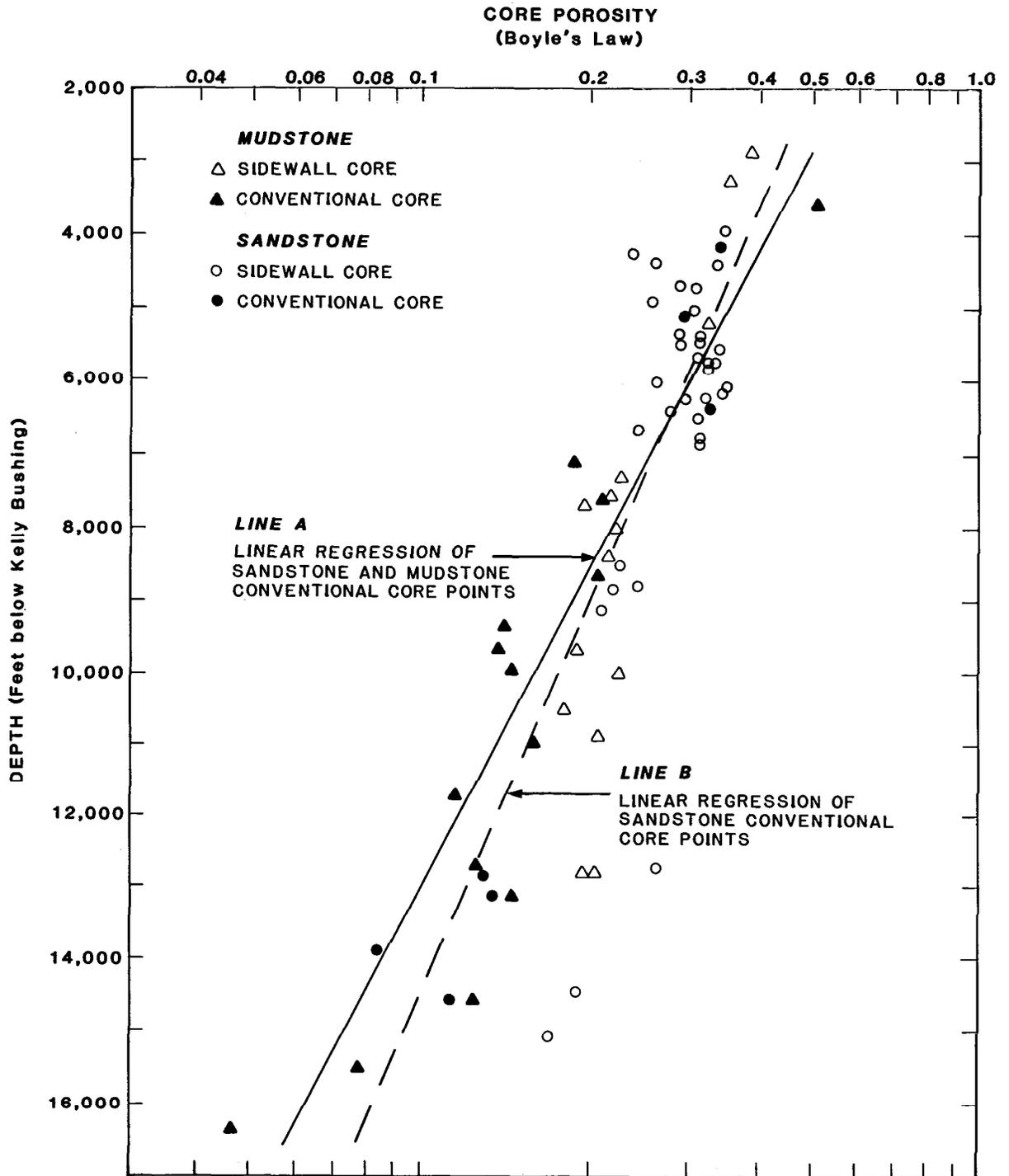
FIGURE 30. Core porosity measurements versus depth, Navarin Basin COST No. 1 well. Line A indicates the loss of porosity with depth for all clastic lithologies. Line B illustrates the loss of porosity with depth for sandstones.

just before the generation of hydrocarbons. The optimum diagenetically driven reservoir enhancement system would place organic-rich source rocks adjacent to "pre-reservoir" sandstones with enough primary porosity and permeability to allow the initial transmission of highly reactive fluids. Unfortunately, the best potential reservoir and source rocks in the COST well are stratigraphically separated by as much as 4,000 feet of shale. In order to bring these sandstones into hydraulic contact with source rocks, migration along faults or across fault planes or unconformities is probably necessary. If the migration path is long, the highly reactive organic acids will probably be consumed within the migration conduit before reaching potential reservoir rocks (Surdam and others, 1984, p. 146).

POSSIBLE TURBIDITE DEPOSITS AND FRACTURED RESERVOIRS

Although no potential reservoir sandstones were encountered in the COST well in the Eocene and early Oligocene deep-water shale sequences (lithologic zones E and F) that contain the organic-rich source rocks, coarser grained facies may be present elsewhere in the basin. Several lines of evidence suggest turbidites may have been deposited along the flanks of basement highs during this time: (1) seismic reflectors onlap local structural highs near the continental shelf break; (2) coarse-grained materials, including conglomerates, were dredged from equivalent rocks on the continental slope; and (3) early Oligocene to Mesozoic basement rocks were exposed to erosion in the late Oligocene and supplied local sediment sources adjacent to deep water. (Further information is given in the Seismic Stratigraphy chapter.)

The diagenetic model proposed by Surdam and others (1984) suggests that where these turbidites interbed and interfinger with organic-rich source rocks, the potential for secondary enhancement of porosity and accumulation of liquid hydrocarbons should be high. Similar prospective facies associations could conceivably occur higher in the stratigraphic section within the late Oligocene to Miocene rocks. If deeper water facies were developed laterally to sandstone shelf deposits in more distal locations, perhaps near subbasin depocenters where subsidence was greater, fine-grained organic-rich rocks may be interbedded or interfingered with potential reservoir sandstones.

Fractured reservoirs similar to the Monterey Shale type of the Santa Maria area, California, could conceivably occur in the Navarin Basin in the diagenetically altered part of the Miocene diatomite sequence. The Monterey Shale and the Miocene rocks of the Navarin Basin are genetically and diagenetically similar in that they are both brittle, siliceous, fine-grained rocks whose character derives in large part from the dissolution and redeposition of silica from in situ diatom frustules.

Reservoirs in the Monterey Shale occur in breccias in dolomitized sections of siliceous shales. The fracturing is not directly due to folding or faulting (Redwine, 1981), although fracture development is most abundant in areas of strike-slip faulting. Roehl (1981) and Redwine (1981) proposed that the breccias originated from tectonically initiated compressive stress which induced dilatancy, fluid expulsion, natural hydraulic fracturing, and dolomitization. The Monterey Shale is an organic-rich source rock, and the dilatancy mechanism was sufficient to allow expulsion and migration of indigenous hydrocarbons. The excess pore pressures believed to have been associated with this mechanism enhanced hydraulic fracturing and fluid flow.

The diagenetically altered section of the Miocene diatomite-rich rocks in the Navarin Basin also could have been subject to a similar fracturing process. The Navarin Basin has undergone analogous tectonic stress, and excess pore pressures were observed in the Miocene in the COST well (Sherwood, 1984). The Navarin/Monterey analogy breaks down with respect to source rock potential. The Miocene siliceous rocks of the Navarin Basin are thermally immature and generally organically poor (less than 0.5 percent organic carbon). Hydrocarbon accumulation would therefore require migration from deeper in the basin along faults or unconformities.

Seals and Migration

SEALS

Many basins contain regional sealing horizons, and where these seals overlie mature source rocks and reservoirs, they are major factors in controlling the emplacement and entrapment of large hydrocarbon accumulations (Murris, 1980; Downey, 1984). Important properties of seals include lithology, ductility, thickness, lateral extent, and uniformity of internal capillary properties. Lithology is generally the most important determinant of a good seal. Fine-grained, ductile mudstones, claystones, and shales of Oligocene and Eocene age (lithologic zones D-1, D-2, E, and F) probably represent the thickest and most regionally extensive seals in the Navarin Basin.

Another potential regional seal in the Navarin Basin is the relatively thin zone of diatomite diagenesis in which biogenic opal-A has been altered to opal-CT, other forms of quartz, and silicate minerals (Turner and others, Navarin COST No. 1, 1984, p. 129-138). The areal extent of this "diagenetic front" can often be delimited by mapping an associated bottom-simulating seismic reflector (BSR) which is regionally apparent on seismic profiles from the Bering Sea shelf (Hein and others, 1978; Hammond and Gaither, 1983; Turner and others, Navarin COST No. 1, 1984). This seal generally occurs at depths of 4,000 feet or less in diatomaceous marine rocks of Miocene age.

Because this diagenetic process is temperature dependent (Hein and others, 1978; Isaacs and others, 1983), it occurs at a relatively constant burial depth and is discordant with dipping, folded, or faulted strata. The effectiveness of this type of seal, however, depends on mineralogical and mechanical diagenesis altering and plugging pore spaces across variable lithologies. In general, diagenetic seals do not form continuous, uniform sealing surfaces for entire commercial hydrocarbon accumulations (Downey, 1984, p. 1762).

On a less than regional scale, the mudstones in the lower part of lithologic zone C-2 (fig. 27, part A) are of sufficient thickness

to suggest that they may be laterally extensive enough to serve as seals. Unfortunately, higher in the section seen in the well (the upper part of zone C-2 and zone C-1; fig. 27, parts B and C), similar claystone and mudstone interbeds are thin or missing.

Other potential sealing surfaces in the Navarin Basin include unconformities, fault planes, lateral facies changes, gas hydrate zones, and hydrodynamic boundaries. All of these may act as seals when they juxtapose sediments of varying permeabilities and fluid pressures. Of these types, unconformities may be of either local or regional significance.

Fault planes can be particularly effective seals when they are associated with geopressured zones. Where geopressured impermeable sediments are juxtaposed with normally pressured permeable sandstones, such as along the faulted sheaths surrounding the shale diapirs in the Navarinsky subbasin, seal effectiveness may be considerably enhanced. In addition, fault plane seals are often enhanced by clay smears that form along faults that intersect thick, undercompacted claystones and mudstones interbedded with reservoir sands (Downey, 1984, p. 1757).

Lateral facies changes that could form stratigraphic traps can reasonably be expected to exist in the Navarin Basin. The rate of change from reservoir to seal is the most important factor in the formation of stratigraphic traps created by updip facies changes (Downey, 1984, p. 1757). If the facies change is too gradual, most of the hydrocarbons will be trapped in low-quality "waste zones" which cannot be economically produced (Schowalter and Hess, 1982).

In the Navarin Basin, both the postulated turbidites (early Oligocene, Eocene, and possible Paleocene) and the offshore bar sands (late Oligocene) represent potential stratigraphic traps. Submarine-fan channel and distributary sands probably exhibit abrupt lateral contacts between reservoir sands and sealing interchannel muds and silts (Bouma, 1984), and offshore sandbar deposits commonly are excellent stratigraphic traps and prolific hydrocarbon producers in the Cretaceous Western Interior Seaway of North America (Slatt, 1984).

Gas hydrate zones, which appear to be ubiquitous in shallow sediments in the Navarin Basin (Carlson and others, 1985), could conceivably form shallow seals. These zones are pressure and temperature dependent and generally occur at burial depths of less than 900 feet. Hydrocarbon gas migrating updip could precipitate pore-filling gas hydrates (ice-like mixtures of water and gas), thus trapping gas and oil downdip (Marlow and others, 1981, p. 42; Downey, 1984, p. 1763).

MIGRATION

Major directions of fluid movement in the Navarin Basin are controlled by lithology, diagenesis, and subsurface geometry. Where interbedded sandstone and shale sequences are present, as within the late Oligocene to Miocene section, fluid flow will be mainly toward the basin edges parallel to strata. Below this, in the thick early Oligocene and Eocene shale section, the main flow direction is probably vertical.

The dominant route for upward migration of fluids in thick overpressured shale sections is thought to be through pressure-generated microfractures (Bruce, 1984; Palciauskas and Domenico, 1980; Powley, 1983). As sealed rock bodies are subjected to progressive burial and temperature increase, they undergo episodic pressure cycles consisting of a buildup to lithostatic fracture-pressure, followed by the fracturing of the seal and the venting of fluids until the lithostatic fracture-healing pressure is reached and pressure buildup is resumed (Powley, 1983). This natural hydrofracturing process may be the principal means of primary hydrocarbon migration from Eocene source rocks in the Navarin Basin.

The generation of excess pore water during smectite/illite diagenesis is the principal cause of abnormal pore pressure in the Tertiary section of the Gulf Coast (Bruce, 1984). Observations from the Navarin COST well (fig. 17) indicate that it is probably the principal cause in the Navarin Basin also (Sherwood, 1984). Because this mineralogical change begins to occur just above, and extends across, the zone of peak oil generation in the well, this diagenetically driven process was probably responsible for flushing hydrocarbons from the organic-rich Eocene claystones. Excess pore water from smectite dehydration provides for the slow release of large volumes of trapped water, which allows hydrocarbon flushing to continue for longer periods and extend to greater depths than otherwise possible (Bruce, 1984).

Several lines of evidence from well logs and cores suggest that hydrocarbon migration may have occurred by upward movement through pressure-generated fractures. Core 14, from the organic-rich Eocene claystones of lithologic zone F, exhibits abundant calcite-filled fractures and small faults that indicate several episodes of fracturing (AGAT, 1983, p. D-423-14). In the strata overlying these fractured, organic-rich rocks, the SP log displays several baseline shifts unrelated to lithologic changes. Such shifts may be indicative of hydrocarbon movement. The observed shifts consist of a positive SP gradient (or drift to the right) as the log is viewed from bottom to top (pl. 1, basal part of lithologic zone E). Such positive SP gradients, often termed "oil gradients," are believed to be genetically related to reducing conditions caused by the presence of small amounts of hydrocarbons (Pirson, 1983, p. 23). Gas peaks and high background gas associated with the SP

shifts in the Navarin Basin COST No. 1 well are further indications of hydrocarbons. Although these lines of evidence appear to suggest that vertical migration of hydrocarbons has occurred, they could be attributed to other causes. The fracturing observed may be the result of structural rather than geopressure-induced stress. The SP baseline shift could also be due to various electrochemical factors. Electrical instability between the spontaneous potential tool electrodes and drilling muds of varying chemical compositions causes problems in determining SP gradients (Pirson, 1983, p. 24). In any event, it seems unlikely that vertical movement alone could result in significant migration through the thick shale sequences present in the Navarin Basin (over 4,000 feet in the COST well). Other natural conduits, such as faults or unconformities, are probably necessary for sufficient hydrocarbon migration from Eocene (and older?) source rocks to form economic accumulations in late Oligocene sandstones.

Play Concepts

Hydrocarbon exploration plays in the Navarin Basin are almost purely conceptual at this juncture due to the dearth of detailed geological data. However, preliminary analyses of geochemical, petrological, petrophysical, and sedimentological data from the Navarin Basin COST No. 1 well suggest that there may be good reservoir and source rocks elsewhere in the basin, as well as a variety of traps. The source rock volume is large enough to have generated significant amounts of hydrocarbons. Local, and possibly regional, sealing horizons abound. Seismic mapping has delineated a number of areas exhibiting significant closure. There are stratigraphic and structural plays both above and below the regional Cretaceous-Tertiary unconformity that marks acoustic basement. Most of the prospective areas are quite close to the generative zone of the basin.

PRE-TERTIARY BASEMENT PLAYS

Mesozoic strata and lithologies are involved in potential structural and stratigraphic traps and reservoirs. At the COST well, the Late Cretaceous section is very mature. The Maastrichtian section at the well is represented by coal-bearing, dominantly nonmarine lithologies, although some dredge sample evidence indicates a correlative marine facies near the shelf edge. The Campanian? section is marine, but has a low total organic carbon content. In the most favorable situation, such as near the shelf edge, this section might have some source potential.

In the COST well, the Late Cretaceous rocks generally displayed poor reservoir qualities, although some secondary and fracture porosity was present. No doubt there are areas characterized by far better development of secondary porosity. Moreover, extensive zones of good reservoir rock may well be associated with the Cretaceous-Tertiary unconformity. Where such Mesozoic reservoirs are in hydrodynamic contact with thick Paleogene source rock sequences, the possibility of significant hydrocarbon accumulations exists (fig. 31).

TERTIARY PLAYS

Most of the Tertiary plays in the Navarin Basin involve Eocene and Oligocene strata (figs. 32 and 33). Regional seismic profiles suggest the presence of thick accumulations of Eocene (and possibly Paleocene) sediments in the deeper parts of the subbasins. This is particularly significant because the relatively thin Eocene section in the COST well (lithologic zone F) represents the best potential source rock encountered. The presence of at least two unconformities within the presumably middle and early Eocene age section bodes well for the occurrence of reservoir lithologies, favorable facies changes, and sealing horizons in the deeper parts of the basin. The existence of Eocene reservoirs is somewhat more conjectural than the almost certain existence of an expanded Eocene section with good source rock potential.

The best reservoir rocks encountered in the COST well are late Oligocene shelf sands (lithologic zone C-2) that probably represent offshore bar deposits. In addition, Oligocene and Eocene turbidite deposits may be present along subbasin margins. The depositional package geometries, the basin configurations, and the paleobathymetric history developed at the COST well all support this contention. Both the late Oligocene shelf sands and the postulated older turbidites represent good stratigraphic or combination plays in some parts of the basin (figs. 31 and 32); both depositional types have favorable facies characteristics, and both pinch out over and against structural highs. There is also a chance that C-1 and C-2 reservoir sands could be sealed by a relatively shallow Miocene silica diagenetic zone of subregional extent (fig. 32). In fact, if fractured, the diagenetic zone could also serve as a reservoir.

Probably the best initial hydrocarbon plays in the Navarin Basin are structural traps or a combination of structural and stratigraphic traps. Many of these plays are in settings characterized by synkinematic deposition (figs. 31, 32, and 33). These traps may occur against the upthrown and downthrown flanks of pull-apart structures, in fault-controlled closures over horsts, and in roll-overs in some of the grabens (fig. 33). Other plays include drapes and pinch-outs over a variety of Tertiary structures and pre-Tertiary basement highs.

Similar fault-buttressed traps are associated with shale diapirs located in the disputed area near the United States-Soviet border. These diapirs structurally involve some of the C-1 and C-2 sandstones and are themselves in part composed of source rocks (fig. 33). A probable gas plume (Carlson and Marlow, 1984) associated with a diapir may represent thermogenic gas leaking directly into the water column, which could be an indication of significant hydrocarbon generation.

TIMING OF OIL GENERATION

Because the most favorable potential source rocks are bounded by seismic horizons C and D (seismic sequence IV), it is possible, by
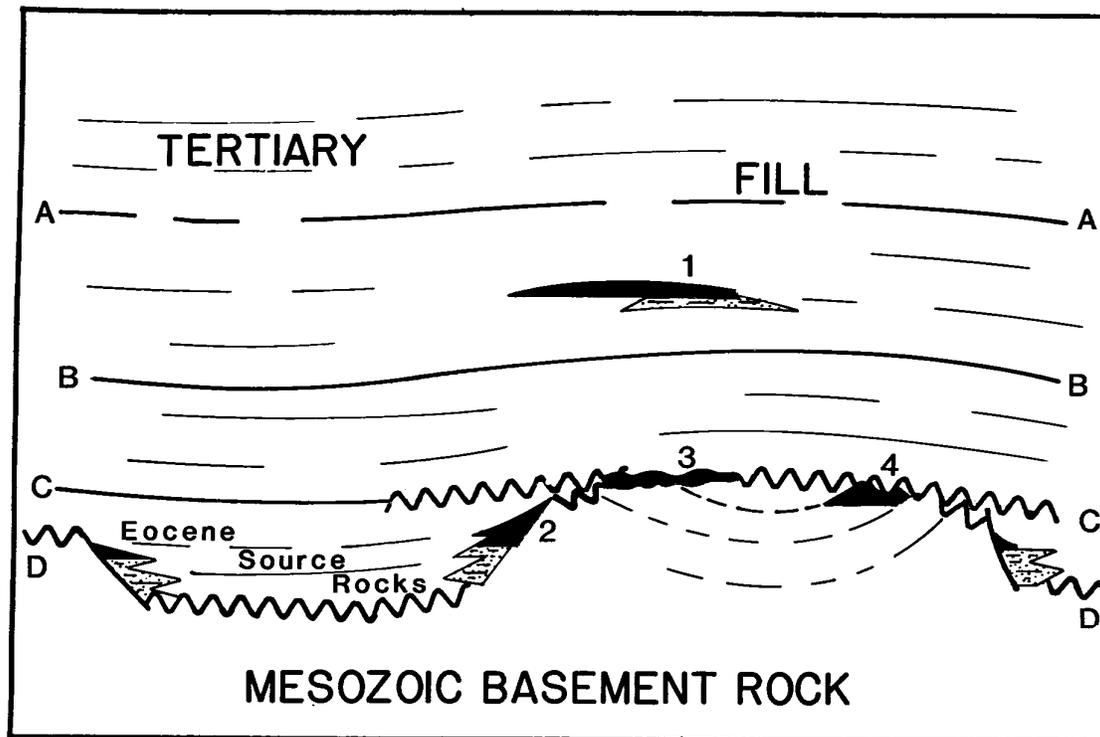
FIGURE 31. Possible structural and stratigraphic trap configurations associated with the Mesozoic basement and the overlying Tertiary basin fill. Seismic horizons A through D are depicted. Potential traps include (1) the C-1/C-2 offshore bar sands (early Miocene to late Oligocene); (2) detrital apron derived from Mesozoic high; (3) Tertiary pinch-out over a basement high; (4) Mesozoic and possible Paleocene reservoir associated with the horizon D truncation event.

FIGURE 32. Possible trap configurations associated with growing basement ridge. Seismic horizons A through D are depicted. Potential traps include (1) proximal turbidite deposits; (2) C-1/C-2 offshore bar sands trapped against an impermeable silica diagenesis zone; (3) sedimentary drape over a growing anticline; (4) stratigraphic pinch-out.

FIGURE 33. Possible trap configurations associated with shale diapir. Seismic horizons A and B are depicted. Potential traps include (1) the C-1/C-2 offshore bar sands tilted by and trapped against a growing shale diapir; and (2) roll-overs associated with normal faulting.
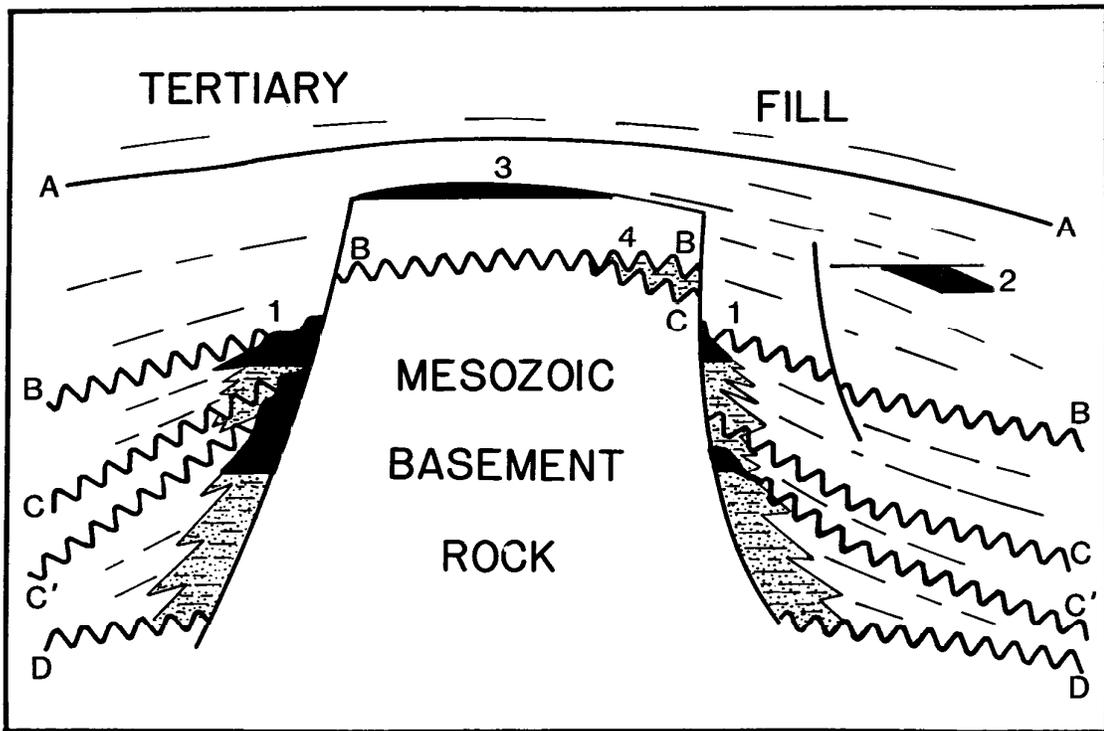
FIGURE 32.
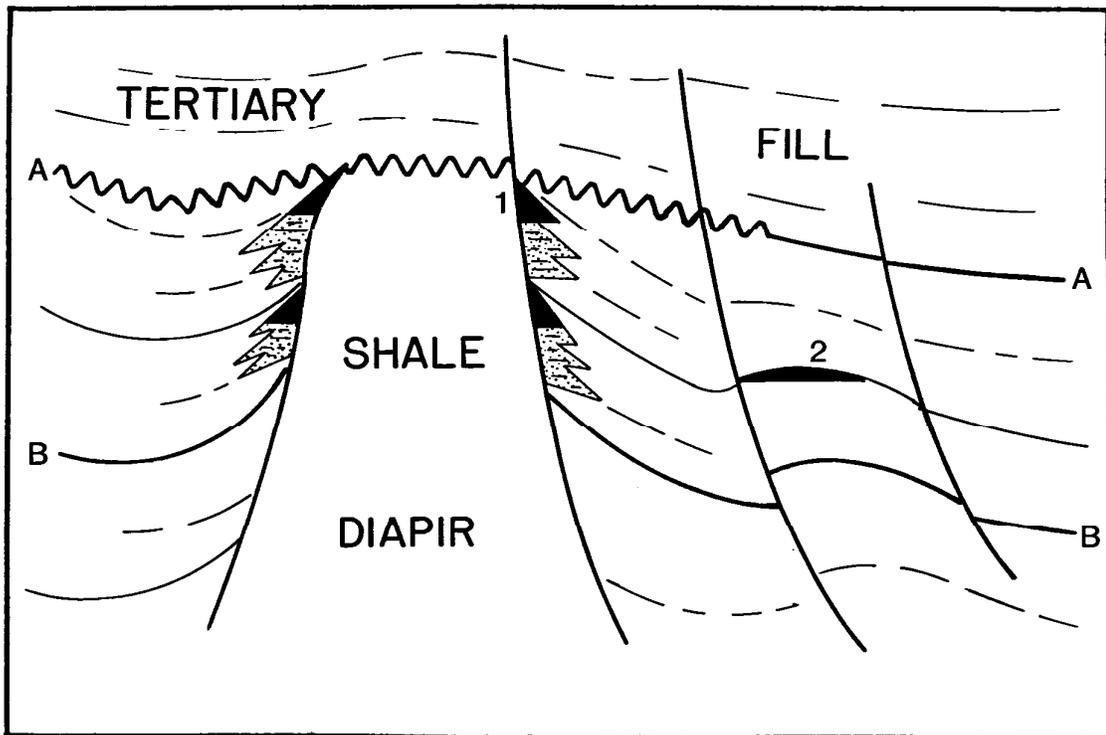
FIGURE 33.

using the Lopatin model, to make estimates concerning the relative timing of thermal maturity. At the COST well, horizon C entered the oil generation window about 3.5 m.y. ago (early Pliocene); horizon D entered the oil window about 9.3 m.y. ago (late Miocene); and the hypothetical Late Cretaceous horizon K (at about 15,000 feet) entered the oil window approximately 21 m.y. ago (early Miocene).

By tracing these seismic horizons into the basins, it is possible to estimate when the C and D horizons would first have been capable of generating oil. A point in the Pinnacle Island subbasin was selected where the D horizon is estimated to drop below 30,000 feet. In this area, seismic horizon C would probably have been within the oil generation window from about 29 m.y. ago (early late Oligocene) to about 12 m.y. ago (middle Miocene). Horizon D entered the oil window about 31 m.y. (early Oligocene) and passed out of it about 27 m.y. ago (late Oligocene).

TIMING OF TRAP FORMATION

The basement ridges that border the subbasins were positive tectonic elements until the late Oligocene and could have been the source for locally derived sediments, including the postulated Eocene and Oligocene turbidite deposits. Growth of these ridges through Tertiary time produced anticlinal structures composed of early Mesozoic and Tertiary strata. Detached and basement-controlled growth faults associated with these ridges may have served as conduits for hydrocarbon migration. However, the continuous growth of some of these faults (into the present) may have kept some otherwise prospective traps from being sealed.

When seismic sequence IV source rocks entered the oil window (early Oligocene), some basement-associated traps (anticlines, flanking turbidite deposits) were already present in the basin. Traps formed by the basement ridges that separate the Pervenets from the Pinnacle Island and Navarinsky subbasins have been in the oil generation window since the early Oligocene, whereas the basement ridge along the shelf break may never have entered the oil window. Anticlinal traps along the southwestern flank of the Pinnacle Island subbasin are located within 20 miles of the probable hydrocarbon generative zone (fig. 24), a reasonable distance for hydrocarbons to have migrated since the early Oligocene (Demaison, 1984). Continuous growth of these anticlines has provided additional structural settings in which the late Oligocene to early Miocene C-1 and C-2 offshore bar sands may be hydrocarbon reservoirs.

In the northwest part of the basin, emplacement of shale diapirs resulted in the tilting and subsequent truncation of the C-1 and C-2 sands by the late Miocene. Diapir-associated closures located within 10 miles of the probable generative zone have been present long enough to represent potential hydrocarbon traps.

SUMMARY

The volume and distribution of potential source rock, reservoir rock, seals, and trapping configurations is sufficient to ensure further exploration efforts in the Navarin Basin. Maturity, migration, and timing do not appear to pose significant problems at this juncture. Reservoir quality may be the most important limiting factor in the basin, but this can only be assessed by a series of exploratory wells.

III. Shallow Geology, Geohazards, and Environmental Considerations

Shallow Geology

The remoteness of the Navarin Basin has long inhibited the investigation of the surface and near-surface geology. Government, academic, and industry programs to identify geologic hazards in the basin before Sale 83 (March 1984) were initiated independently. As a result of these efforts, a basin-wide shallow geologic model is currently being established. The limited high-resolution seismic reflection data base is sufficient for the gross recognition of geohazard types and patterns and for the lease-block-specific identification of submarine slides.

DATA BASE

Shallow geologic characteristics and potential geohazards at the COST well drill site were identified by Nekton, Inc. (1980a). This site-clearance survey, part of the stipulations in the Application for Permit to Drill (APD), included a geotechnical study of the upper 5 feet of sediment and a high-resolution seismic reflection survey of the sea floor and its near-surface features. The regional description of the Navarin Basin oil and gas lease planning area is a synopsis of work done by the USGS as summarized by Carlson and Karl (1981a) and Karl and Carlson (1984). The summary is based on a composite of government and university data. These reconnaissance surveys included shallow geotechnical sampling and analog high-resolution and multichannel seismic reflection surveys.

PHYSIOGRAPHY

The Navarin Basin Planning Area contains representative elements of four physiographic provinces: continental shelf, continental slope, continental rise, and submarine canyons (fig. 34). The largest province, the shelf, covers 66 percent of the planning area. The 500-mile-wide Bering Sea continental shelf is one of the world's largest compared to a world average width of 40 miles (Shepard, 1963). Shelf water depths range from less than 320 feet to 500 feet at the shelf break. Approximately 26 percent

of the shelf area can be considered a middle-shelf environment
(165 to 320 feet); the remaining 74 percent is an outer-shelf
environment (320 to 500 feet). The broad, flat shelf has a very
gentle slope of 0.02° to the southwest, which is consistent with
a world average slope of 0.11° (Shepard, 1963). About 35 miles
east of the planning area, St. Matthew Island rises above the
shelf.

The shelf grades into the continental slope, which trends
relatively straight to the northwest and represents 19 percent of
the planning area. The Navarin continental slope has a width of 11
to 30 miles, typical of the world average, and gradients of 3° to
8°, consistent with the world average of 4°17' for the first 6,000
feet of water depth (Shepard, 1963). The slope bathymetry is
irregular because of slump blocks, fault scarps, submarine canyons,
and hummocky mounds characterized by chaotic internal seismic
reflections. The slope environment is depicted in the line
interpretation of a seismic profile (fig. 10). Degradational
processes on the slope have exposed rocks ranging in age from Late
Jurassic to Holocene.

Three large submarine canyons, the Zemchug, Pervenets, and
Navarinsky, cut the shelf and slope. All three canyons begin as
erosional channels in water depths of less than 500 feet and widen
distally into vast canyons with large subsea fans. The toes of
the fans extend into water depths greater than 9,800 feet. Dredge
sampling indicates that the channels have eroded through the Cenozoic
fill of the Navarin Basin and into Mesozoic basement rock (Marlow
and others, Description of Samples, 1983). Navarinsky, the longest
canyon (211 miles), has a relief of 2,300 feet and a width of 62
miles at the shelf break; its two main channels have thalweg
gradients of 0.33° and 0.50°. Pervenets, the shortest canyon (78
miles), has a relief of 2,600 feet and a width of 19 miles at the
shelf break; its two main channels have thalweg gradients of 0.30°
and 0.33°. The Zemchug Canyon, 150 miles long, has a relief of
8,500 feet and a width of 62 miles at the shelf break; its thalweg
gradients range from 1.2° to 2.2°.

The remaining 15 percent of the planning area falls within a
continental rise environment characterized by depths greater than
9,200 feet. The continental rise here is a transitional zone between
the slope and the Aleutian abyssal plain. The width of the rise
ranges from 15 miles near Zemchug Canyon to 50 miles at the US-USSR
international border. Slopes range from 0.5° at the canyon mouths
to 1.8° northwest of Zemchug Canyon. The rise contains both
submarine-canyon mouths and the toe deposits of subsea fans. Karl
and others (1981) describe sand lenses of possible turbidite flows
from cores taken in the dissecting canyons and the adjacent rise.
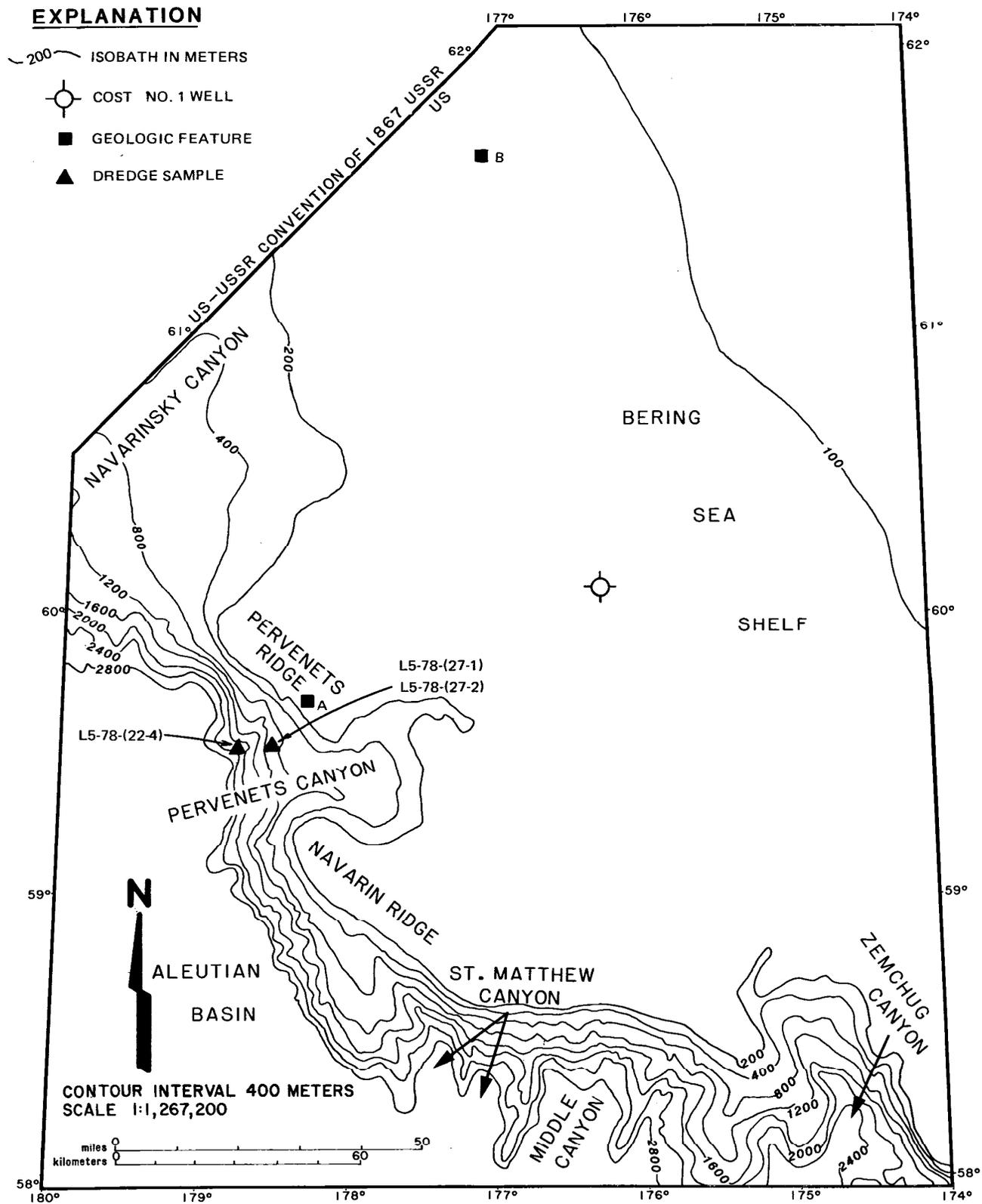
FIGURE 34. Bathymetry, physiographic features, and locations of geologic features and dredge samples.
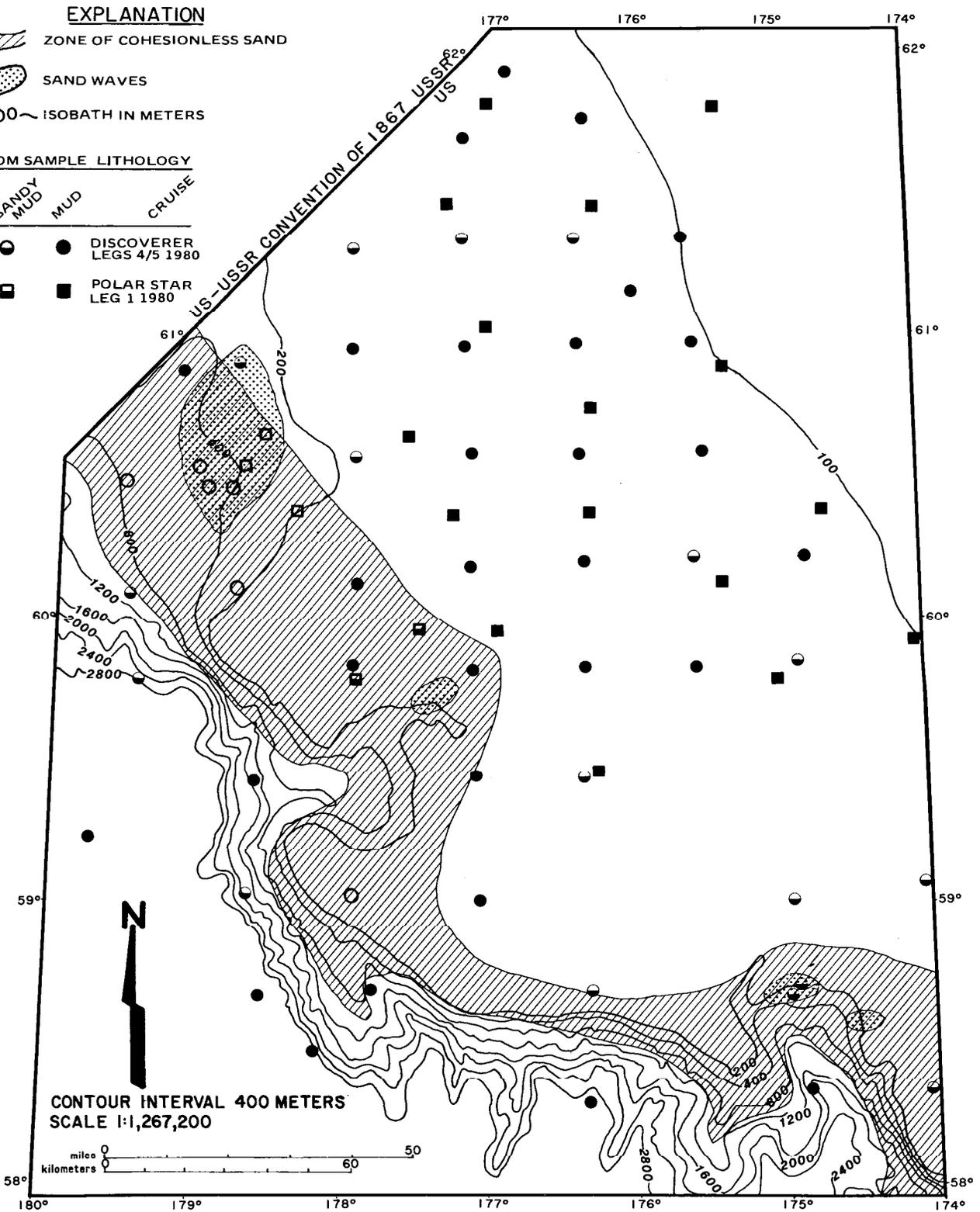
FIGURE 35. Location and lithology of bottom samples, and distribution of cohesionless sand and sand waves. After Carlson and Karl (1984), Edwards and Lee (1984), and Karl and others (1981).

QUATERNARY GEOLOGY

The Navarin Basin is part of the broad, flat Bering Sea continental shelf that has been relatively stable through most of the Cenozoic. During Pleistocene glaciations (and associated low stands of sea level), parts of the inner to outer shelf were exposed to erosion and terrigenous deposition. Sediments eroded from the exposed shelf along with sediments carried by the ancestral Anadyr and Yukon Rivers were deposited across the basin and onto the continental slope and rise. Quaternary deposits blanket much of the Navarin Basin, with at least 115 feet of unconsolidated fine- to coarse-grained sediment covering some areas (Carlson and others, 1983). The interglacials and their associated high-stands of sea level were intervals of little or no sediment accumulation on the Bering Sea shelf.

Quaternary sedimentation rates vary over the shelf, slope, and rise (Carlson and Karl, 1984). Shelf rates range from 3.3 inches/1,000 years north of the shelf break to 8.3 inches/1,000 years at the head of the submarine canyons, with a shelf average of 5.6 inches/1,000 years. Slope sedimentation rates range from 2.0 inches/1,000 years at the upper slope to 5.9 inches/1,000 years on the lower slope. This range reflects the mass movement of large amounts of sediment down gradient. Continental rise sedimentation rates range from 2.8 to 8.3 inches/1,000 years, with an average of 5.9 inches/1,000 years. The areas of highest sediment accumulation are in turbidite fan deposits that are interbedded with hemipelagic muds.

Bottom sampling indicates a zone of sandy mud and sand along the outer shelf edge and upper slope (fig. 35). The sandiest areas are at the canyon heads, where large sediment waves may occur (Carlson and Karl, 1981b). The 1,000-meter isobath appears to delimit the deepwater boundary of this sandy zone. A steepening of the gradient also occurs below the 1,000-meter isobath. In the Navarinsky Canyon area the change in gradient is from 0.03° to 0.28°, and in the Pervenets Canyon area the change is from 0.23° to 5.75°. There are two possible sediment sources for the sandy zone: relict Pleistocene, fine-grained terrigenous deposits that have been winnowed by bottom currents or recent outer-shelf sand deposition. The absence of a proximate sediment source coupled with the presence of weak bottom currents suggests a relict rather than recent origin for this sand.

On the middle and outer shelf, the largest potential sources of sediment are the Yukon, Kuskokwim, and Anadyr Rivers, with average surface runoffs of 71, 17, and 16 cubic miles, respectively. A dominantly northward current has been carrying the Yukon sediment load through the Bering Strait to the southern Chukchi Sea since 11,000 years before present (Knebel and Creager, 1973). The sediment loads carried by the Kuskokwim and Anadyr Rivers could supply the

Navarin shelf area if the bottom currents are strong enough to transport sediment. Storm- or tide-induced bottom currents dominate this part of the shelf. These currents rework existing deposits but bring little or no new sediment into the basin. The remaining part of the middle and outer shelf is covered by Holocene muds that become progressively sandier toward the southeast corner of the planning area (fig. 35). Drop cores collected at the COST well site showed the upper 60 inches of sediment to be soft marine clay and clayey silt, part of the thin veneer of unconsolidated Holocene sediment that covers the inner and middle shelf of the region.

Muds represent the dominant sediment type in the lower slope and rise. Lenticular, coarse-grained, turbidite deposits are present in the dissecting channels. An isopach map of a probable Quaternary reflector (Carlson and others, 1983) shows that this is a structurally controlled depositional environment. Isopach trends and fault offsets indicate an actively subsiding basin. In the Pinnacle Island subbasin, a northwest-trending trough of Quaternary sediment parallels and is slightly offset to the northeast from a similar trough of Tertiary sediment. Structural control of Quaternary sedimentation is also seen in the Navarinsky subbasin. High-resolution seismic data show faults that offset Quaternary reflections and parallel basement-controlled faults.

Geohazards

The presence of shallow gas-charged sediments, deeper
abnormally pressured zones, and sea-floor-instability factors
represent the major potential geologic hazards in the Navarin
Basin. A geologic process or condition is considered a potential
hazard if it threatens the structural integrity of a drill rig
foundation or the safety of men and equipment working in the
area. High-resolution seismic reflection data, geotechnical
borehole information, and surface sample analysis allowed the
identification of types and characteristics of potentially hazardous
conditions. The limited amount of public data, however, prohibited
lease-block-specific identification of geohazard locations with
the exception of submarine slides.

SEA-FLOOR INSTABILITY

Sea-floor-instability hazards which may affect bottom-founded
structures include faulting, seismicity, slides, and erosion.
Foundation support failure results from a reduction in shear strength
of the supporting substrate or from removal of the surrounding
sediment by geologic processes. Seismicity and near-surface faulting
can cause a loss of foundation support by differential displacement,
earthquake-induced shaking, and substrate liquefaction induced by
vibration.

Both detached growth faulting and basement-controlled faulting
appear to be active in the Navarin Basin. Figure 16 displays
numerous large basement faults that offset the overlying Tertiary
deposits.

High-resolution seismic data reveal fault offsets of sediment
as young as Pleistocene near the well site and throughout the
margins of the individual subbasins. Fault offsets of no more
than 10 feet were identified near the Navarin Basin COST well in
reflectors considered to be Pliocene in age (Nekton, Inc., 1980b).
Near-surface offsets ranging from 33 to 67 feet were reported by
Carlson and Karl (1981b) to be present in the Navarin Basin.

The dynamic effects of earthquakes on bottom-founded structures are estimated by calculating the inertial stress generated by ground acceleration (Sowers, 1979). Both body and surface waves generated by an earthquake can cause ground acceleration. Any kinetic energy applied to a structure that is not absorbed by elastic or plastic deformation of the superstructure will result in damage (Leonards, 1962). Vertical acceleration imposes a vertical load on a structure which may cause temporary uplift, followed by foundation settlement. Horizontal acceleration is translated into a shear stress applied to the foundation substrate which may cause lateral displacement of the foundation.

When wet, cohesionless, fine sand that is not at critical density is subjected to vibration, a rapid decrease in soil mass volume may occur (Leonards, 1962). This volumetric decrease results from a decrease in water content. If water is not expelled, and if the reorientating grains are supported by water and not by grain-to-grain contact, the sand mass liquefies, causing a loss of shear strength. Material susceptible to this type of failure has been identified by Edwards and Lee (1984) at the outer shelf edge and upper slope of the Navarin Basin (fig. 35).

The Navarin Basin Planning Area has experienced little recent seismic activity. Meyers (1976) lists only seven reported earthquakes of unspecified magnitude in the area since 1786. The remoteness of the area and the lack of a proper seismic detection network has inhibited an accurate assessment of the region's seismicity. A study of potential earthquake hazards of the Alaskan continental shelf (Woodward-Clyde Consultants, 1978) predicts a maximum ground acceleration of 55 cm/sec^2, with a return period of 100 years.

Submarine slides are a common hazard on the continental slope and in the dissecting submarine canyons. USGS reconnaissance surveys identified slides in water depths of 500 to 3,900 feet. One slide covered an area of over 480 square miles, and composite slides affected the upper 960 feet of sediment. Gravity cores of the upper 16 feet of slide material recovered a mixture of pebbly mud and very soft mud. The slides were classified as slumps, debris flows, or mud flows on the basis of their seismic reflection characteristics (Nardin and others, 1979).

Rapidly deposited, cohesionless, fine-grained material on the Navarin outer shelf edge and upper slope is prone to sliding (fig. 35). Previous sliding may have been initiated either by cyclic wave-loading induced by storms during low stands of sea level or by earthquakes. Carlson and others (1982) and Marlow and others (Resource Report Supplement, 1983) discount cyclic wave-loading as a triggering mechanism for present-day submarine slides. Navarin area storms commonly have winds more than 60 miles per hour and may have winds in excess of 100 miles per hour. Waves generated by storms of this magnitude range from 50 to 65 feet. Repeated strains produced by

earthquakes, however, can increase the pore pressure and cause a loss of shear strength in a sand mass (Sowers, 1979). The increased pore pressure enables the material to withstand even larger strains until failure ensues. The ensuing liquefaction depends on the ability of the sand mass to dissipate pore pressure, the initial density of the material, and the amount of applied stress.

Lease blocks characterized by active or potential submarine sliding were identified in the Notice of Sale for Sale 83 (fig. 36). The criteria used included the presence of fault scarps, proclivities greater than 2°, disrupted reflection sequences, hummocky bathymetry, and detached slump blocks. Where a potential hazard was inferred, the inference was justified by bathymetry and proximity to blocks with direct seismic evidence of slides. Relict and recent movements could not be differentiated by seismic criteria.

Active erosion and redistribution of sediment could reduce the support of bottom-founded structures. Such processes are expressed as sediment waves and sea-floor depressions. USGS surveys have identified relict large sediment waves formed at the heads of the three submarine canyons during low stands of sea level. At the Navarinsky Canyon, these waveforms cover an area of 230 to 270 square miles between the 700- and 1,475-foot isobaths. In some areas, these sediment waves are covered by a thin veneer of recent sediments. Sea-floor depressions parallel to bathymetric contours are present on the down-slope sides of the sediment waves. The depressions are about 165 feet wide and 16 to 33 feet deep and are located 330 to 6,500 feet apart. Sediment transport by bottom currents generated by surface waves has been proposed as a mechanism for the formation of these depressions (Carlson and Karl, 1981b).

GAS-CHARGED SEDIMENTS

Gas-charged sediments are ubiquitous in the Navarin Basin. Shallow occurrences of gas-charged sediment can cause an increase in pore pressure and a decrease in shear strength, which may result in unstable foundation conditions. Gas-charged sediments are identified on analog high-resolution seismic reflection data as anomalous acoustic events recognized by polarity reversal, amplitude increase, reflector "wipe out," and reflector "pull down." Biogenic gas was present in all of the USGS gravity cores taken in the Navarin Basin (Vogel and Kvenvolden, 1981). No significant shows of thermogenic gas were identified. Shallow gas was also encountered in the Navarin Basin COST No. 1 well. Most of this shallow gas is probably biogenic, although some fraction may be thermogenic. There is no obvious zone in which shallow gas accumulated. Anomalous seismic events that might be gas associated are present in all three subbasins in zones correlative with lithologic zones A-1, A-2, B, C-1, and C-2 of the Navarin COST well. In the continental slope and rise areas, gas hydrate accumulations may be

present in the form of a solid-phase mixture of water and gas. This phenomenon is well documented in the Bering Sea (Kvenvolden and McMenamin, 1980; Marlow and others, 1981; Hammond and Gaither, 1983). The gas hydrate is identifiable because the acoustic impedance contrast between it and the overlying sediment produces a seismic reflection. Because the gas hydrate is temperature-pressure dependent, the reflection mimics the sea floor and appears to be a time-transgressive reflection (bottom-simulating reflector, or BSR) in areas of structural relief.

OVERPRESSURING

Unpredicted abnormal pore-fluid pressure can be extremely hazardous if encountered during drilling operations. If encountered near the surface it can also endanger bottom-founded structures. Evidence from the Navarin Basin COST well and from seismic reflection surveys indicates the presence of abnormal pore-fluid pressures in the Navarin Basin (Sherwood, 1984). In the late Miocene to early Pliocene section (2,500 to 3,840 feet), formation test and well log data indicated the presence of abnormally high pore-fluid pressures. Sherwood postulated that this overpressuring is associated with the diagenesis of diatomite-rich sediments and the restricted flow of expelled pore fluid from compacting shales. In the Oligocene section (below 9,430 feet), pore-fluid pressure begins to deviate significantly from the expected pressure gradient for the Bering Sea region. This second, and major, abnormally pressured section apparently continues down into the Cretaceous section. The presence of abnormal pore-fluid pressures in the Navarinsky subbasin is suggested by the presence of shale diapirs (fig. 9). These diapirs are probably derived from Paleocene and Eocene clays that were buried in a rapidly subsiding basin. The basinward divergence of continuous, coherent seismic reflections, and their subsequent disappearance in the center of the basin, suggest continuous, rapid deposition. Rapid deposition increases the likelihood of overpressured shales by increasing the pressure on a porous medium having restricted flow (Gretener, 1981).

Hedberg (1976) postulated that shales which produce gas under restricted-flow conditions enhance their own diapiric capabilities. COST well data indicate that lithologic zones E, F, and perhaps part of D-2, are within the oil window. Lithologic zones E and F contain appropriate types and amounts of kerogen for hydrocarbon generation. The time-equivalent sections of zones E and F thicken considerably in the center of the northern subbasin. Thus, the source beds for the shale diapirs may also be prone to hydrocarbon generation. Therefore, at least in the Navarinsky subbasin, the presence of overpressured shale is likely and, if not prepared for, could pose a hazard to drilling operations.
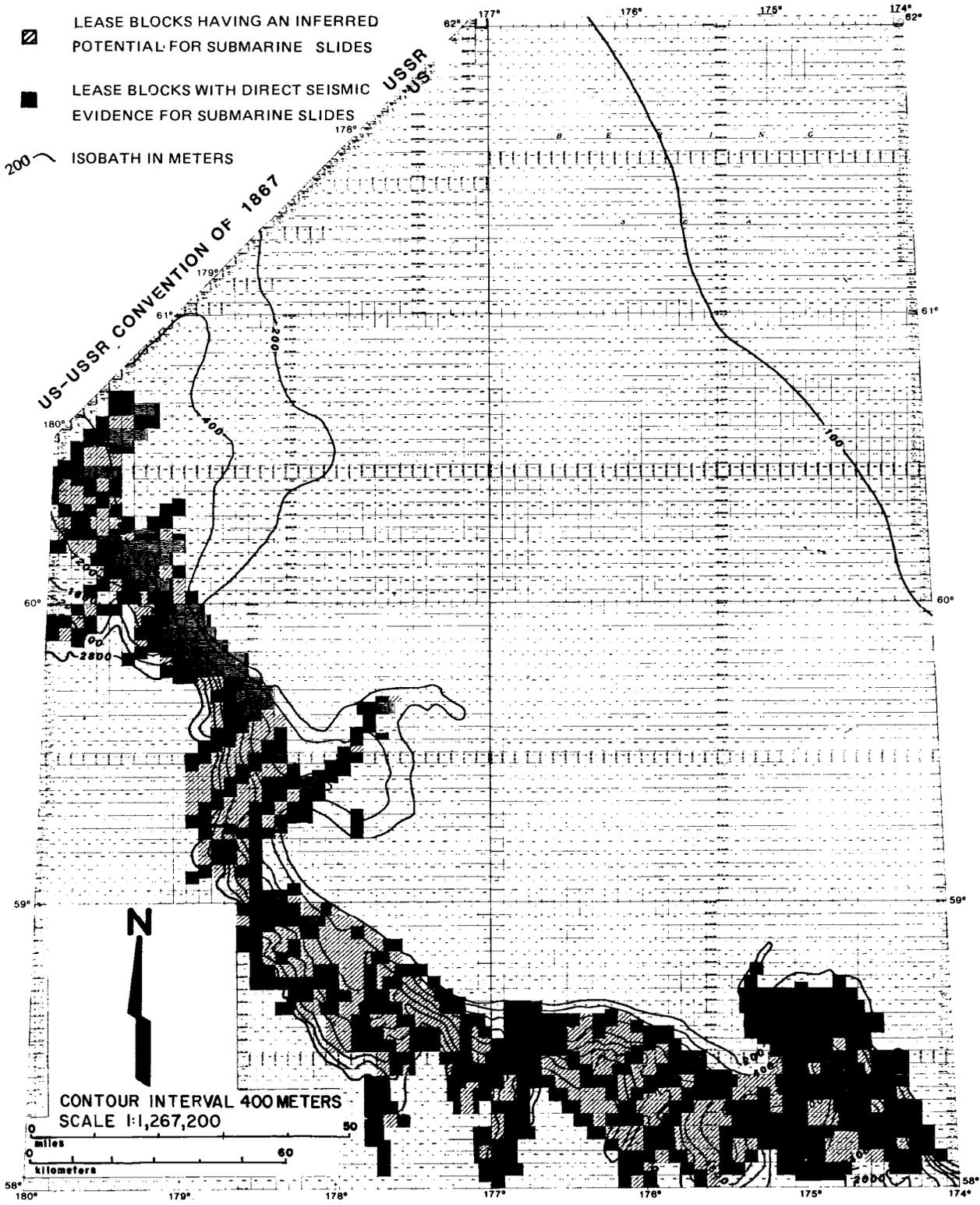
FIGURE 36. Lease blocks identified as having active or potential submarine slides. Adapted from Steffy (1984a).

Environmental Considerations

Very little site-specific biologic, meteorologic, or
oceanographic data exist for the Navarin Basin Planning Area.
Most of the meteorologic and oceanographic information pertaining
to the area is summarized in the Climatic Atlas of the Outer
Continental Shelf Waters and Coastal Regions of Alaska (Brower and
others, 1977) and The Alaska Marine Ice Atlas (Labelle and others,
1983), from data compiled by the National Weather Service and
other Federal agencies, and by the Arctic Environmental Information
and Data Center. The most complete recent biological data available
for the area come from a site-specific survey done for ARCO Alaska,
Inc., by Nekton, Inc. (1980b). The above-enumerated sources and
the Environmental Considerations chapter of the Navarin Basin COST
well report (Adams, 1984) represent the data base for environmental
considerations in the planning area.

METEOROLOGY AND OCEANOGRAPHY

Most of the Bering Sea lies in subarctic latitudes. Cyclonic
atmospheric circulation predominates, and cloudy skies, moderately
heavy precipitation, and strong surface winds characterize the
marine weather. The weather is controlled by high pressures over
the Pacific and Arctic Oceans and Siberia, which results in low
pressures in the Aleutian area. Oceanic current flow in the area
is northerly. Currents range from 0.5 knot in the south to 1.0
knot in the north, where the flow is accelerated toward the Bering
Strait. Wave energy in the Bering Sea is variable. At the center
of the planning area, wave heights greater than 5 feet occur less
than 50 percent of the time from April to July and more than 70
percent of the time from October through January (Brower and others,
1977). Average wave heights are greater toward the southwest part
of the area and smaller to the northeast. Before the Navarin COST
well was drilled, the maximum recorded storm wave heights in the
planning area ranged from 20 feet in June and July to 49 feet in
December.

The planning area is ice free, based on 10-year-average data,
from mid-July to mid-November, at which time the ice edge (generally
about 50 percent ice concentration) begins to encroach from the

northeast. Annual variations in these dates can amount to several weeks, however; National Weather Service analysis of satellite photos has indicated that in 1985, for instance, the area was ice free by June 19. The northeast corner of the planning area may be fully covered by sea ice from early December to late June, with a 75-percent probability of being covered from January through mid-June and a virtual certainty of being covered from mid-February through May. The center of the planning area may be covered with sea ice from early January to mid-June, with a greater than 50-percent chance that it will be covered from early April to late May. The southwest corner of the planning area is generally ice free, with only a 10-percent chance that the ice will extend beyond this point at the sea ice maximum in late April.

The most recent detailed information on meteorological and sea ice conditions in the planning area was gathered by Nortec, Inc. (1984), at the Navarin Basin COST No. 1 well, which was located 120 miles west of Pinnacle Island of the St. Matthew and Hall Islands. The well was begun on May 26, 1983, and completed on October 22, 1983. During this time, meteorologic conditions and wave heights were monitored daily at the rig. Three significant wind events, with 1-minute average surface winds of 34 knots (gale force) or more, were recorded. These occurred from September 12 to September 14, and on September 29 and October 8, 1983. The highest gust (47 knots) was recorded during the first event. The highest seas (with significant wave heights of 29 feet and maximum heights of 50 feet) occurred during the October 8 event.

The pack ice advance near the COST No. 1 well reached a maximum on March 11, 1983, with the ice edge extending to about 60 miles south of the well site. The only other recent recorded pack ice advances which have exceeded this were in 1960 and 1978. The 1978 advance covered about 70 percent of the planning area. Ice coverage of the Sale 83 area within the planning area during this advance was about 90 percent.

BIOLOGY

The Bering Sea shelf edge, and to a lesser extent the rest of the planning area, is characterized by high primary productivity. This is due to the upwelling of nutrient-rich oceanic water at the shelf edge, which supports a complex ecosystem of culturally and commercially valuable stocks of fish, invertebrates, and marine mammals. In addition, St. Matthew and Hall Islands, a wilderness area approximately 30 miles east of the planning area, support a large number of bird species. These islands have been nominated as an area meriting special attention in the Alaska Coastal Management Plan.

A site-specific marine biological survey was designed by MMS in concert with other Federal and State agencies to obtain biological data at both the Navarin COST No. 1 well site and the

alternate site 13 miles to the west. Through the use of underwater video and photographic documentation, plankton tows, infaunal sampling, and trawling, Nekton, Inc. (1980b), determined the relative abundance and types of organisms present in various habitats. These surveys were conducted from August 15 to August 17, 1980. The results, which are probably characteristic of the biologic makeup of much of the planning area, are summarized below:

1. Copepods (small crustaceans) were the most abundant element of the plankton, accounting for about 99 percent of the total organisms. Smaller amounts (approximately 1 percent) of euphausids (shrimp-like crustaceans) and chaetognaths (arrow worms) were also present. Decapod crustaceans (crabs, shrimp, etc.) accounted for less than 1 percent of the plankton in all of the samples. No fish eggs or fish larvae were found at either site.

2. Epibenthic invertebrates were the numerically dominant component of the trawl catch at both sites. The most abundant invertebrates were asteroids (starfish) and ophiuroids (brittle stars). One commercial shrimp species was taken in low numbers at both sites.

3. Video and still photography of the seabed at both sites revealed, in decreasing order of abundance, eelpouts, roundfish, near-bottom plankton organisms, starfish, and sea snails. Benthic grabs at both sites revealed that polychaete annelids (bristle worms) were the dominant animals, followed by arthropods, priapulids (small wormlike animals), and echinoderms (sea urchins, etc.).

The biological survey indicated that the area contained no unique habitats or species that would require rejection or modification of the COST well drilling program. No additional biological resources were discovered during drilling operations. No adverse effects on existing biological resources were apparent from drilling activities.

MARINE MAMMALS, ENDANGERED SPECIES, AND BIRDS

Marine mammal and bird resources of the planning area include overwintering whales and pinnipeds (seals and walrus), migrating whales, and migrating and resident sea birds and other waterfowl. Few endangered mammals frequent the planning area. Bowhead whales overwinter in the vicinity of the ice front; beluga whales are occasionally present; and sperm whales feed along the shelf break along the western boundary of the area.

The proposed drilling program was submitted to the National Marine Fisheries Service (NMFS) and the U.S. Fish and Wildlife

Service for review and comment regarding potential effects of the operation on living resources in the area. A letter was received from NMFS, included as an attachment to the Environmental Assessment (EA), recommending stipulations to be carried out in concert with the Alaska OCS Orders. NMFS recommended minimum approach distances for air and surface support craft, gave guidelines for reinitiation of consultation, and recommended continued whale research.

Eleven species of birds were observed at the COST well site, and ten species at the alternate site. The most abundant bird species at both sites was the northern fulmar. Other species frequently encountered at the COST well site included tufted puffins, common murres, fork-tailed storm petrels, black turnstones, Aleutian terns, Arctic terns, and black-legged kittiwakes. Black-legged kittiwakes and common murres were also frequently sighted at the alternate site. Both of these species have recently received special attention because of population declines related to shortages of food, chiefly pollack (Springer and others, 1983; MMS contract avian recensusing, in progress).

FISHERIES

The planning area contributes significantly to Bering Sea fisheries production. In the past, Bering Sea fishery resources have been largely exploited by Japanese, Korean, and Soviet fishing fleets; however, with the advent of the Federal 200-mile extended jurisdiction, these resources may be more intensively harvested by U.S. fishermen. Approximately 315 species of fish are present in the Bering Sea, of which 25 are commercially valuable. Herring, salmon, pollack (cod), ocean perch, and halibut and various other flatfish (turbot and sole) are the most important of the commercial species. Noteworthy also are valuable populations of King and Tanner crab and western Alaska salmon.

CULTURAL RESOURCES

The COST well and alternate sites were located in a deepwater area where the probability for the occurrence of cultural resources (campsites, burial sites, etc., occupied during Pleistocene low-sea-level stands) was low. TV transects, side-scan sonar, and magnetometer surveys discovered no unexplained anomalies, and no cultural resources were identified during the COST well drilling operations. The northeastern quarter of the planning area is shallower (165 to 600 feet) and may require further investigations for Pleistocene cultural artifacts.

Summary and Conclusions

The Navarin Basin Planning Area includes significant acreage on the continental shelf as well as in the deepwater continental slope province. At this juncture, the only part of the planning area considered to have economic hydrocarbon potential is the continental shelf and shelf basins. The advent of improved deep-water drilling technology coupled with the collection of new data from the slope and rise could someday alter this perception.

Sea-floor instability (earthquake shaking, submarine slides, gas-charged sediment) and abnormal formation pressures could impose engineering constraints on drilling operations. Deep water, extreme weather conditions, and floating ice are also significant inhibiting environmental considerations in this offshore frontier area.

Rocks of Holocene to Jurassic age are present under the Navarin Basin shelf. Mesozoic strata are exposed at the shelf break. The acoustic basement appears to be Mesozoic in most areas, probably Late Cretaceous. Acoustic basement and economic basement may not be synonymous. The base of Tertiary fill may be as deep as 36,000 feet in some of the subbasins.

The best source rocks in the COST well are organic-rich Eocene mudstones. Good source rock sections elsewhere in the basin may be several thousand feet thick. Type II kerogens containing 1.0 to 2.0 percent organic carbon were observed in the Eocene section of the well. Gas plumes associated with shale diapirs appear to represent leaking thermogenic gas. Sediments as young as late Oligocene and as old as Late Cretaceous exhibit some source rock potential. The oil window seen in the COST well extends from about 9,400 to 15,000 feet.

The best reservoir rocks in the Navarin Basin COST well are the late Oligocene offshore bar sandstones of lithologic zone C-2. Reservoir sands of somewhat lesser quality are present in lithologic zone C-1 (Miocene). Potential reservoirs associated with possible Oligocene and Eocene turbidite deposits appear to be present along the subbasin margins and as detrital aprons around basement highs. These possible turbidite reservoirs apparently

interfinger downdip with thermally mature, organic-rich mudstones.
In some settings, the Mesozoic section may have good reservoir
characteristics due to the development of secondary porosity.

There are a number of hydrocarbon trap configurations present
in the Navarin Basin. Most of the traps are associated with Tertiary
pull-apart structures characterized by normal faulting. Other plays
include pinch-outs, drape deposits over basement highs, and truncations
associated with shale diapirism. There are also a number of potential
stratigraphic traps related to facies changes and diagenetic zones.

The presence of thermally mature, organically rich source beds,
abundant sealing horizons, good trapping configurations, and timing
considerations all bode well for petroleum exploration and development.
Reservoir quality may prove to be the most important limiting factor
in the basin.

REFERENCES

Adams, A. J. 1984. Environmental considerations. In Geological
    and operational summary, Navarin Basin COST No. 1 well, Bering
    Sea, Alaska, 222-229. See Turner and others, 1984.

AGAT Consultants, Inc. 1983. Reservoir quality study, ARCO Navarin
    Basin COST Well No. 1. 8 vols. Denver. Independent consultant
    report prepared for ARCO Exploration Company.

Alaska Geological Society. 1975. Oil and gas fields in the Cook
    Inlet Basin, Alaska. Anchorage.

Al-Chalabi, Mahboub. 1974. An analysis of stacking, RMS, average,
    and interval velocities over a horizontally layered ground.
    Geophysical Prospecting 22:458-75.

Al-Chalabi, Mahboub. 1979. Velocity determination from seismic
    reflection data. In Developments in Geophysical Exploration
    Methods-1. London: Applied Science Publication, Ltd.

Aleksandrov, A. A.; Bogdanov, N. S.; Byalobzheskig, S. G.; Marlow,
    M. S.; Tilman, S. M.; Khain, V. Ye.; and Chekhov, A. D. 1976.
    New data on the tectonics of the Koryak-highlands. Geotectonics
    9:292-99.

Anstey, N. A. 1977. Seismic interpretation: The physical aspects.
    Boston: International Human Resources Development Corp.

ARCO Alaska, Inc. 1981. Environmental report for Navarin Basin
    COST No. 1. Anchorage. Report submitted to U.S. Minerals
    Management Service, Alaska OCS Region.

Asquith, G. E., and Gibson, C. G. 1982. Basic well log analysis
    for geologists. Tulsa: AAPG.

Badaut, Denise, and Risacher, Francois. 1982. Authigenic smectite
    on diatom frustules in Bolivian saline lakes. Geochimica et
    Cosmochimica Acta 47:363-75.

Banik, N. C. 1983. Velocity anisotropy of shales and depth anomalies
    in the North Sea. In 53rd Annual International Society of
    Exploration Geophysicists meeting, September 11-15, 1983,
    Las Vegas, Nevada: Expanded abstracts with biographies, 1983
    Technical Program, 540-42. Tulsa.

Barker, Colin. 1974. Pyrolysis techniques for source-rock evaluation.
    AAPG Bulletin 58:2349-61.

Barron, J. A. 1980. Lower Miocene to Quaternary diatom biostratigraphy of Leg 57, off northeastern Japan, Deep Sea Drilling Project. In Initial reports of the Deep Sea Drilling Project, vol. 56, 57, part 2, 507-38. Washington, D.C.: National Science Foundation.

Barron, J. A. 1981. Late Cenozoic diatom biostratigraphy and paleoceanography of the middle latitude eastern Pacific, Deep Sea Drilling Project. In Initial reports of the Deep Sea Drilling Project, vol. 63, 507-73. Washington, D.C.: National Science Foundation.

Barron, J. A., and Keller, G. 1982. Widespread Miocene deep-sea hiatuses: Coincidence with periods of global cooling. Geology 10:577-81.

Bayliss, G. S., and Smith, M. R. 1980. Source rock evaluation reference manual. Houston: Geochem Laboratories.

Beikman, H. M. 1980. Geologic map of Alaska. U.S. Geological Survey. 2 sheets. Scale 1:2,500,000.

Belyi, V. F. 1973. Okhotsk-Chukotsk fold belt and the problem of volcanic arcs in northeast Asia. In AAPG Memoir 19, 252-58.

Berg, R. R. 1975. Depositional environment of Upper Cretaceous Sussex Sandstone, House Creek Field, Wyoming. AAPG Bulletin 59:2099-2110.

Bernard, Bernie; Brooks, J. M.; and Sackett, W. M. 1977. A geochemical model for characterization of hydrocarbon gas sources in marine sediments. In Ninth annual Offshore Technology Conference, proceedings, paper 2934.

BioStratigraphics Consulting Micropaleontology. 1983. ARCO Navarin Basin COST No. 1, Bering Sea, Alaska. 5 parts. Ventura, Calif.: BioStratigraphics, a unit of McClelland Engineers.

Blanton, Jr., S. L. 1977. Geology of the Bering Shelf. In The relationship of plate tectonics to Alaskan geology and resources, ed. A. Sisson, E-1-6. Proceedings of 6th Alaska Geological Society Symposium, April 4-6, Anchorage.

Blow, W. H. 1969. Late middle Eocene to Recent planktonic foraminiferal biostratigraphy. In Proceedings, first International Conference of Planktonic Microfossils, Geneva, 1967, vol. 1, 199-422. Leiden: E. J. Brill.

Boles, J. R. 1984. Principles of chemical diagenesis with applications in Gulf Coast Tertiary sandstones. In Sandstone Diagenesis Course Notes, 1-86. Tulsa: AAPG

Bolli, H. M. 1957. Planktonic foraminifera from the Oligocene-Miocene Cipero and Lengua Formations of Trinidad, B.W.I.: U.S. National Museum Bulletin, No. 215, 97-123.

Bouma. 1984. Quoted in Gentz, J. 1984. Mississippi Fan findings studied. AAPG Explorer (Oct. 1984):22-24.

Bray, E. E., and Evans, E. D. 1961. Distribution of n-paraffins as a clue to recognition of source beds. Geochemica et Cosmochimica Acta 22:2-15.

Brenner, R. L., and Davies, D. K. 1974. Oxfordian sedimentation in Western Interior United States. AAPG Bulletin 58:407-28.

Brower, W. H.; Diaz, H. F.; Prechtel, H. S.; Searby, H. W.; and Wise, J. L. 1977. Climatic atlas of the outer continental shelf waters and coastal regions of Alaska. Vol. 2, Bering Sea. AEIDC Publication B-77. Anchorage: Alaska Environmental Information and Data Center, University of Alaska.

Brown, L. F., and Fisher, W. L. 1980. Seismic stratigraphic interpretation and petroleum exploration. AAPG Continuing Education Course Note Series No. 16. Tulsa.

Bruce, C. H. 1984. Smectite dehydration--Its relation to structural development and hydrocarbon accumulation in northern Gulf of Mexico Basin. AAPG Bulletin 68:673-83.

Bujak, J. P. 1984. Cenozoic dinoflagellate cysts and acritarchs from the northern North Pacific. Micropaleontology 60:100-212.

Burckle, Lloyd. 1981. Paleomagnetic data on the Dictyocha aspera/D. fibula crossover in the equatorial Pacific. Micropaleontology 27:332-34.

Burst, J. F. 1969. Diagenesis of Gulf Coast clayey sediments and its possible relation to petroleum migration. AAPG Bulletin 53:73-93.

Byun, B. S. 1983. Characteristics of reflection traveltimes for layer models. In 53rd Annual International Society of Exploration Geophysicists meeting, September 11-15, 1983, Las Vegas, Nevada: Expanded abstracts with biographies, 1983 technical program, 447-48. Tulsa.

Carlson, P. R.; Fischer, J. M.; Karl, H. A.; and Larkin, Christopher. 1983. Isopach map of unit A, youngest sedimentary sequence in Navarin Basin. In Surface and near-surface geology, Navarin Basin province: Results of the 1980-81 field seasons, ed. H. A. Karl and P. R. Carlson. U.S. Geological Survey Open-File Report 84-89.

Carlson, P. R.; Golan-Bac, Margaret; Karl, H. A.; and Kvenvolden,
K. A. 1985. Seismic and geochemical evidence for shallow
gas in sediment on Navarin continental margin, Bering Sea.
AAPG Bulletin 69:422-36.

Carlson, P. R., and Karl, H. A. 1981a. Seafloor geologic hazards,
sedimentology, and bathymetry: Navarin Basin province,
northwestern Bering Sea. U.S. Geological Survey Open-File
Report 81-1217.

Carlson, P. R., and Karl, H. A. 1981b. Seafloor geologic hazards. In
Seafloor geologic hazards, sedimentology, and bathymetry: Navarin
Basin province, northwestern Bering Sea, ed. P. R. Carlson and
H. A. Karl, 58-73. U.S. Geological Survey Open-File Report 81-
1217.

Carlson, P. R., and Karl, H. A. 1984. Rate of sediment accumulation.
In Surface and near-surface geology, Navarin basin province:
Results of the 1980-81 field season, ed. H. A. Karl and P. R.
Carlson. U.S. Geological Survey Open-File Report 84-89.

Carlson, P. R.; Karl, H. A.; Fischer, J. M.; and Edwards, B. D.
1982. Geologic hazards in Navarin Basin province, northern
Bering Sea. In Fourteenth annual Offshore Technology Conference,
Houston, proceedings, paper 4172.

Carlson, P. R., and Marlow, M. S. 1984. Discovery of a gas plume in
Navarin Basin. Oil and Gas Journal 82(2 April):157-58.

Claypool, G. E., and Reed, P. R. 1976. Thermal-analysis technique
for source rock evaluation: Quantitative estimates of organic
richness and effects of lithologic variation. AAPG Bulletin
60:608-26.

Cooper, A. K.; Scholl, D. W.; and Marlow, M. S. 1976. Plate tectonic
model for the evolution of the Bering Sea basin. GSA Bulletin
87:1119-26.

Core Laboratories, Inc. 1983. Core analysis report for ARCO Alaska,
Inc., Navarin COST No. 1 stratigraphic test, Navarin Basin,
Alaska. Dallas.

Davey, R. J.; Downie, Charles; Sarjeant, W. A. S.; and Williams,
G. L. 1966. Studies on Mesozoic and Cainozoic dinoflagellate
cysts. Bulletin of the British Museum (Natural History),
Geology, Supplement 3. London.

Deffeyes, K. S. 1959. Zeolites in sedimentary rocks. Journal of
Sedimentary Petrology 29:602-9.

Demaison, G. J. 1981. Stratigraphic aspects of source bed occurrence: The organic facies concept. In Geochemistry for geologists. Short Course Notes. Dallas: AAPG.

Demaison, Gerard. 1984. The generative basin concept. In Petroleum geochemistry and basin evaluation, ed. Gerard Demaison and R. J. Murris, 1-14. AAPG Memoir 35. Tulsa.

Demaison, G. J., and Moore, G. T. 1980. Anoxic environments and oil source bed genesis. AAPG Bulletin 64:1179-1209.

Dickinson, W. R. 1970. Relations of andesites, granites and derivative sandstones to arc-trench tectonics. Rev. Geophys. Space Phys. 8:813-60.

Dix, C. H. 1955. Seismic velocities from surface measurements. Geophysics 20:68-86.

Dow, W. G. 1977. Kerogen studies and geological interpretations. Journal of Geochemical Exploration 7(2):79-99.

Dow, W. G., and Coleman, S. H. 1983. Geochemical analysis of Navarin Basin No. 1 COST well, Alaska. Houston: Robertson Research (U.S.), Inc. Prepared for ARCO Exploration Co., Anchorage.

Dow, W. G., and O'Connor, D. J. 1982. Kerogen maturity and type by reflected light microscopy applied to petroleum exploration. In How to assess maturation and paleotemperatures, 133-57. SEPM Short Course No. 7. Tulsa: Society of Economic Paleontologists and Mineralogists.

Downey, M. W. 1984. Evaluating seals for hydrocarbon accumulations. AAPG Bulletin 68:1752-63.

Dresser Atlas, Dresser Industries, Inc. 1979. Log interpretation charts. Houston.

Dundo, O. P. 1974. Stratigraphic scheme of the Cretaceous deposits of the Koryak highlands (design of unified and correlational schemes). In Stratigraphy and lithology of the Cretaceous, Paleogene, and Neogene deposits of the Koryak-Anadyr District, 5-15. Leningrad: Scientific Research Institute of Arctic Geology (NIIGA), Ministry of Geology of the USSR.

Dutro, Jr., J. T. 1981. Geology of Alaska bordering the Arctic Ocean. In The ocean basins and margins, ed. A. E. M. Nairn, M. Churkin, Jr., and F. G. Stehl, 21-36. New York: Plenum Press.

Edwards, B. D., and Lee, H. J. 1984. Summary of geotechnical characteristics. In Surface and near-surface geology, Navarin Basin province: Results of the 1980-81 field seasons, ed. H. A. Karl and P. R. Carlson. U.S. Geological Survey Open-File Report 84-89.

Elsik, W. C. 1977. Paralecaniella indentata (Defl. and Cooks. 1955) Cookson and Eisenack 1970 and allied dinocysts. Palynology 1:95-102.

ERT biostrat. 1983. Micropaleontology report, Navarin Basin COST well program, Bering Sea, Alaska. Fort Collins, Colo.: ERT biostrat, a division of Environmental Research and Technology, Inc.

Espitalie, J.; Laporte, J. L.; Madec, M.; Marquis, F.; Leplat, P.; Paulet, J.; and Boutefeu, A. 1977. Methode rapide de caracterisation des roches meres, de leur potentiel petrolier et de leur degre d'evolution. Revue de l'Institute Francais Petrolier 32:23-42.

Exploration Logging (USA), Inc. 1983. Final operational report, ARCO Alaska, Inc., Navarin Basin COST well No. 1, May 1983 to October 1983. Anchorage.

Exploration Logging (USA), Inc., see also Russ, 1983, Geochemical final well report.

Fertl, W. H. 1976. Abnormal formation pressures. Developments in Petroleum Science, 2. New York: Elsevier.

Fertl, W. H., and Wichmann, P. A. 1977. How to determine static BHT from well log data. World Oil 184:105-6.

Fisher, M. A.; Patton, W. W.; Thor, D. R.; Holmes, M. L.; Scott, E. W.; Nelson, C. H.; and Wilson, C. L. 1979. Resource report for proposed OCS Lease Sale 57: Norton Basin, Alaska. U. S. Geological Survey Open-File Report 79-720.

Folk, R. L. 1974. Petrology of sedimentary rocks. Austin, Tex.: Hemphill.

Fullam, T. J.; Supko, P. R.; Boyce, R. E.; and Stewart, R. J. 1973. Some aspects of Late Cenozoic sedimentation in the Bering Sea and north Pacific Ocean. In Initial reports of the Deep Sea Drilling Project, vol. 19, ed. P. R. Supko, 887-96. Washington, D. C.: National Science Foundation.

Geological Society of America. 1970. Rock color chart, by E. N. Goddard, P. D. Trask, R. K. DeFord, O. N. Rove, J. T. Singewald, Jr., R. M. Overbeck. Boulder.

Gladenkov, Y. B. 1977. Stages in the evolution of mollusks and
    subdivisions of the North Pacific Neogene. In Proceedings of
    the first International Congress on Pacific Neogene stratigraphy,
    Tokyo, 1976, ed. Tsunemesa Saito and Hiroshi Ujiie, 89-91.
    Tokyo: International Union of Geological Sciences, Science
    Council of Japan, and Geological Society of Japan.

Gladenkov, Y. B. 1980. Stratigraphy of marine Paleogene and Neogene
    of northeast Asia (Chukotka, Kamchatka, Sakhalin). AAPG
    Bulletin 64:1087-93.

Golan-Bac, Margaret, and Kvenvolden, K. A. 1984a. Hydrocarbon
    gases in sediments from Navarin Basin, Bering Sea: Results
    from 1982 field season. U.S. Geological Survey Open-File
    Report 84-97.

Golan-Bac, Margaret, and Kvenvolden, K. A. 1984b. Hydrocarbon gases
    in sediments: Results from 1981 field season. In Surface
    and near-surface geology, Navarin Basin province: Results
    of 1980-81 field seasons, ed. H. A. Karl and P. R. Carlson.
    U.S. Geological Survey Open-File Report 84-89.

Gretener, P. E. 1981. Pore pressure: Fundamentals, general
    ramifications, and implications for structural geology (revised).
    Education Course Note Series No. 4. Tulsa: AAPG.

Hammond, R. D., and Gaither, J. R. 1983. Anomalous seismic character -
    Bering Sea shelf. Geophysics 48:590-605.

Harding, T. P. 1973. Newport-Inglewood trend, California--An example
    of wrenching style of deformation. AAPG Bulletin 57:97-116.

Harland, Rex. 1978. Quaternary and Neogene dinoflagellate cysts. In
    Distribution of biostratigraphically diagnostic dinoflagellate
    cysts and miospores from the northwest European continental
    shelf and adjacent areas, ed. Bindra Thusu, 7-17. Continental
    Shelf Institute Publication No. 100. Trondheim, Norway.

Harms, J. C.; Southard, J. B.; Spearing, D. R.; and Walker, R. G.
    1975. Depositional environments as interpreted from primary
    sedimentary structures and stratification sequences. SEPM
    Short Course No. 2. Dallas: Society of Economic Paleontologists
    and Mineralogists.

Harms, J. C.; Southard, J. B.; and Walker, R. G. 1982. Structures and
    sequences in clastic rocks. Lecture Notes for Short Course No. 9.
    Society of Economic Paleontologists and Mineralogists.

Hayes, J. B. 1984. Sandstone porosity evolution. In Sandstone
    Diagenesis Course Notes, 1-36. Tulsa: AAPG.

Hayes, J. B.; Harms, J. C.; and Wilson, T. 1976. Contrasts between braided and meandering stream deposits, Beluga and Sterling Formations (Tertiary), Cook Inlet, Alaska. In Recent and ancient sedimentary environments in Alaska, Alaska Geological Society Symposium Proceedings, J1-J27.

Hedberg, H. D. 1976. Relation of methane generation to under-compacted shales, shale diapirs and mud volcanoes. AAPG Bulletin 58:661-73.

Hein, J. R.; O'Neil, J. R.; and Jones, M. G. 1979. Origin of authigenic carbonates in sediment from the deep Bering Sea. Sedimentology 26:681-705.

Hein, J. R., and Scholl, D. W. 1978. Diagenesis and distribution of late Cenozoic volcanic sediment in the southern Bering Sea. Geological Society of America Bulletin 89:197-210.

Hein, J. R.; Scholl, D. W.; Barron, J. A.; Jones, M. G.; and Miller, Jacquelyn. 1978. Diagenesis of late Cenozoic diatomaceous deposits and formation of the bottom simulating reflector in the southern Bering Sea. Sedimentology 25:155-81.

Helander, D. P. 1983. Fundamentals of formation evaluation. Tulsa: Oil and Gas Consultants, Inc.

Hottmann, C. E., and Johnson, R. K. 1965. Estimation of formation pressures from log-derived shale properties. Journal of Petroleum Technology (June 1965):717-22.

Hunt, J. M. 1979. Petroleum geochemistry and geology. San Francisco: W. H. Freeman.

Hunt, J. M. 1984. Generation and migration of light hydrocarbons. Science 226:1265-1270.

Iijima, Azuma. 1980. Geology of natural zeolites and zeolitic rocks. Pure and Applied Chemistry 52:2115-30.

Iijima, Azuma, and Utada, Minoru. 1983. Recent developments in the sedimentology of siliceous deposits in Japan. In Siliceous deposits in the Pacific region, ed. A. Iijima, J. R. Hein, and R. Siever, 45-64. Developments in Sedimentology No. 36. Amsterdam: Elsevier.

Isaacs, C. M.; Pisciotto, K. A.; and Garrison, R. E. 1983. Facies and diagenesis of the Miocene Monterey Formation, California: A summary. In Siliceous deposits in the Pacific region, ed. A. Iijima, J. R. Hein, and R. Seiver, 247-82. Developments in Sedimentology No. 36. Amsterdam: Elsevier.

Gladenkov, Y. B. 1977. Stages in the evolution of mollusks and
    subdivisions of the North Pacific Neogene. In Proceedings of
    the first International Congress on Pacific Neogene stratigraphy,
    Tokyo, 1976, ed. Tsunemesa Saito and Hiroshi Ujiie, 89-91.
    Tokyo: International Union of Geological Sciences, Science
    Council of Japan, and Geological Society of Japan.

Gladenkov, Y. B. 1980. Stratigraphy of marine Paleogene and Neogene
    of northeast Asia (Chukotka, Kamchatka, Sakhalin). AAPG
    Bulletin 64:1087-93.

Golan-Bac, Margaret, and Kvenvolden, K. A. 1984a. Hydrocarbon
    gases in sediments from Navarin Basin, Bering Sea: Results
    from 1982 field season. U.S. Geological Survey Open-File
    Report 84-97.

Golan-Bac, Margaret, and Kvenvolden, K. A. 1984b. Hydrocarbon gases
    in sediments: Results from 1981 field season. In Surface
    and near-surface geology, Navarin Basin province: Results
    of 1980-81 field seasons, ed. H. A. Karl and P. R. Carlson.
    U.S. Geological Survey Open-File Report 84-89.

Gretener, P. E. 1981. Pore pressure: Fundamentals, general
    ramifications, and implications for structural geology (revised).
    Education Course Note Series No. 4. Tulsa: AAPG.

Hammond, R. D., and Gaither, J. R. 1983. Anomalous seismic character
    Bering Sea shelf. Geophysics 48:590-605.

Harding, T. P. 1973. Newport-Inglewood trend, California--An example
    of wrenching style of deformation. AAPG Bulletin 57:97-116.

Harland, Rex. 1978. Quaternary and Neogene dinoflagellate cysts. In
    Distribution of biostratigraphically diagnostic dinoflagellate
    cysts and miospores from the northwest European continental
    shelf and adjacent areas, ed. Bindra Thusu, 7-17. Continental
    Shelf Institute Publication No. 100. Trondheim, Norway.

Harms, J. C.; Southard, J. B.; Spearing, D. R.; and Walker, R. G.
    1975. Depositional environments as interpreted from primary
    sedimentary structures and stratification sequences. SEPM
    Short Course No. 2. Dallas: Society of Economic Paleontologists
    and Mineralogists.

Harms, J. C.; Southard, J. B.; and Walker, R. G. 1982. Structures and
    sequences in clastic rocks. Lecture Notes for Short Course No. 9.
    Society of Economic Paleontologists and Mineralogists.

Hayes, J. B. 1984. Sandstone porosity evolution. In Sandstone
    Diagenesis Course Notes, 1-36. Tulsa: AAPG.

Issler, D. R. 1984. Calculation of organic maturation levels for offshore eastern Canada - implications for general application of Lopatin's method. Canadian Journal of Earth Sciences 21: 477-88.

Jacobson, R. A. 1984. Age determination of dredge samples. Denver: Jacobson Consulting, Inc.

Jones, D. M.; Kingston, M. J.; Marlow, M. S.; Cooper, A. K.; Barron, J. A.; Wingate, F. H.; and Arnal, R. E. 1981. Age, mineralogy, physical properties, and geochemistry of dredge samples from the Bering Sea continental margin. U.S. Geological Survey Open-File Report 81-1297.

Jorden, J. R., and Shirley, O. J. 1966. Application of drilling performance data to overpressure detection. AIME-SPE Paper No. 1407. Journal of Petroleum Technology 18:1387-94.

Karl, H. A., and Carlson, P. R. 1984. Surface and near-surface geology, Navarin Basin province: Results of the 1980-1981 field seasons. U.S. Geological Survey Open-File Report 84-89.

Karl, H. A.; Carlson, P. R.; Fischer, J.; Johnson, K.; and Lamb, B. 1981. Textural variations and composition of bottom sediment. In Seafloor geologic hazards, sedimentology, and bathymetry: Navarin Basin province, northwestern Bering Sea, ed. P. R. Carlson and H. A. Karl, 28-33. U.S. Geological Survey Open-File Report 81-1217.

Keigwin, Lloyd, and Keller, Gerta. 1984. Middle Oligocene cooling from equatorial Pacific DSDP site 77B. Geology 12:16-19.

Keller, Gerta. 1983. Biochronology and paleoclimatic implications of middle Eocene to Oligocene planktonic foraminiferal faunas. Marine Micropaleontology 7(6):463-86.

Keller, Gerta, and Barron, J. A. 1983. Paleoceanographic implications of Miocene deep-sea hiatuses. Geological Society of America Bulletin 94:590-613.

Keller, Gerta; Von Huene, R.; McDougall, K.; and Bruns, T. R. 1984. Paleoclimatic evidence for Cenozoic migration of Alaskan terranes. Tectonics 3:473-495.

Kerr, R. A. 1984. Ice cap of 30 million years ago detected. Science 224(13 April):141-42.

Knebel, H. J., and Creager, J. S. 1973. Yukon River: Evidence for extensive migration during the Holocene transgression. Science 179:1230-32.

Koizumi, Itaru. 1973. The Late Cenozoic diatoms of sites 183-193, Leg 19 Deep Sea Drilling Project. In Initial reports of the Deep Sea Drilling Project, vol. 19, ed. P. R. Supko, 805-55. Washington, D. C.: National Science Foundation.

Korotkevich, V. D. 1974. Late Cretaceous spore-pollen assemblages of the Koryak highlands. In Stratigraphy and lithology of the Cretaceous, Paleogene, and Neogene deposits of the Koryak-Anadyr District, 31-37. Leningrad: Scientific Research Institute of Arctic Geology (NIIGA), Ministry of Geology of the USSR.

Kvenvolden, K. A., and McMenamin, M. A. 1980. Hydrates of natural gas: A review of their geologic occurrence. U.S. Geological Survey Circular 825.

Kvenvolden, K. A., and Redden, G. D. 1980. Hydrocarbon gas in sediment from the shelf, slope, and basin of the Bering Sea. Geochimica et Cosmochimica Acta 44:1145-50.

Labelle, J. C.; Wise, J. L.; Voelker, R. P.; Schulze, R. H.; and Wohl, G. M. 1983. Alaska marine ice atlas. Anchorage: Alaska Environmental Information and Data Center, University of Alaska.

Larskaya, Y. S., and Zhabrev, D. H. 1964. Effects of stratal temperatures and pressures on the composition of dispersed organic matter from the example of the Mesozoic-Cenozoic deposits of the western Ciscaspian region. Dokl. Akad. Nauk SSSR 157(4):135-39.

Lentin, J. K., and Williams, G. L. 1977. Fossil dinoflagellates: Index to genera and species. Bedford Institute of Oceanography Report Series BI-R-77-8. Dartmouth, Canada.

Leonards, G. A. 1962. Foundation Engineering. New York: McGraw-Hill.

Levin, F. K. 1978. The reflection, refraction, and diffraction of waves in media with an elliptical velocity dependence. Geophysics 48:528.

Ling, H. Y. 1973. Silicoflagellates and Ebridians from Leg 19. In Initial reports of the Deep Sea Drilling Project, vol. 19, ed. P. R. Supko, 751-75. Washington, D. C.: National Science Foundation.

Ling, H. Y. 1977. Late Cenozoic silicoflagellates and Ebridians from the eastern North Pacific region. In Proceedings of the first International Congress on Pacific Neogene Stratigraphy, Tokyo, 1976, ed. Tsunemasa Saito and Hiroshi Ujiie, 205-33. Tokyo: International Union of Geological Sciences, Science Council of Japan, and Geological Society of Japan.

Link, T. A.; Downing, J. A.; Raasch, G. O.; Byrne, A. W.; Wilson, D. W.
    R.; and Reece, A. 1960. Geological map of Arctic. Prepared by
    First International Symposium on Arctic Geology, Alberta Society of
    Petroleum Geology. 1 oversized map. Scale 1:1,750,000.

Lopatin, N. V. 1971. Temperature and geologic time as factors in
    coalification (in Russian). Izv. Akad. Nauk SSSR, Seriya
    geologicheskaya, No. 3, 95-106. Cited in Waples, 1981.

Lowell, J. D. 1984. Structural geology. Tulsa: Oil and Gas
    Consultants International, Inc. Short course offered in Jackson
    Hole, Wyoming, Sept. 17-22.

Lynch, M. B. 1984. Lithology. In Geological and operational summary,
    Navarin Basin COST No. 1 well, Bering Sea, Alaska, 39-93. See
    Turner and others, 1984.

MacGregor, J. R. 1965. Quantitative determination of reservoir
    pressures from conductivity log. AAPG Bulletin 49:1502-11.

Macmillan. L. 1980. Oil and gas of Colorado: A conceptual view
    (abstract). In Rocky Mountain Association of Geologists, 1980
    Symposium, 191-197.

Magoon, L. B., and Claypool, G. E. 1983. Petroleum geochemistry of the
    North Slope of Alaska: Time and degree of thermal maturity. In
    Advances in organic geochemistry, ed. Malvin Bijorov, 28-38. New
    York: John Wiley.

Maison, Gerard. 1984. The generative basin concept. In Petroleum
    geochemistry and basin evaluation, ed. Gerard Demaison and
    R. J. Murris, 1-14. AAPG Memoir 35. Tulsa.

Marks, J. G. 1983. Molluscan fossils from third Alaska deep test, a
    report for ARCO Exploration Company: Preliminary reports and
    summary. Englewood, Colo.

Marlow, M. S.; Carlson, P.; Cooper, A. K.; Karl, H.; McLean, H.;
    McMullin, R.; and Lynch, M. B. 1981. Hydrocarbon resource
    report for proposed OCS sale No. 83, Navarin Basin, Alaska.
    U.S. Geological Survey Open-File Report 81-252.

Marlow, M. S., and Cooper, A. K. 1984. New discoveries along the
    Bering Sea continental margin. In Abstracts with programs of
    80th annual meeting of Cordilleran Section, Geological Society of
    America, May 30-June 1, 1984, Anchorage.

Marlow, M. S.; Cooper, A. K.; Carlson, P. R.; Karl, H. A.; and
    Edwards, B. D. 1983. Supplement resource report for OCS
    lease sale #83, Navarin Basin, Alaska. U.S. Geological Survey
    Open-File Report 83-707.

Marlow, M. S.; Cooper, A. K.; and Childs, J. R. 1983. Tectonic evolution of Gulf of Anadyr and formation of Anadyr and Navarin Basins. AAPG Bulletin 67:646-65.

Marlow, M. S.; Scholl, D. W.; Cooper, A. K.; and Buffington, E. C. 1976. Structure and evolution of Bering Sea shelf south of St. Lawrence Island. AAPG Bulletin 60:161-83.

Marlow, M. S.; Scholl, D. W.; Cooper, A. K.; and Jones, D. L. 1979. Mesozoic rocks from the Bering Sea: The Alaska-Siberia connection. In Vol. II, Geological Society of America Abstracts Programs, 90.

Marlow, M. S.; Vallier, T. L.; Cooper, A. K.; Barron, J. A.; and Wingate, F. H. 1983. A description of dredge samples collected in 1982 from the Bering Sea continental margin west of Navarin Basin. U.S. Geological Survey Open-File Report 83-325.

Martin, G. C. 1984. Well log interpretation. In Geological and operational summary, Navarin Basin COST No. 1 well, Bering Sea, Alaska, 139-166. See Turner and others, 1984.

Mason, Brian, and Sand, L. B. 1960. Clinoptilolite from Patagonia: The relationship between clinoptilolite and heulandite. American Mineralogist 45:341-50.

Matthews, R. K., and Poore, R. Z. 1980. Tertiary ^{18}O record and glacio-eustatic sea-level fluctuations. Geology 8:501-4.

McClure, L. J. 1977. Drill abnormal pressure safely. Manual for a short course offered by the author. Houston.

McGeary, S. E., and Ben-Avraham, Zvi. 1981. Allochthonous terranes in Alaska: Implications for the structure and evolution of the Bering Sea shelf. Geology 9:608-14.

McLean, Hugh. 1979a. Review of petroleum geology of Anadyr and Khatyrka Basins, U.S.S.R. AAPG Bulletin 63:1467-77.

McLean, Hugh. 1979b. Sandstone petrology: Upper Jurassic Naknek Formation of the Alaska Peninsula and coeval rocks on the Bering shelf. Journal of Sedimentary Petrology 49:1263-68.

McLean, Hugh. 1979c. Pribilof segment of the Bering Sea continental margin: A reinterpretation of Upper Cretaceous dredge samples. Geology 7:307-10.

Meyer, B. L., and Nederlof, M. H. 1984. Identification of source rocks on wireline logs by density/resistivity and sonic transit time/resistivity crossplots. AAPG Bulletin 68:121-29.

Meyerhoff, A. A. 1980. Petroleum basins of the Soviet Arctic. Geological Magazine (Cambridge) 117:101-210.

Meyers, Herbert. 1976. A historical summary of earthquake epicenters in and near Alaska. U.S. National Oceanic and Atmospheric Administration Technical Memorandum EDS NGSDC-1.

Milow, Dean. See Biostratigraphics, 1983.

Mitchell, J. G., and Maher, J. C. 1957. Suggested abbreviations for lithologic descriptions. AAPG Bulletin 41:2103-7.

Murata, K. J.; Friedman, I.; and Gleason, J. D. 1977. Oxygen isotope relations between diagenetic silica minerals in Monterey shale, Temblor Range, California. American Journal of Science 277:259-72.

Murata, K. J., and Whiteley, K. R. 1973. Zeolites in the Miocene Briones Sandstone and related formations of the central Coast Ranges, California. Journal of Research of the U.S. Geological Survey 1:255-65.

Murris, R. J. 1980. Middle East: Stratigraphic evolution and oil habitat. AAPG Bulletin 64:597-618.

Nardin, T. R.; Hein, F. J.; Gorsline, D. S.; and Edwards, B. D. 1979. A review of mass movement processes, sediment and acoustic characteristics, and contrasts in slope and base-of-slope systems versus canyon-fan-basin-floor systems. In Geology of continental slopes, ed. L. J. Doyle and O. H. Pilkey, 61-73. Society of Economic Paleontologists and Mineralogists Special Publication No. 27. Tulsa.

Nekton, Inc. 1980a. Alaskan COST program. Vol. VII, Biological investigation operations plan. San Diego. Report to ARCO Oil and Gas Company.

Nekton, Inc. 1980b. Biological survey: Proposed continental offshore stratigraphic test No. 1, Navarin Basin, Alaska. San Diego. Report to ARCO Oil and Gas Company.

Nekton, Inc. 1980c. Shallow drilling hazards survey: Proposed continental offshore stratigraphic test No. 1, Navarin Basin, Alaska. San Diego. Report to ARCO Oil and Gas Company.

Nortec, Inc. 1984. Forecast service report, Navarin Basin COST well No. 1. Prepared for ARCO Alaska, Inc.

Oil and Gas Journal. 1984. Soviets report Chukchi Peninsula gas/condensate find. Oil and Gas Journal 82(26 November):57.

Palciauskas, V. V., and Domenico, P. A. 1980. Microfracture development
    in compacting sediments - relation to hydrocarbon-maturation kinetics.
    AAPG Bulletin 64:927-37.

Patton, Jr., W. W. 1973. Reconnaissance geology of the northern Yukon-
    Koyukuk Province, Alaska. U.S. Geological Survey Professional Paper
    774-A.

Patton, Jr., W. W., and Dutro, Jr., J. T., 1969. Preliminary report on
    the Paleozoic and Mesozoic sedimentary sequence on St. Lawrence
    Island, Alaska. In Geological Survey research 1969, 138-143.
    U.S. Geological Survey Professional Paper 650-D.

Patton, W. W., Jr.; Lanphere, M. A.; Miller, T. P.; and Scott, R. A.
    1975. Age and tectonic significance of volcanic rocks on St. Matthew
    Island, Bering Sea, Alaska. U.S. Geological Survey Open-File
    Report 75-150.

Pennebaker, E. S. 1968a. An engineering interpretation of seismic
    data. SPE 2165, 43rd AIME Fall Meeting, Houston, Texas. Dallas:
    Society of Petroleum Engineers of AIME.

Pennebaker, E. S. 1968b. Seismic data indicate depth, magnitude of
    abnormal pressures. World Oil 166:73-78.

Phillipi, G. T. 1957. Identification of oil source beds by chemical
    means. In 20th International Geological Congress, proceedings,
    Mexico City, Sec. 3, 25-28.

Pichugina, G. K.; Kristofovich, L. V.; and Yegiazarov, B. Kh. 1974.
    Stratigraphic scheme of the Paleogene and Miocene deposits of
    the northwestern part of the Olyutorskiy-Kamchatskiy fold system.
    In Stratigraphy and lithology of the Cretaceous, Paleogene, and
    Neogene deposits of the Koryak-Anadyr District, 42-47. Scientific
    Research Institute of Arctic Geology, Ministry of Geology of the
    U.S.S.R.

Pirson, S. J. 1983. Geologic well log analysis. Houston: Gulf
    Publishing Co.

Pisciotto, K. A. 1981. Distribution, thermal histories, isotopic
    compositions, and reflection characteristics of siliceous rocks
    recovered by the Deep Sea Drilling Project. In Society of
    Economic Paleontologists and Mineralogists Special Publication
    No. 32, 129-147.

Powers, M. C. 1967. Fluid-release mechanisms in compacting marine
    mudrocks and their importance in oil exploration. AAPG
    Bulletin 51:1240-54.

Powley, D. 1983. Pressures: Normal and abnormal. In Advanced
    petroleum exploration. AAPG Course Notes. Tucson.

Radke, Matthias; Schaffer, R. G.; Leythaeuser, Detlev; and Teichmuller, Marlies. 1980. Composition of soluble organic matter in coals: Relation to rank and liptinite fluorescence. Geochemica et Cosmochemica Acta 44:1787-1800.

Redwine, L. E. 1981. Hypothesis combining dilation, natural hydraulic fracturing, and dolomitization to explain petroleum reservoirs in Monterey Shale, Santa Maria area, California. In The Monterey Formation and related siliceous rocks of California: Proceedings of an SEPM research symposium, ed. R. E. Garrison, 221-48. Los Angeles: Society of Economic Paleontologists and Mineralogists, Pacific Section.

Robertson Research (U.S.), Inc., see Dow and Coleman, 1983.

Robinson, G. S. 1970. Change of the bathymetric distribution of the genus Cyclammina. In Vol. 20, Transactions, Gulf Coast Association of Geological Societies, ed. N. G. Shaw, 201-9. Shreveport.

Roehl, P. O. 1981. Dilation brecciation--a proposed mechanism of fracturing, petroleum expulsion, and dolomitization in the Monterey Formation, California. In The Monterey Formation and related siliceous rocks of California: Proceedings of an SEPM research symposium, ed. R. E. Garrison, 285-315. Los Angeles: Society of Economic Paleontologists and Mineralogists, Pacific Section.

Rouse, G. E. 1977. Paleogene palynomorph ranges in western and northern Canada. In Contributions of stratigraphic palynology (with emphasis on North America): Vol. 1, Cenozoic palynology, ed. W. C. Elsik, 48-65. American Association of Stratigraphic Palynologists Contribution Series No. 5 A.

Russ, Tony. 1983. Geochemical final well report, ARCO Alaska, Inc., Navarin Basin COST No. 1. Anchorage: Exploration Logging (USA), Inc.

Schlumberger Well Services, Inc. 1972. Log interpretation manual. Vol. 1, Principles. Houston.

Schlumberger Well Services, Inc. 1974. Log interpretation manual. Vol. 2, Applications. Houston.

Schlumberger Well Services, Inc. 1981. Dipmeter interpretation. Vol. 1, Fundamentals. Houston.

Schmidt, G. W. 1973. Interstitial water composition and geochemistry of deep Gulf Coast shales and sandstones. AAPG Bulletin 57:321-37.

Schmidt, V. 1984. Secondary porosity in reservoir sandstones. In Sandstone Diagenesis Course Notes, 1-97. Tulsa: AAPG.

Scholl, D. W.; Buffington, E. C.; and Marlow, M. S. 1975. Plate tectonics and the structural evolution of the Aleutian-Bering Sea region. In Contributions to the geology of the Bering Sea basin and adjacent regions, ed. R. B. Forbes, 1-32. Geological Society of America Special Paper 151.

Scholl, D. W.; and Creager, J. S. 1973. Geologic synthesis of Leg 19 (DSDP) results: Far North Pacific, and Aleutian Ridge, and Bering Sea. In Initial reports of the Deep Sea Drilling Project, vol. 19, ed. P. R. Supko, 897-913. Washington, D. C.: National Science Foundation.

Scholle, P. A., and Spearing, D. R., ed. 1982. Sandstone depositional environments. AAPG Memoir No. 31. Tulsa.

Schowalter, T. T., and Hess, P. D. 1982. Interpretation of subsurface hydrocarbon shows. AAPG Bulletin 66:1302-27.

Schrader, Hans. 1973. Cenozoic diatoms from the northeast Pacific, Leg 18. In Initial reports of the Deep Sea Drilling Project, vol. 18, 673-797. Washington, D. C.: National Science Foundation.

Selly, R. C. 1978. Concepts and methods of subsurface facies analysis. AAPG Education Course Notes Series No. 9. Tulsa.

Serova, M. Y. 1976. The Caucasina eocaenica kamchatica Zone and the Eocene-Oligocene boundary in the northwestern Pacific. In Progress in micropaleontology: Selected papers in honor of Prof. Kiyoshi Asano, ed. Yokichi Takayanagi and Tsunemasa Saito, 314-28. New York: The American Museum of Natural History, Micropaleontology Press.

Shepard, F. P. 1963. Submarine geology. 2d ed. New York: Harper and Row.

Sheriff, R. E. 1978. A first course in geophysical examination and interpretation. Boston: International Human Resources Development Corp.

Sherwood, K. W. 1984. Abnormal formation pressure. In Geological and operational summary, Navarin Basin COST No. 1 well, Bering Sea, Alaska, 167-192. See Turner and others, 1984.

Slatt, R. M. 1984. Continental shelf topography: Key to understanding distribution of shelf sand-ridge deposits from Cretaceous Western Interior Seaway. AAPG Bulletin 68:1107-20.

Snowdon, L. R., and Powell, T. G. 1982. Immature oil and condensate: Modification of hydrocarbon generation model for terrestrial organic matter. AAPG Bulletin 66:775-88.

Sowers, G. F. 1979. Introductory soil mechanics and foundations: Geotechnical engineering. 4th ed. New York: Macmillan.

Spearing, D. R. 1976. Upper Cretaceous Shannon Sandstone: An offshore shallow-marine sand body. In Wyoming Geological Association 28th annual guidebook, 65-72.

Springer, A. M.; Roseneau, D. G.; Murphy, E. C.; Springer, M. I. 1983. Population and trophics studies of seabirds in the northern Bering and eastern Chukchi Seas, 1982: Final report. Research Unit 460. NOAA Outer Continental Shelf Environmental Assessment Program.

Stach, E.; Mackowsky, M.-Th.; Teichmuller, M.; Taylor, G. H.; Chandra, D.; and Teichmuller, R. 1982. Stach's textbook of coal petrology. Berlin: Gebruder Borntraeger.

Staplin, F. L. 1969. Sedimentary organic matter, organic metamorphism, and oil and gas occurrence. Bulletin of Canadian Petroleum Geology 17:47-66.

Steffy, D. A. 1984a. Shallow geology and geohazards. In Geological and operational summary, Navarin Basin COST No. 1 well, Bering Sea, Alaska, 14-19. See Turner and others, 1984.

Steffy, D. A. 1984b. Seismic stratigraphy. In Geological and operational summary, Navarin Basin COST No. 1 well, Bering Sea, Alaska, 103-128. See Turner and others, 1984.

Stewart, M. I. 1983. Well planning, part I. Seminar given at U.S. Minerals Management Service, Alaska OCS Region, Anchorage, Alaska, August 1-5, 1983.

Stoll, R. D.; Ewing, J.; and Bryan, G. M. 1971. Anomalous wave velocity in sediments containing gas hydrates. Journal of Geophysical Research 76:2090.

Stone, D. B.; Panuska, B. C.; and Packer, D. R. 1982. Paleolatitudes versus time for southern Alaska. Journal of Geophysical Research 87(no.B5):3697-3707.

Stover, L. E., and Evitt, W. R. 1978. Analyses of pre-Pleistocene organic-walled dinoflagellates. Stanford University Publications Geological Sciences vol. 15. Stanford.

Surdam, R. C.; Boesc, S. W.; and Crossey, L. J. 1984. The chemistry of secondary porosity. In Sandstone Diagenesis Course Notes, 127-149. Tulsa: AAPG.

Teledyne Isotopes. 1983. Potassium-argon age determination on three samples from the ARCO Navarin Basin COST Well No. 1 for ARCO Alaska, Inc. Westwood, N.J.: Teledyne Isotopes.

Tipsword, H. L.; Setzer, F. M.; and Smith, F. L., Jr. 1966.
Interpretation of depositional environment in Gulf Coast
petroleum exploration from paleoecology and related stratigraphy.
Transactions, Gulf Coast Association of Geological Societies,
vol. 16, ed. F. W. Bates, 119-30. Houston.

Tissot, B. P., and Welte, D. H. 1984. Petroleum formation and
occurrence. 2d ed. New York: Springer-Verlag.

Turner, R. F.; Bolm, J. G.; McCarthy, C. M.; Steffy, D. A.; Lowry,
Paul; and Flett, T. O. 1983. Geological and operational
summary, Norton Sound COST No. 1 well, Norton Sound, Alaska.
U.S. Geological Survey Open-File Report 83-124.

Turner, R. F.; Bolm, J. G.; McCarthy, C. M.; Steffy, D. A.; Lowry,
Paul; Flett, T. O.; and Blunt, David. 1983. Geological and
operational summary, Norton Sound COST No. 2 well, Norton
Sound, Alaska. U.S. Geological Survey Open-File Report
83-557.

Turner, R. F.; McCarthy, C. M.; Comer, C. D.; Larson, J. A.; Bolm,
J. G.; Banet, A. C., Jr.; and Adams, A. J. 1984. Geological
and operational summary, St. George Basin COST No. 1 well,
Bering Sea, Alaska. OCS Report MMS 84-0016. Anchorage:
U.S. Department of the Interior, Minerals Management Service.

Turner, R. F.; McCarthy, C. M.; Comer, C. D.; Larson, J. A.; Bolm,
J. G.; Flett, T. O.; and Adams, A. J. 1984. Geological
and operational summary, St. George Basin COST No. 2 well,
Bering Sea, Alaska. OCS Report MMS 84-0018. Anchorage: U.S.
Department of the Interior, Minerals Management Service.

Turner, R. F.; McCarthy, C. M.; Steffy, D. A.; Lynch, M. B.; Martin,
G. C.; Sherwood, K. W.; Flett, T. O.; and Adams, A. J. 1984.
Geological and operational summary, Navarin Basin COST No. 1
well, Bering Sea, Alaska. OCS Report MMS 84-0031. Anchorage:
U.S. Department of the Interior, Minerals Management Service.

U.S. Department of the Interior. 1985. Draft of 5-year leasing
schedule, March 1985. Photocopy.

U.S. Minerals Management Service, Alaska OCS Region, Field Operations.
1981. OCS environmental assessment No. AK 81-6. Anchorage.
Photocopy.

Vail, P. R.; Mitchum, R. M., Jr.; and Thompson, S., III. 1977.
Seismic stratigraphy and global changes of sea level, part 4:
Global cycles of relative changes of sea level. In Seismic
stratigraphy: Applications to hydrocarbon exploration, ed. C.
E. Payton, 83-97. American Association of Petroleum Geologists
Memoir 26. Tulsa.

Vallier, T. L.; Underwood, M. B.; Jones, D. L.; and Gardner, J. V. 1980. Petrography and geologic significance of Upper Jurassic rocks dredged near Pribilof Islands, southern Bering Sea continental shelf. AAPG Bulletin 64:945-50.

Van Alstine, D. R. 1983. Paleomagnetism of core from the Navarin Basin COST Well No. 1. Vol. 1, Interpretation. Walnut Creek, Calif.: Z Axis, a subsidiary of Woodward Clyde Consultants. Prepared for the Bering Sea COST Group.

Van Bennekom, A. J., and Van der Gaast, S. J. 1976. Possible clay structures in frustules of living diatoms. Geochimica et Cosmochimica Acta 40:1149-52.

Vogel, T. M., and Kvenvolden, K. A. 1981. Hydrocarbon gases in Navarin Basin province sediments. In Sea floor geologic hazards, sedimentology, and bathymetry: Navarin Basin province, northwestern Bering Sea, ed. P. R. Carlson and H. A. Karl, 80-99. U.S. Geological Survey Open-File Report 81-1217.

Voloshinova, N. A., and Budasheva, A. I. 1961. Lituolids and trochamminids from the Tertiary deposits of Sakhalin Island and the Kamchatka Peninsula. Microfauna of the USSR, Trudy sbornik 12, vol. 170, p. 199, Leningrad (VNIGRI).

Voloshinova, N. A.; Kuznetsova, V. N.; and Leonenko, L. S. 1970. Neogene Foraminifera of Sakhalin: Proceedings of the All Union Petroleum Scientific Research, Geological Exploration Institute. 3 vols. National Translations Center TT 76-53241. Washington, D. C.: Smithsonian Institution and National Science Foundation; Translated from Russian.

Von Rad, U., and Rosch, H. 1972. Mineralogy and origin of clay minerals, silica and authigenic silicates in Leg 14 sediments. In Initial reports of the Deep Sea Drilling Project, vol. 14, ed. A. C. Pimm, 727-51. Washington, D. C.: National Science Foundation.

Wall, David, and Dale, Barnie. 1971. A reconsideration of living and fossil Pyrophacus Stein, 1883 (Dinophyceae). Journal of Phycology 7:221-35.

Wallace, W. E. 1965. Application of electric log measured pressures to drilling problems and a new simplified chart for well site pressure computation. Log Analyst 6:26-38.

Waples, D. W. 1980. Time and temperature in petroleum formation: Application of Lopatin's method to petroleum exploration. AAPG Bulletin 64:916-926.

Waples, D. W. 1981. Organic geochemistry for exploration geologists.
Minneapolis: Burgess Publishing Company.

Waples, D. W. 1984. Course Notes Organic Geochemistry for Petroleum
Explorationists. Houston: International Human Resources
Development Corporation.

Weber, K. J.; Mandl, G.; Pilaar, W. F.; Lehner, F.; and Precious,
R. G. 1978. The role of faults in hydrocarbon migration and
trapping in Nigerian growth fault structures. In Tenth annual
Offshore Technology Conference, proceedings, paper 3356.

Whitney, J. W., and Wallace, W. K. 1984. Oceanic plate motions and
tectonic evolution of the Bering Sea shelf. In 80th annual
meeting, Cordilleran Section, Geological Society of America,
May 30-June 1, 1984, Anchorage, Alaska: Abstracts with programs,
340.

Williams, G. L. 1975. Dinoflagellate and spore stratigraphy of the
Cenozoic, offshore eastern Canada. Geological Survey of Canada,
paper 74-30, 2, 107-161.

Williams, G. L., and Bujak, J. P. 1977. Cenozoic palynostratigraphy
of offshore Eastern Canada. In Contributions of stratigraphic
palynology (with emphasis on North America): Vol. 1, Cenozoic
palynology, ed. W. C. Elsik, 14-48. American Association of
Stratigraphic Palynologists Contribution Series No. 5A.

Wills, J. C.; Bolm, J. G.; Stewart, G. H.; Turner, R. F.; Lynch, M. B.;
Petering, G. W.; Parker, John; and Schoof, Brian. 1978.
Geological and operational summary, Atlantic Richfield Lower
Cook Inlet, Alaska, COST well No. 1. U.S. Geological Survey
Open-File Report 78-145.

Wilson, G. J., and Bush, R. E. 1973. Pressure prediction with
flowline temperature gradients. AIME-SPE Paper No. 3848.
Journal of Petroleum Technology 25:135-42.

Woodward-Clyde Consultants. 1978. Offshore Alaska seismic exposure
study, vol. V. Prepared for Alaska Subarctic Operators'
Committee.

Zieglar, D. L., and Spotts, J. H. 1978. Reservoir and source-bed
history of Great Valley, California. AAPG Bulletin 62:813-26.

ERA	PERIOD	EPOCH	AGE	PALEOBATHYMETRY	MEASURED DEPTH (FEET BELOW KELLY BUSHING)	GAMMA-RAY LOG INCREASING RADIOACTIVITY →	SP LOG	LITHOLOGY	DEEP RESISTIVITY LOG INCREASING RESISTIVITY →	DENSITY LOG INCREASING DENSITY →	SONIC LOG INCREASING VELOCITY →	LITHOLOGIC ZONE	SEISMIC HORIZON AND SEQUENCE

Right-side descriptive text:

Quaternary (sea floor to 1,536 feet)
Quaternary deposits consist of poorly sorted silt, clay, sand, and diatomaceous ooze.

Pliocene (1,536 to 3,180 feet)
The Pliocene interval contains poorly sorted, silty, sandy mudstone and diatomaceous ooze. Primary sedimentary structures were destroyed by extensive bioturbation. Concentrations of granule-s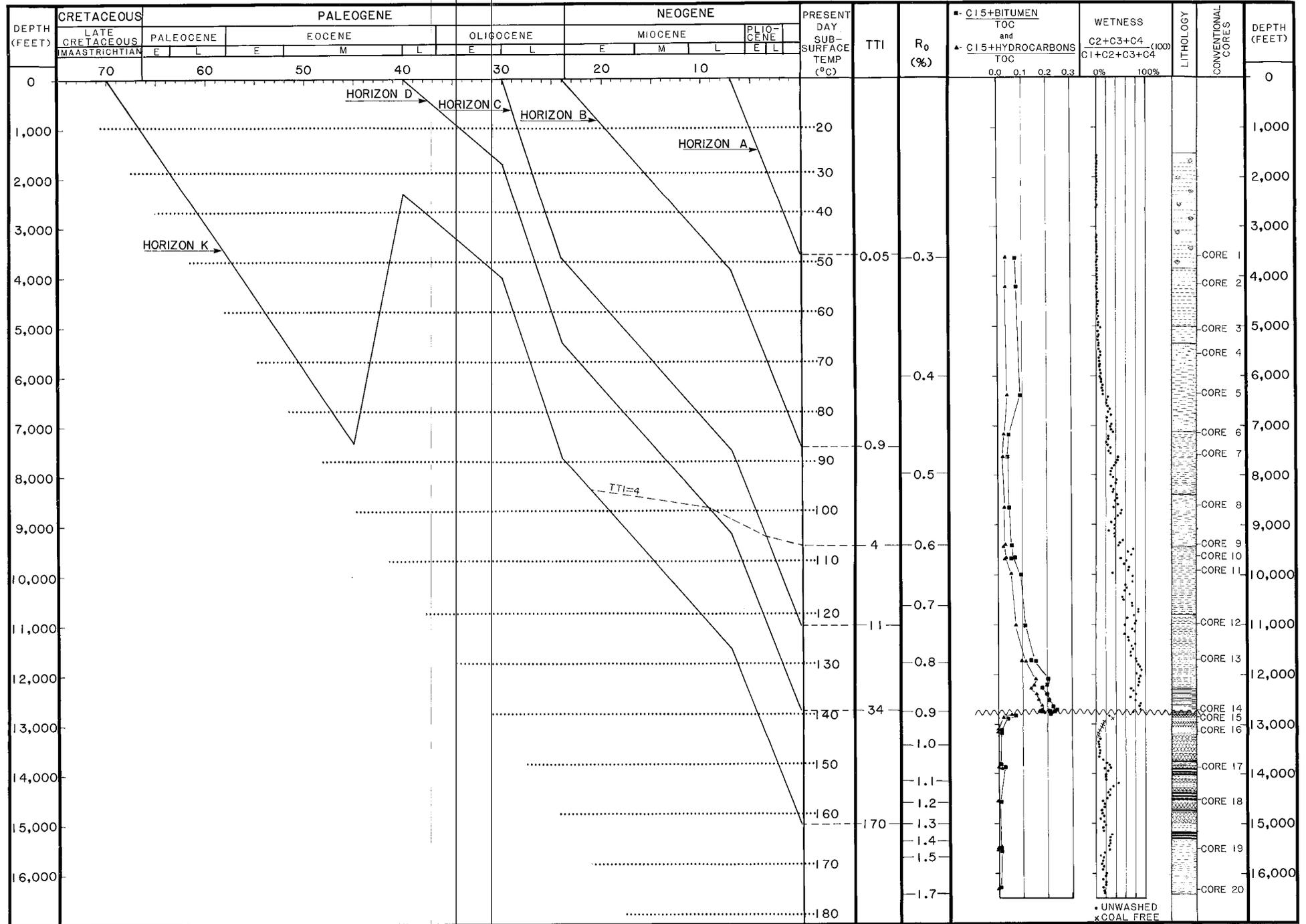ized rock and shell fragments are associated with scour surfaces. Coarser grained material may represent basal lag deposits on erosional surfaces created by storm-generated currents. The framework grains are mainly volcanic lithic fragments, angular quartz, and feldspars. Diatom and clay matrix content ranges from 50 to 80 percent. Most of the diatom fragments are broken and angular. The lithic components are dominated by basaltic and intermediate volcanic fragments, mica, plutonic rock, chert, and clay. Accessory minerals include hornblende, epidote, apatite, and pyroxene. Diagenetic changes included weak alteration and dissolution of lithic fragments and development of authigenic pyrite and chlorite.

Miocene (3,180 to 5,704 feet)
From 3,180 to 3,860 feet the section consists of interbedded, moderately indurated sandstone and mudstone. Most of the diatoms (opal-A) have been altered to clinoptilolite and minor amounts of opal-CT by the depth of 3,860 feet. Secondary carbonates (high-magnesium calcite, protodolomite, and rhodochrosite) are common.

The interval from 3,860 to 5,010 feet is composed of fine- and very fine-grained sandstones interbedded with sandy mudstones. The sandstones are poorly to well sorted, and locally cemented with calcite. In core 2, the primary sedimentary structures not destroyed by bioturbation consist of discontinuous, wavy laminations. Some diatoms have been replaced by framboidal pyrite. Visual analysis suggests that some diatoms altered to authigenic quartz may be present. Precipitation of smectite and zeolite has reduced porosity and permeability.

The section from 5,010 to 5,360 feet is similar to the upper part of the Miocene section, but contains more siltstone than mudstone.

From 5,360 feet to 5,704 feet there are thick, coarsening-upward sandstone beds interbedded with claystones and mudstones. The sandstone is fine to very fine grained, poorly to well sorted, bioturbated, and locally cemented by calcite. Broken and intact molluscan shells and lithic pebbles are present. Primary sedimentary structures in cores include wavy to horizontal interlaminations. Glauconite is common. The framework grains include chert, monocrystalline and polycrystalline quartz, lithic fragments, and feldspars. Plagioclase is the dominant feldspar. Most of the lithic fragments are volcanic in origin. Minor constituents include chert, hornblende, pyroxene, epidote, zircon, garnet, and rare tourmaline. Diagenetic alterations include compaction, alteration, and dissolution of feldspars and volcanic lithic fragments, and the precipitation of clinoptilolite and authigenic pyrite.

Oligocene (5,704 to 12,280 feet)
The lithology from 5,704 to 7,130 feet is similar to the lithology of the Miocene section between 5,360 and 5,704 feet, and together they constitute a single lithostratigraphic unit.

The interval from 7,130 to 10,800 feet is characterized by sandy mudstone, fine-grained muddy sandstone, and claystone with rare siltstone lenses. Isolated coarse-sand- to pebble-sized volcanic rock fragments are present. The sediments have been bioturbated and burrowed. Whole and broken molluscan shells are present. The only primary sedimentary structures seen in the cores are wavy laminations. The framework clasts consist of subrounded and subangular quartz, feldspar, and lithic grains. Other minerals present include glauconite, micas, clays, chert, and hornblende. Authigenic minerals include smectite, mixed-layer illite-smectite, calcite, siderite, pyrite, zeolites, gypsum, chlorite, quartz, and feldspar.

The zone from 10,800 to 12,280 feet consists of moderately burrowed, laminated claystone. Calcite concretions are present. Silt-sized monocrystalline quartz, plagioclase, micas, chert, organic material, and volcanic rock fragments are present as framework clasts. Other minerals include pyrite, siderite, ankerite, calcite, pyroxene, clinoptilolite, laumontite, leonhardite, glauconite, hornblende, gypsum, and clays. Clays, which constitute about 40 to 70 percent of the rock, include chlorite, kaolinite, illite, and mixed-layer illite-smectite. Authigenic minerals include chert matrix, mixed-layer clays, pyrite, calcite, zeolites, quartz, potassium feldspar, and ankerite. The provenance was probably chiefly volcanic with a minor metamorphic input.

Eocene (12,280 to 12,780 feet)
The Eocene section contains dark gray, calcareous, organic-rich claystone. Calcite-filled fractures are present throughout the cored interval. No primary sedimentary structures are visible. The mineralogy and provenance are similar to that of the Oligocene section above from 10,800 to 12,280 feet, but the Eocene rocks contain much more organic material. This interval contains the best potential hydrocarbon source rocks encountered in the well.

Cretaceous (12,780 to 16,400 feet)
The Cretaceous section penetrated by the well is nonmarine from 12,780 to 15,300 feet and marine from 15,300 to 16,400 feet. The nonmarine section contains siltstone, very fine grained sandstone, mudstone, and claystone intruded by Miocene diabase and basalt sills or dikes. These strata were deposited as a sequence of fluvial, paludal, and possibly intertidal sediments. Sedimentary structures include fining-upward sequences, flaser bedding, microfaults associated with the slumping of semiconsolidated sediments, root-mottled zones, and continuous to discontinuous, wavy- and parallel-laminated coal, claystone, mudstone, and sandstone. Framework grains in the sandstone and mudstone include quartz (both monocrystalline and polycrystalline), chert, plagioclase feldspar, mica, hornblende, carbonaceous material, and volcanic and metamorphic rock fragments. Chert matrix and clay are abundant. Authigenic minerals include calcite, pyrite, kaolinite, chlorite, siderite, clinoptilolite, chert, and mixed-layer illite-smectite. The coal occurs in beds up to 20 feet thick, as thin layers in the sediments, and as fragments disseminated through clastic beds. The intrusives are hard dark-greenish-gray diabase characterized by an intersertal texture. Interstices between plagioclase and clinopyroxene laths are filled with alteration products such as clay, calcite, and minor amounts of quartz.

The marine deposits below 15,300 feet are composed of claystone, siltstone, mudstone, and tuff. Bioturbation, rare leaf fossils, Inoceramus fragments, discontinuous wavy laminations, and isolated thin tuff layers are present in conventional cores. These strata were deposited in marine shelf and possibly prodelta environments. Clay minerals make up 70 to 80 percent of the rocks in the zone. Chlorite is the most abundant clay, followed by mixed-layer illite-smectite, kaolinite, and illite. Volcanic rock fragments, quartz, plagioclase feldspar, potassium feldspar, pyrite, siderite, calcite, clinopyroxene, clinoptilolite, heulandite, hornblende, organic fragments, and mica are also present.

Lithostratigraphy, Navarin Basin COST No. 1 Well

Organic Richness and Classification of Organic Matter, Navarin Basin COST No. 1 Well

UNITED STATES DEPARTMENT OF THE INTERIOR
MINERALS MANAGEMENT SERVICE

A Hypothetical Depositional History, Tectonic History, and Temperature Gradient, plus Selected Geochemical and Lithologic Profiles, for the Navarin Basin